ELECTRICAL COMMUNICATION

1958
VOLUME 35
NUMBER 2

THE TECHNICAL JOURNAL OF ITT

INTERNATIONAL TELEPHONE AND TELEGRAPH CORPORATION

ELECTRICAL COMMUNICATION

Technical Journal Published Quarterly by

INTERNATIONAL TELEPHONE and TELEGRAPH CORPORATION

67 Broad Street, New York 4, New York

President: Edmond H. Leavey

Secretary: C. Douglas Webb

Subscription: $2.00 per year; 50¢ single copy

ELECTRICAL COMMUNICATION

The Technical Journal of
INTERNATIONAL TELEPHONE AND TELEGRAPH CORPORATION
AND ASSOCIATE COMPANIES

CONTENTS

VOLUME 35 **1958** **NUMBER 2**

Electronic 20-Line Private Automatic Telephone Exchange 75

Electron-Beam Voltage-Indicator Tube EM-84 *by A. Lieb* 76

Direct-Voltage Instantaneous Breakdown of Oil-Impregnated Paper Capacitors as a Function of Area *by D. S. Girling* 83

Characteristics and Applications of the Iatron Storage Tube *by Dean W. Davis* 93

Storage Tube Projects Radar Plan-Position-Indicator Display *by Harry W. Gates* 103

Carrier Telecommunications Over the High-Tension Power Network in Algeria *by Edmond A. Thomas* 109

Crossbar Toll Offices in the Finnish Group Network *by Nikolaus Lewen and Heinz Kürten* 116

Two-Wire Repeater Employing Negative Impedance *by Theodor G. Grewe* 123

Telephone Statistics of the World 138

United States Patents Issued to International Telephone and Telegraph System; November 1957-January 1958 143

Recent Telecommunication Developments—

Electronic Spectroanalysis 82

Space-Charge Waves (Book) 102

Contributors to This Issue 145

Electronic 20-Line Private Automatic Telephone Exchange

DEVELOPED and manufactured by Laboratoire Central de Télécommunications, Paris, and by Bell Telephone Manufacturing Company, Antwerp, a fully electronic 20-line private automatic branch exchange was a center of interest at Bell's pavilion at the 1958 Brussels World Fair.

The frontispiece photograph shows typical visitors from the stream that continually placed call after call to each other using the telephones on the table and marvelled to see their connections quickly established by purely electronic means.

The exchange can handle 4 simultaneous conversations and will process 2 calls simultaneously by means of 20 subscribers' line circuits, 4 junction circuits, and 2 registers. The fundamental circuit elements used[1] are silicon junction speech-switching diodes controlled by magnetic flip-flop circuits made of a saturable reactor in series with a capacitor to form a ferroresonant circuit. By completely excluding moving contacts, such as those on relays, the life of the equipment becomes practically indefinite.

The subscriber's set used with the equipment differs from the conventional design in that digits are transmitted from a keyboard and not from a dial and that the bell has been replaced by an electroacoustical device driven by a transistor amplifier in the set.

In the exchange, the subscriber's line circuit incorporates a line transformer and the device setting the condition of the line, busy or free, et cetera. The silicon-diode speech-switching circuits use two miniature diodes to establish a speech path between subscribers. In the blocking condition, the diodes are equivalent to a 1000-megohm resistor in parallel with a 5 picofarad capacitor. In the conducting condition, they have a resistance of only 4 ohms.

The peak power transmitted is 50 milliwatts and the total attenuation from line to line is 1 decibel.

The diode switches are operated by the magnetic flip-flops, which also form the register counters. These flip-flops are driven by an 8-kilocycle-per-second 10-volt supply. At this voltage, they have two operating conditions; in one state, the current passed is 15 times that of the other condition. After conversion to direct current by selenium rectifiers, the flip-flop output polarizes the diodes in conducting or blocking conditions.

Printed-circuit construction is used in the exchange; its dimensions are but 22 by 53 by 61 centimeters (8.8 by 21 by 24 inches). The power consumed by the exchange itself (excluding the microphone currents of the subscribers' sets) is only 30 watts at 24 volts.

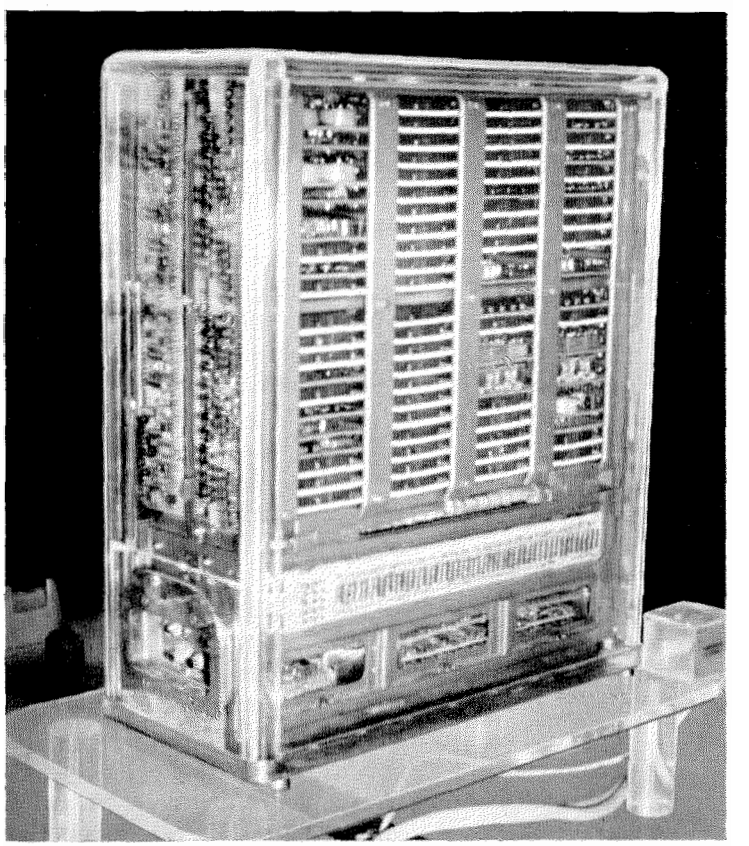

[1] C. Dumousseau, "Fully Electronic 20-Line Automatic Telephone Exchange," *Electrical Communication*, volume 34, pages 92–101; June, 1957.

Electron-Beam Voltage-Indicator Tube EM84

By A. LIEB

Lorenz Werke, division of Standard Elektrik Lorenz A.G.; Stuttgart, Germany

INDICATOR TUBES are simplified cathode-ray tubes in which the magnitude of a voltage is made visible on a target by electron-optical means. The vacuum-tight envelope and the constructional principles correspond to those of ordinary vacuum tubes. The voltage indication of such tubes is not impaired by inertia effects as in the case of mechanical instruments and the tube is insensitive to reasonable voltage overloads. Moreover, the tube is usually so designed that no power is drawn from the measured circuit.

Commonly known indicator tubes have also been called magic eye or magic fan, depending on the shape of the luminous image. They are widely used in superheterodyne receivers with automatic gain control, where they facilitate tuning. In such applications, the tube indicates the magnitude of the gain-control voltage. Accurate tuning results in the maximum value of this voltage. Tuning by ear alone is difficult, as the automatic gain control causes almost the same volume level whether the receiver is tuned or detuned. Proper tuning is particularly important for sets with high selectivity and good reproduction as a slight detuning from the center of the carrier frequency will cause distortion; particularly with frequency-modulation receivers. Tuning-indicator tubes have therefore found wide application, particularly in Europe where the customer demands very-high-quality sound reproduction. Thus, 80 percent of all radio receivers made in Germany are equipped with tuning-indicator tubes.

In the United States, few receivers had such indicator tubes previously. However, the trend toward high-fidelity reproduction has brought about their wider use.

The principle of this tube dates back to the magic eye developed in the 1930's. The target of the magic eye is a metal funnel coated inside with luminous phosphor. An axial cathode with a parallel control electrode are inside the target. The control electrode produces a shadow on the target. The shadow varies in size depending on the voltage applied to the control electrode.

This magic-eye indicator tube has the disadvantage of a small target area. The concave target is mounted in the narrow end of the glass tube envelope. The person tuning a receiver often has to change position to observe the tube indication. Moreover, the target brightness of the tube has a relatively short life.

The observation angle of the *EM84* tube is much greater and the decrease of the luminous intensity during life is much smaller. The luminous image is simple and facilitates accurate reading. In addition, voltage values can be calibrated on a scale attached to the outside of the tube. This property of the tube makes it suitable for indicating not only minimum and maximum values of a voltage, as is the case with conventional tubes, but also specific voltages. Because of this expanded application, the tube is designated a voltage-indicator tube rather than a tuning-indicator tube.

1. Constructional Principles

The luminous pattern of an indicator tube can be observed best and from the greatest angle if this pattern is produced directly on the glass envelope. This is particularly true when the moving edge of the luminous image is on the envelope portion having the greatest curvature. These requirements are most conveniently met with a luminous pattern whose moving edge is at a right angle to the tube axis for any possible value indicated. The pattern of the new tube consists of two luminous bands parallel to the tube axis so that the length of both bands changes along the tube axis.

Figure 1A is a photograph of the tube and Figure 1B shows the luminous pattern. Distance *A* between the edges is a measure of the voltage. If the tube is placed in a radio set so that a portion of the side of the glass envelope protrudes from the panel, good observation is ensured from the whole area in front of the cabinet.

The principle described allows for simple calibration that can be accomplished, for instance, by projecting a thermometer-like scale against

the exterior wall of the glass bulb. Since the luminous pattern is directly on the bulb wall, all parallax errors that might affect the reading are precluded. The measuring scale can be calibrated after completion of the tube, thus compensating for manufacturing tolerances.

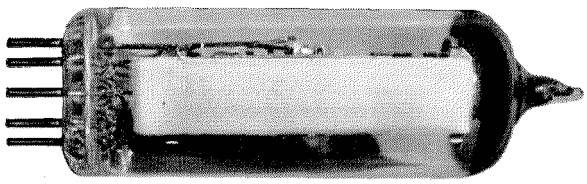

Figure 1A—Photograph of tube.

In conventional indicator tubes, zinc silicate is generally used for the target phosphor. This phosphor yields a relatively high light output in the green spectral range even if the excitation energy is small. However, the durability of this phosphor when exposed to electron bombardment is not very favorable. Beside zinc silicate, a suitably prepared phosphor of zinc oxide will also emit sufficient light and the decrease caused by electron bombardment is much less than for zinc silicate. This has been known for many years, but the bluish-green tint of the zinc-oxide emission did not favor its general introduction. Contrariwise, the zinc silicate produces an emission of pure green color. The pale color of the zinc oxide is caused by a high white component in the emitted light, which is less easily identifiable in ambient illumination than light from zinc silicate.

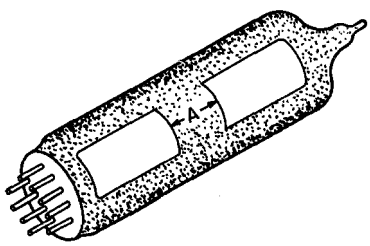

Figure 1B—Drawing of tube showing the fluorescent bands. Dimension *A* varies with the control voltage.

In the *EM84* indicator tube, however, a phosphor of zinc oxide is used. The problem of the emitted color has been solved by a color filter mounted so that it covers the luminous areas of the tube. The interfering white component thus serves a useful purpose; in addition, the advantage is obtained that the resulting color can be controlled by the spectral transmission factor of the filter. This advantage can be used to mark in a simple and effective way that portion of the luminous band that corresponds to a given voltage.

In the case under discussion, provision was made to change the color of the luminous bands as they expand along the scale. This arrangement will be seen in Figure 2; the tube bulb carries optical filters with different transmission factors at sections designated *F1* and *F2*. As soon as the luminous-band edges move over the distance *B*, the color of the bands will also change. The filter also increases the contrast and this is an advantage in bright daylight or artificial illumination.

The measured voltage is preamplified as in the case of conventional tubes. This ensures high indicating sensitivity and high input impedance. For economic reasons, the amplifier system is built into the indicator tube. The amplifier system of the indicator tube should be as simple as possible so that the tube can be manufactured on an economical basis and will give stable operation. In the new magic-band indicator tube, the design is simplified inasmuch as one cathode is utilized for both the indicator system and the amplifier system. The amplifier system is further simplified by using two rods to take the place of the usual control grid. These two control electrodes are arranged in the space-charge region of a grid at cathode potential. This grid surrounds the cathode and also functions as a grid for the indicator system.

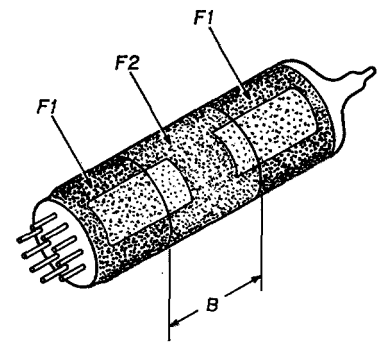

Figure 2—Colored filters can be placed over the fluorescent strip to identify certain values of measured voltage.

2. *Design Details*

Constructional details of the magic-band tube may be seen in Figure 3. The electrodes are held in place by the aperture frame, which is at target potential. This frame is welded to the leads

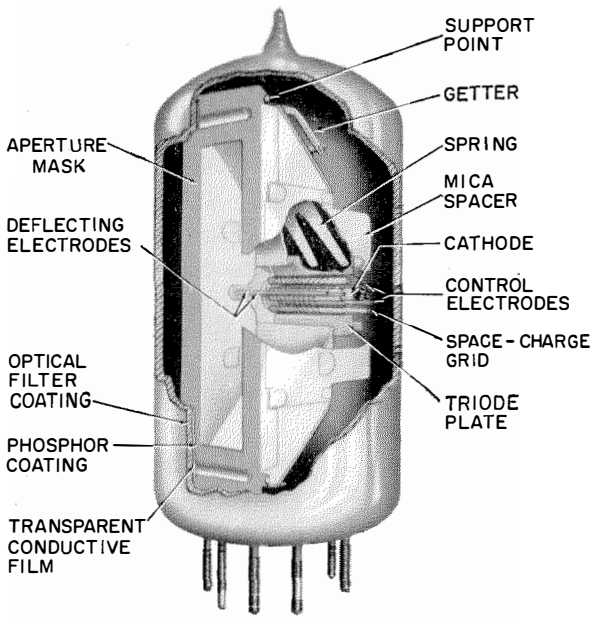

Figure 3—Electrode arrangement in the *EM84* voltage-indicator tube.

passing through the glass button stem and has a slot-like aperture opposite the target on the glass bulb. The slot determines the width and the total length of the fluorescent patterns and, moreover, forms a shield between the mica spacers and the discharge space of the indicator system to prevent formation of disturbing charges on the mica spacers.

The target is on the inside wall of the bulb in front of the frame aperture. It consists of a transparent conductive film and the phosphor coating. The optical filter can be a transparent lacquer film applied to the exterior of the bulb. Instead of the lacquer, a colored transparent glass or heat-resistant plastic foil can be placed on the tube or in front of it.

By varying the transmission factor of the filter, a large number of various colors can be obtained. However, blue, green, and yellow have a particularly high light output owing to the preferred emission of the zinc-oxide phosphor.

For a two-color filter, it is expedient to select two complementary colors to achieve as great a color contrast as possible. The complementaries blue and yellow have the highest luminous intensity when zinc oxide is employed.

The length of the fluorescent bands, or the distance between their opposite ends, is varied by the deflecting electrodes. These deflecting electrodes are electrically connected to each other and this parallel connection results in a very-high deflection sensitivity and in particularly sharp edges of the fluorescent patterns.

The cathode is surrounded by a space-charge grid. That portion of the cathode facing the target serves as an electron source for the indicator system. The other side of the cathode forms the amplifier system. It consists of the control electrodes, the space-charge grid, and the plate. The control electrodes are two rods arranged between the cathode and space-charge grid. The amplifier section can be regarded as a special type of space-charge-controlled two-grid tube.

The electodes are supported by two mica spacers that, contrary to conventional design, are mounted parallel to the bulb axis. The electrode system is pressed against the glass bulb by the spring shown in Figure 3. Only a few points of the frame are in contact with the glass so that intolerable thermal glass strains during pumping are prevented. These points of support and the spring also ensure the parallel position of the

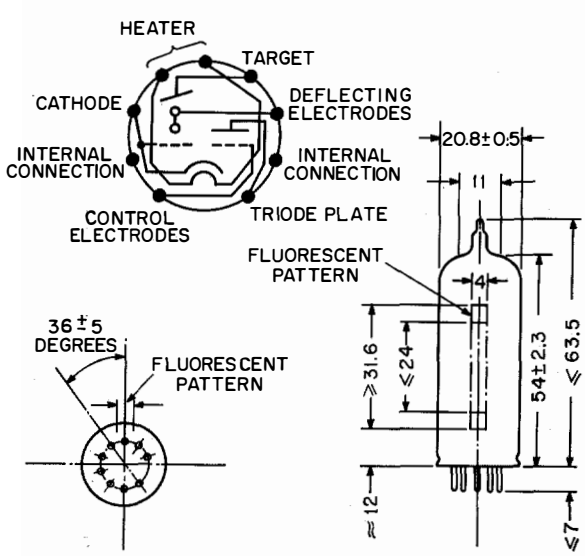

Figure 4—Socket connections, dimensions in millimeters, and position of fluorescent pattern on the tube.

frame with respect to the target. Finally, the points of support and the spring connect the target with the frame aperture mask so that both have the same potential.

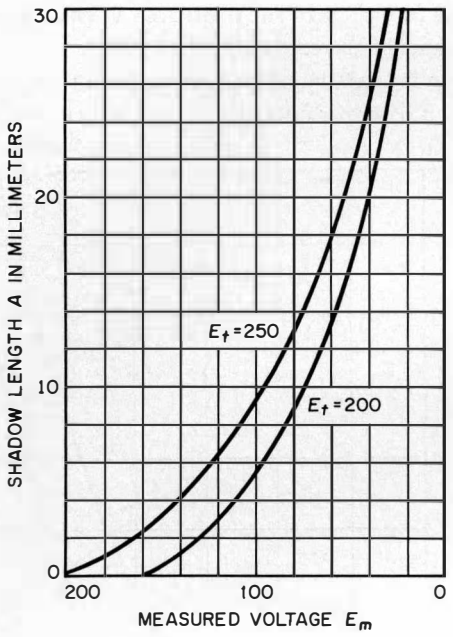

Figure 5—Shadow length A (see Figure 1B) as a function of the measured voltage E_m when applied directly to the deflecting electrodes. The target voltage = E_t.

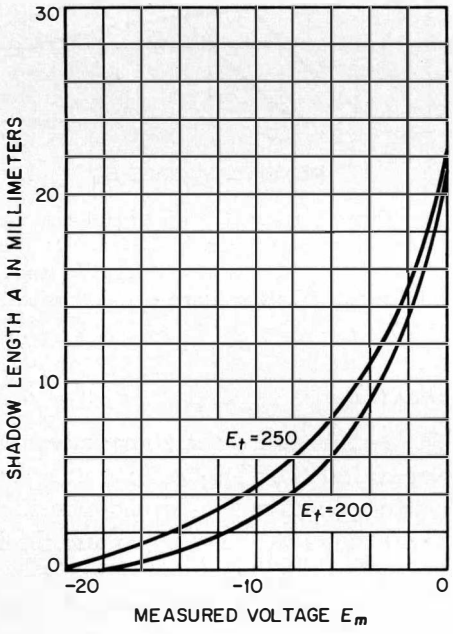

Figure 6—Shadow length A as a function of the measured voltage E_m when applied to the control electrode of the triode preamplifier. The target voltage = E_t. Triode plate load resistor = 470 kilohms.

3. Properties of Tube

The most-important properties of the *EM84* can be seen from Figure 4 and Table 1.

Figure 5 shows the distance A between the pattern edges as a function of the measured voltage when it is applied directly to the deflecting electrodes. Figure 6 is for that voltage applied to the amplifier control electrode. Figure 7 shows the derivative of A to the measured voltage depending on the measured voltage applied to the amplifier. This quantity to a first approximation is a measure of indicator sensitivity. A more-accurate evaluation of sensitivity should take into account not only the variation of A, but also its absolute value at any instant. When A becomes smaller, voltage variations are more-readily perceived, as the observer tends then to observe the doubly sensitive distance variations between the fluorescent edges rather than the changing length of one band.

TABLE 1

OPERATIONAL CHARACTERISTICS OF *EM84*

Heater Values, Parallel Supply	
Heater Voltage	6.3 Volts ± 10 Percent
Heater Current	0.27 Ampere
Cathode	Oxide, Unipotential
Operational Values (Deflecting Electrodes Connected to Plate)	
Plate Voltage	250 Volts
Target Voltage	250 Volts
Plate Load Resistance	470 Kilohms
Control-Electrode Resistor	3.0 Megohms
Control-Electrode Bias	0 to −22 Volts
Plate Current	0.45 to 0.06 Milliampere
Target Current	1.1 to 1.6 Milliamperes
Shadow Length A	22 to 0 Millimeters
Maximum Values (Limiting)	
Cold Plate Voltage	550 Volts
Plate Voltage	300 Volts
Plate Dissipation	0.5 Watt
Cold Target Voltage	550 Volts
Target Voltage	300 Volts
Cathode Current	3.0 Milliamperes
Grid-Leak Resistance	3.0 Megohms
Heater-to-Cathode Voltage	100 Volts
Ambient Temperature Near Target	120 Degrees Centigrade

The subjective reading sensitivity was measured by plotting the smallest increment of voltage resulting in a perceptible change of the pattern over a range of measured voltages. These

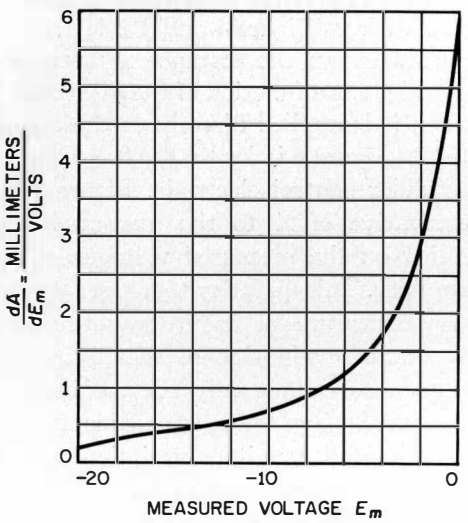

Figure 7—Derivative of length A to measured voltage E_m as a function of measured voltage applied to the grid of the triode preamplifier; Target voltage E_t = 250 volts.

observations were made at a practical distance of 40 centimeters by several persons independently. The resulting mean values obtained by all observers are shown in Figure 8. The measurements reveal the high sensitivity of the human eye to distance variations of parallel edges; perceptibility is far greater than for the varying arc of a luminous sector.

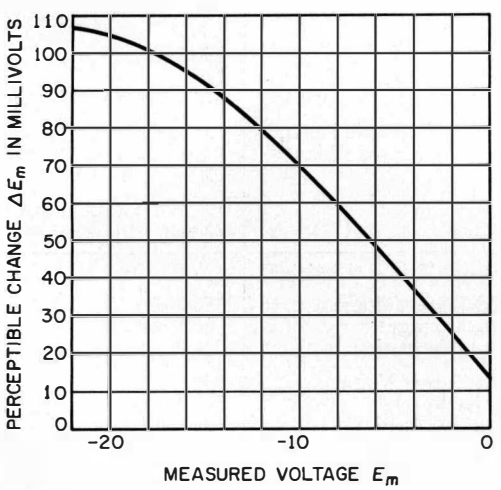

Figure 8—Smallest perceptible change ΔE_m in measured voltage E_m applied to control electrode.

Figure 9 is a plot of the target and plate currents as functions of the measured voltage applied to the amplifier system. The relatively low target current is particularly favorable for receivers with small power supplies.

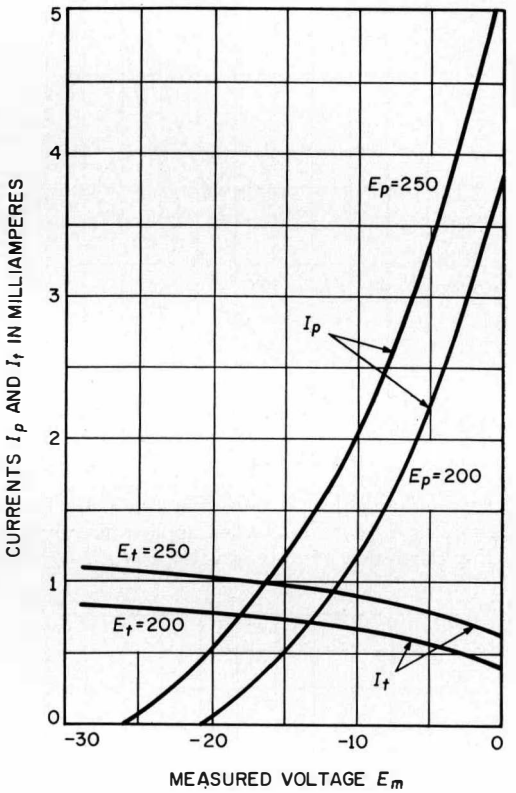

Figure 9—Target current I_t (with triode plate load resistance) and triode plate current I_p (without load resistance) as a function of measured voltage E_m applied to the control electrode. Target voltage = E_t and triode plate voltage = E_p.

4. Applications

The *EM84* tube, with the above advantages, can replace in all their applications the conventional magic-eye and magic-fan indicators.

Figure 10 shows the tube in a radio receiver. The tube is arranged above the tuning scale and in a horizontal position. The possibility of observing the tube from a wide angle is quite apparent with this arrangement. The tube is masked by a cylindrical bezel exposing only that portion of the tube bearing the target.

Another suitable type of mounting is immediately behind the dial or panel of a receiver. Since the target is on the glass envelope, the tube can be mounted so that the target appears in the plane of the tuning scale. In conventional tuning-indicator tubes, the luminous pattern is always set behind the scale so that observation is not as convenient as with the *EM84*.

The tube can even be moved along the scale with the scale pointer. The narrow fluorescent bands varying in length can be better adapted to the shape of the pointer than can the targets of conventional indicator tubes.

The possibility of marking certain values in a convenient scale on the exterior of the bulb, thus excluding parallax errors, makes the tube applicable to all cases where one or more voltage values must be determined. An example is the indication of overmodulation in a tape recorder.

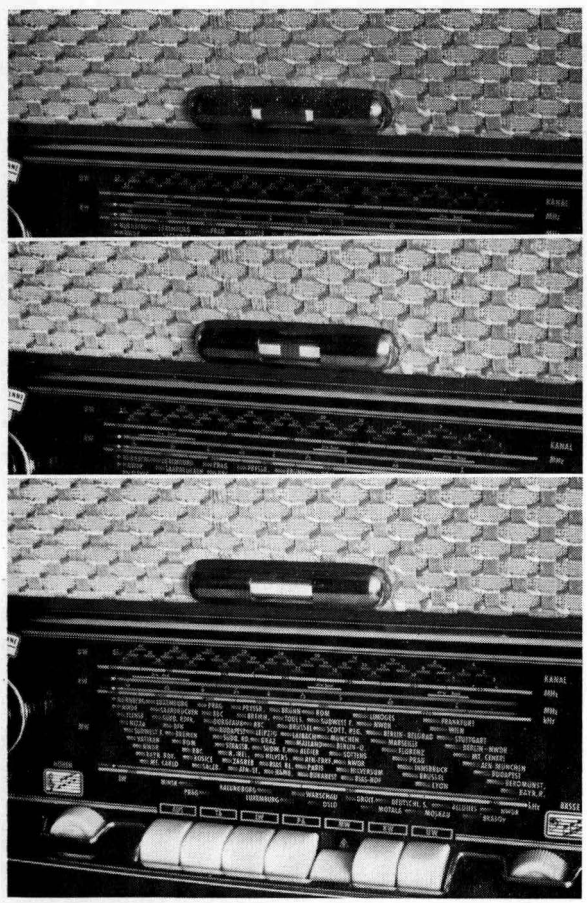

Figure 10—Type-*EM84* tube in receiver operating on weak (top), medium (middle), and strong (bottom) signals.

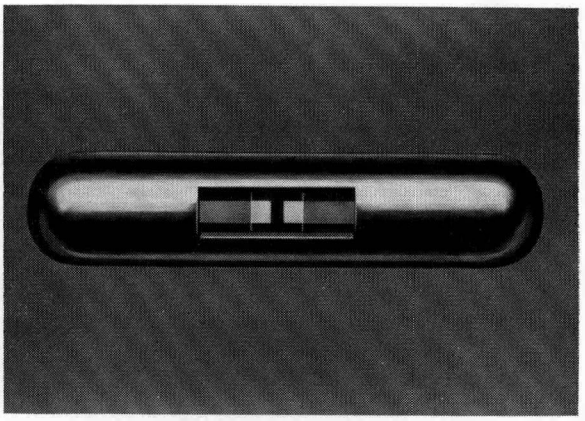

Figure 11—Application with colored filters as an overmodulation indicator in a tape recorder.

So far, tuning-indicator tubes used for this purpose have been arranged so that the fluorescent pattern moves visibly when the adjustment is correct, while maximum permissible amplitude results in disappearance of the shadow. This requires very-careful observation of the fluorescent pattern during the adjustment of the recorder gain and supervision from a distant place, as in home studios, is impossible. When the *EM84* is used in a tape recorder, two filters are employed as shown in Figure 11. The tube is covered by a mask so that only the target is visible. Voltages below the overload value are indicated in blue, while a yellow filter becomes effective as soon as overmodulation takes place.

By adding a third color filter, insufficient gain can be indicated in addition to the mean and overload values. In this case, the recorder must be adjusted so that the fluorescent pattern edges fluctuate only in the color area corresponding to permissible modulation. Adjustments of this kind can be easily comprehended and carried out even by unskilled personnel.

When a scale is fixed to the tube exterior, voltages can be measured with the *EM84*. Two measuring ranges are available without any parallel or series input resistors.

When the voltage to be measured is applied directly to the deflecting electrodes, the measuring range is +35-to-+200 volts. This range can be shifted to +20-to-+250 volts by changing the target voltage. For the case of the preamplified

voltage, the measuring range is 0-to-−22 volts. Here again the range can be shifted to −10-to-−30 volts by varying the plate supply voltage or the load resistance.

Figure 12 shows an *EM84* in such an application. The tube bulb carries a plastic-foil strip with a scale. To facilitate the reading, one of the fluorescent bands is completely masked. The sharp edge of the pattern permits very-accurate reading of the indicated values. The measuring accuracy is 5-to-15 percent due to variations in tube properties such as cathode emission, contact potential between cathode and control electrode, secondary-electron emission of the deflecting electrodes, and the like. Accuracy depends on the care taken in calibrating the scale and the measuring range selected. The tube will be of interest in certain fields of application where the main requirements on the measuring device are insensitivity to physical position, to vibration, and to overload; quick time response, low power drawn from the measured circuit, and economy.

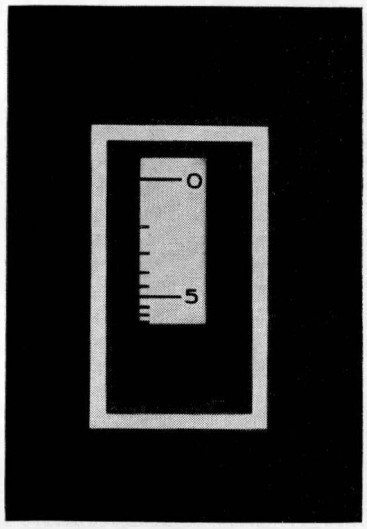

Figure 12—Tube used as a voltmeter.

Recent Telecommunication Development

Electronic Spectroanalysis

ELECTRONIC COMPUTERS have been adapted to the field of infrared spectroscopy to determine the elements that are present in an unknown chemical mixture. Each chemical element will absorb certain wavelengths of radiation to a known relative amount and the chief use of spectroscopy is to determine the elements in an unknown mixture from an examination of its pattern of absorbtivity.

If several elements are present in the specimen and their absorption lines are confusingly mixed together and even fall on the same wavelengths in some instances, the problem of sorting out which lines belong to which element is one that can take many hours or even days to solve by manual methods.

In cooperation with the Sloan–Kettering Institute for Cancer Research, the ITT Laboratories, a division of International Telephone and Telegraph Corporation, has produced equipment for the spectroscopic analysis of steroid compounds using the infrared spectrum. The spectrum is broken into thousands of narrow bands and the relative absorbtivity at each band is recorded numerically on punched paper tape. The tape is then run through a special electronic computer that matches a prerecorded library of known spectrums to that of the unknown mixture to determine its chemical constituents and their concentrations. Only a few minutes is required for the complete analysis. The computer utilizes transistors and other advanced techniques such as plug-in printed circuits.

Direct-Voltage Instantaneous Breakdown of Oil-Impregnated Paper Capacitors as a Function of Area

By D. S. GIRLING

Standard Telephones and Cables Limited; London, England

THEORIES relating to the decrease of breakdown strength of dielectrics with increasing area are reviewed. The breakdown-voltage distribution of 2- and 3-layer capacitors of various areas and dielectric thicknesses are examined and it is shown that these are usually skewed towards lower values and may be double humped. The lower hump increases in importance with increasing area and is due to the coincidence of conducting particles in different layers.

It is shown that the variation of mean breakdown voltage with increasing area is represented adequately by Milnor's equation and that the breakdown voltage between spheres may be taken as the limiting value. Edge effect prevents such values from being approached with normal foil-type capacitors. The errors involved in the assumption of a normal distribution are assessed. The coefficient of variation appears to be independent of area but decreases with increasing thickness of dielectric. This information permits prediction of the voltage below which a given fraction of the sample will fail.

• • •

It has long been recognised that the breakdown voltage of thin sheets of dielectric decreases as the area increases. Small areas have breakdown voltages that are distributed around a relatively high value. Since failure of a larger area is due to the weakest of its constituent smaller areas, the breakdown voltages are distributed around lower values.

This electric strength variation is partly due to variations of the dielectric thickness and of the electric strength and partly to the inclusion of conducting or semiconducting particles generally arising from the tissue manufacturing, but sometimes also the capacitor winding process. Both these conditions result in electric stress variations from point to point in the capacitor area.

If the intrinsic electric strength of the material were uniform, failure in a uniform field would occur at the point of highest stress; that is to say, where the effective dielectric thickness is least. Thus, when failure is due to capacitor-tissue breakdown, the instantaneous breakdown voltage gives information about the minimum effective thickness. This may differ considerably from the nominal dielectric thickness. In connection with the rating of such dielectrics, a knowledge of this minimum effective thickness enables capacitors to be designed on a maximum-stress basis rather than on the nominal stress. It will be shown that on this basis, differing ratings are required for different dielectric areas or for different numbers of layers giving the same total thickness.

1. Summary of Theory

Although the reasons for the decrease in breakdown voltage with increasing area have been appreciated qualitatively for a long time, no completely satisfactory method of predicting breakdown voltage has been established. Milnor[1] and Holmes[4] produced equations based on the assumption that the breakdown distribution function of small areas was Gaussian. The work of Milnor was confirmed experimentally over a small range of areas by Bush and Moon[2].

Brooks[9] suggested that deviations from the true dielectric strength were due to conducting particles that reduced the effective dielectric thickness. After considering the mathematical probability of conducting-particle occurrence in relation to his experimental results, he showed that the conducting-particle sizes were distributed exponentially and that values greater than the paper thickness occurred. This resulted in the particle penetrating more than one layer of tissue. He concluded that it was not necessary to assume that coincidence between particles in the

[1] All footnote references will be found in the bibliography, section 5.

various layers occurs to cause such a condition and, further, it was possible for large conducting particles to become reoriented by such flexing of the sheet as occurs in winding.

In a further paper, Epstein and Brooks[10] applied the theory of extreme values to determine mathematically the effect of an exponential distribution of conducting-particle size on the average and on the distribution of breakdown voltage of capacitors of various areas.

Zingerman[12] gave a statistical theory and established an equation relating the breakdown-voltage distribution of large areas to that of a small area based on a generalised distribution of breakdowns of the small area. He pointed out that this distribution could not be Gaussian since his equations predicted that the breakdown distribution of larger areas would be asymmetrical. Since the small area itself could be regarded as a multiple of smaller areas, the small-area distribution must also be skewed.

If the probability that failure of a small area will occur at a voltage between x and $x + \delta x$ is $f(x)$, then the probability that a sample will break down at a voltage equal to or smaller than x is

$$F(x) = \int_{-\infty}^{x} f(x)\,dx. \qquad (1)$$

It therefore follows that the probability that n such areas will withstand a voltage x is

$$F_n'(x) = [1 - F(x)]^n. \qquad (2)$$

The breakdown voltage distribution is then

$$f_n(x) = dF_n'(x)/dx. \qquad (3)$$

and the mean breakdown voltage

$$\bar{x}_n = \int_{0}^{\infty} F_n(x)\,dx. \qquad (4)$$

1.1 Effect of Conducting Particles

In the experimental results described in the following paragraphs, observations were made over a large range of areas and it was clear from the histograms that the particle-coincidence effect must be considered. The conclusions of Brooks[9] are thought to be due to the assumption that all deviations from the nominal tissue strength were attributable to conducting particles.

The effect of conducting particles embedded in the tissue and penetrating it completely will be to produce a coincidence effect so that a capacitor can be short-circuited if particles in all layers are coincident or partially coincident. In the practical case, the sizes of the conducting particles will be distributed so that the breakdown-voltage distribution of a small area consisting of n tissue layers will consist of a series of distribution functions corresponding to 0, 1, 2 $\cdots$ n coincident conducting particles. The distribution functions will have to take account of :—

A. The inherent variability of the electric strength of the dielectric material (including the effects of density and inhomogeneities other than conducting particles, et cetera).

B. The distribution of dielectric thickness.

C. The distribution of conducting-particle size in the direction normal to the paper.

D. The relation between thickness and breakdown voltage.

In voltage breakdown tests on very-small areas, the probability of conducting-particle occurrence will be so small that tests may not reveal any deviation from a single distribution. Combining small areas to form larger ones increases the probability of the occurrence of lower breakdown values, so that even in the absence of conducting particles, a decrease in electric strength would be observed. The lesser probabilities of failure, however, increase in proportion to the area ratio, so that the breakdown histogram becomes increasingly skewed towards lower values and may exhibit two maxima—the so called double-humped distribution. For normal tissue areas, the frequency of conducting-particle occurrence is such that there will be one somewhere in every layer so that the predominant distribution function will be that corresponding to 1 conducting particle. For larger areas, the occurrence of 2 coincident conducting particles in different layers may give rise to a lower hump. If the area were increased still further, or if the frequency of conducting-particle occurrence were

sufficiently high, the lower hump would become predominant and eventually a further lower hump due to 3 particles would become apparent.

2. *Experimental Results*

The work that is described in the following paragraphs was undertaken originally to ascertain empirically the variation of electric strength with area of a British-made rag-based tissue impregnated with mineral oil. The tests were carried out on groups of units varying from 50 to 500. The units were, in general, tubular for capacitances up to 0·1 microfarad and above that were of the flattened and clamped construction. The smaller tubular units and all the flattened units had tinned copper connecting tapes. The flashover gap at the edges normally varied from $\frac{1}{8}$ to $\frac{1}{4}$ inch (3·2 to 6·4 millimetres) according to the dielectric thickness. The paper width was normally in the range of 1 to 3 inches (2·5 to 7·6 centimetres) and was determined by the availability of supplies. This policy was adopted since it enabled the use of standard units and also because it was desired to obtain information on the units most commonly employed.

The units were impregnated in a mineral oil using a standard vacuum impregnation cycle; after impregnation they were cooled and stored under oil. Testing was carried out as soon as possible after impregnation to avoid any deterioration due to absorption of gas or moisture by the oil. Breakdown testing was carried out under oil. The following tests were made.

A. Quality-control check on capacitance, power factor, and insulance to ensure that impregnation was satisfactory.

B. Instantaneous-breakdown voltage measurement as described below.

C. Examination to eliminate failures due to faulty manufacture (torn papers, et cetera) to determine the nature of and position of failure and to check winding length. If, on examination, failure was proved to be due to faulty winding or mechanical damage to the paper, the observation was excluded.

In calculating the results of the tests described in these paragraphs, all valid observations were included.

In the course of this work it became apparent that the results obtained were consistent with one another and were forming a pattern that agreed qualitatively with the theory already given. The tests using sphere gaps were carried out to determine the limiting value for very-small areas.

2.1 Apparatus

The apparatus for measurement of breakdown voltage was a normal half-wave rectifier set; its input could be controlled by an adjustable-voltage transformer. The output was limited by a 1-megohm resistor. Indication of the breakdown voltage was obtained from an electrostatic voltmeter and the rate of increasing voltage was such that failure occurred in 5 to 10 seconds. Since observations were made on a rising voltage, each observation was liable to some error. It has not been possible to evaluate this, but it is clear that such an error will be nonsystematic and will limit the minimum standard deviation that can be observed.

2.2 Tests for Conducting Particles

Analysis of the results of tests for conducting particles, using the roller method described in British Standard Specification *698* of 1936, shows that the number of particles that completely penetrate the paper decreases rapidly with increasing thickness. This test cannot be regarded as absolute since it depends on the flatness of the plate and the uniformity of the roller; great care must be taken to eliminate dust. An assessment of the effectiveness of the apparatus can be made by carefully testing a piece of paper by making several runs with it and marking all detectable conducting particles. It has been found that in one run at least 60 per cent of all detectable conducting particles is indicated. The number of such conducting particles as a function of thickness is shown in Figure 1.

2.3 Sphere-Gap Tests

To measure the instantaneous-breakdown stress of the smallest practicable area, a series of tests was carried out using a test cell made to British Standard Specification *148* of 1951.

The test results are shown in Figure 2 on which the breakdown stress in volts per micron for 50 tests are plotted as a function of total thickness.

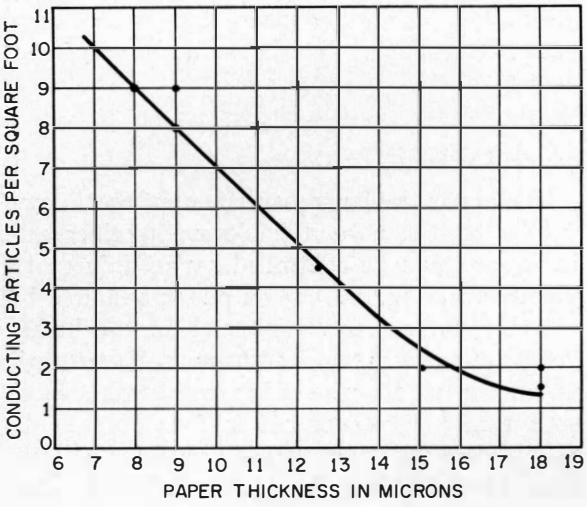

Figure 1—Number of conducting particle per square foot as a function of thickness for rag-based tissue. (1 square foot = 0·093 square metre.) Each point represents the average of 24 1-by-12-inch (2·54-by-30·48-centimetre) samples. Measured in accordance with British Standard Specification *698*.

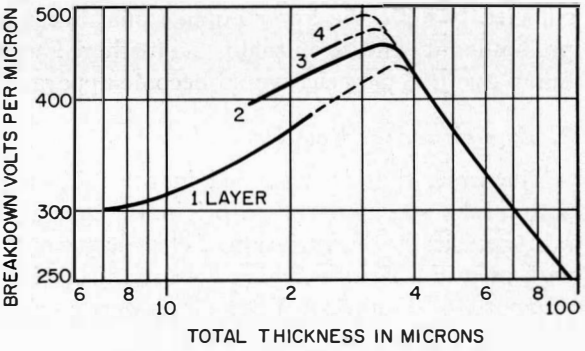

Figure 2—Instantaneous direct-current breakdown voltage of rag-based tissue impregnated with mineral oil. Test was between 0·5-inch (1·25-centimetre) spheres at 20 degrees centigrade.

Depending on the number of layers, increasing thickness of tissue results in increasing strength up to a certain critical value. Increasing the number of layers also results in increased strength. Above the critical value this stress decreases again and, as far as can be seen, is independent of the number of layers. The dependence of breakdown stress on the number of layers has also been observed by Hopkins, Walters, and Scoville[14]. Since the breakdown stress is a function of the number of papers below the critical value, and not above, it is considered that below this value failure is inititated by the paper and above it by the oil. Examination of the failure distribution shows that as far as can be judged on groups of 50 results, they follow a Gaussian law.

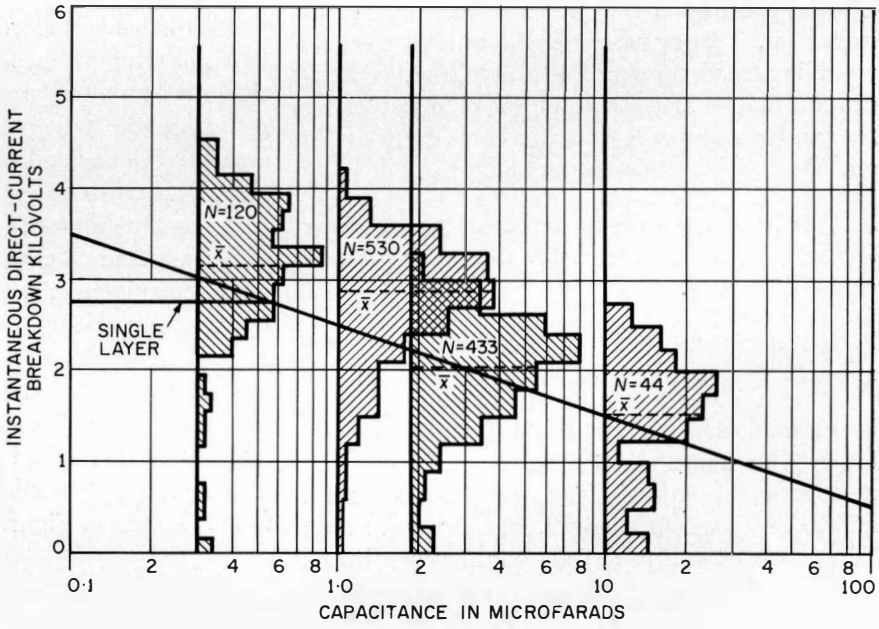

Figure 3—Instantaneous direct-current-breakdown-voltage histograms as a function of capacitance (area). Four values of capacitance, 0·3, 1, 2, and 10 microfarads, were examined. All had 2 layers of 9-micron rag-based tissue impregnated with mineral oil. N = number of capacitors represented in each histogram.

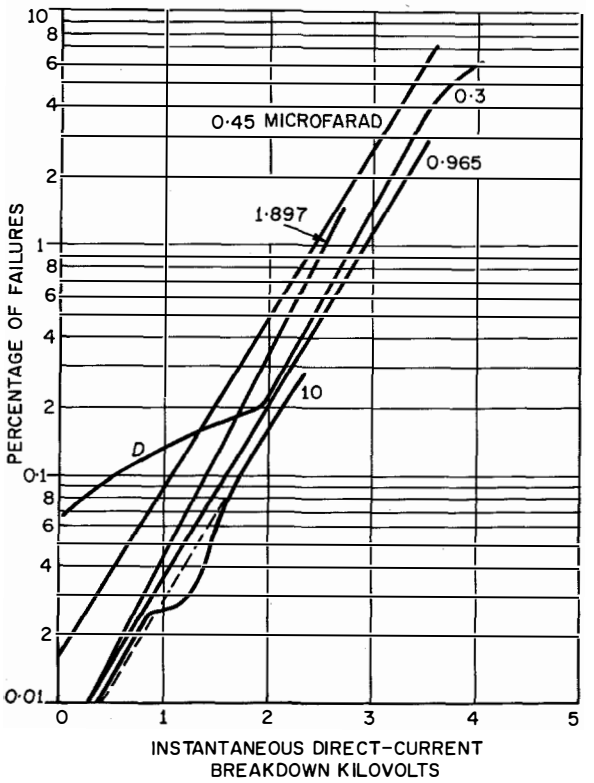

Figure 4—Breakdown voltage of capacitors consisting of 2 layer of 9-micron rag-based tissue impregnated with mineral oil, referred to 0·01 microfarad. The portion of the 0·3-microfarad-capacitor curve marked *D* is a deviation caused by other types of failure; these were the only completely assembled capacitors in these tests.

2.4 Tests on Wound Units

2.4.1 Breakdown Histograms

2.4.1.1 Double-Layer Capacitors

The test results on units wound with 2 layers of 9-micron tissues are shown in Figure 3. This is drawn as a plot of instantaneous-breakdown voltage against capacitance; superimposed on the plots are histograms showing the failure distribution. Two of these are based on 433 and 530 units and it can be seen that these present a smooth and slightly skewed appearance. These 4 distributions demonstrate fairly clearly the points suggested by the theory.

The 1-microfarad-capacitor results show a slight skewness towards lower breakdown voltage values. The increase to 2 microfarads shows a similiar distribution about a rather lower value and a marked increase in the failures in the lowest cell. This trend continues still further with the increase to 10 microfarads. The strength of a single-layer 9-micron tissue can be obtained from Figure 2 as 2·75 kilovolts. Since in the 0·2-microfarad capacitor there will be on the average about 4 conducting particles in each layer of paper, it may be assumed that in most capacitors, only one layer will be effective. The probability of two coincident conducting particles is still too small to be noticeable.

Figure 4 shows the failure distribution for 0·01-microfarad capacitors calculated from the above results using (2). If the breakdown voltage were a function of area only, then all these curves would coincide. It is quite clear that they tend to do so but the extreme cases show a discrepancy by a factor of 3 in the failure percentage. It is interesting to note that what appeared as a double hump in the 10-microfarad-capacitor experiment does not appear to be so by comparison with the other curves. The divergence of the results for the 0·3-microfarad capacitor (the only complete capacitor tested) at the lower voltages clearly demonstrates the existence of faults resulting from causes other than dielectric failures. Figure 5 shows the percentage of failures

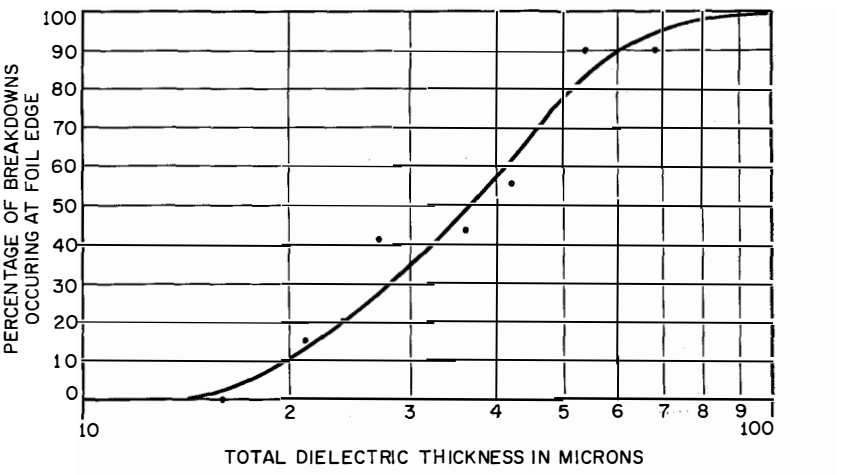

Figure 5—Relation between percentage of failure occurring at foil edge and total dielectric thickness. Plotted points are average values.

that occurred at the paper edge in tests on capacitors of various dielectric thicknesses and demonstrates the increasing importance of edge effect with increasing thickness.

2.4.1.2 Triple-Layer Capacitors

A set of results similar to Figure 3 is shown in Figure 6 for the case of 3 layers of 8-micron tissue. These are shown over a wider area range. The

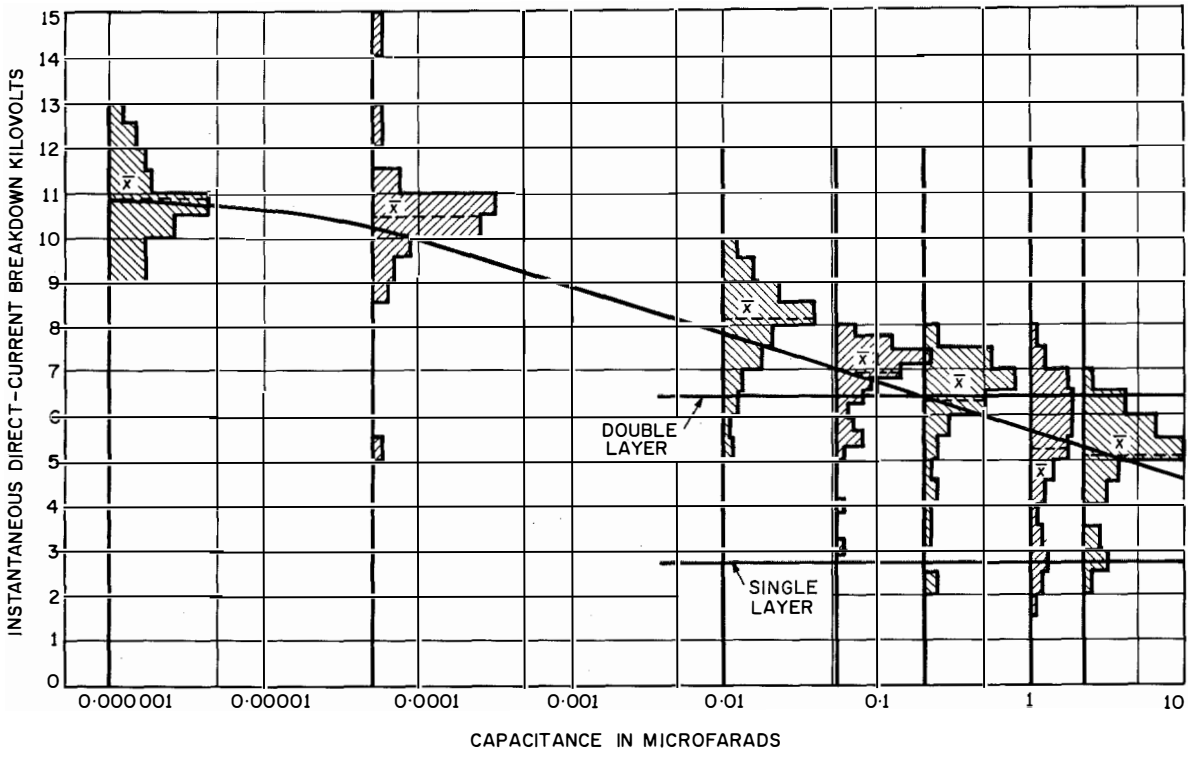

Figure 6—Instantaneous-breakdown-voltage histograms as a function of capacitance (area). Values of capacitance tested were 0·000 001 (sphere gap), 0·0001, 0·01, 0·05, 0·2, 1, and 3 microfarads. All had 3 layers of 8-micron rag-based tissue impregnated with mineral oil. Each histogram is based on 100 results.

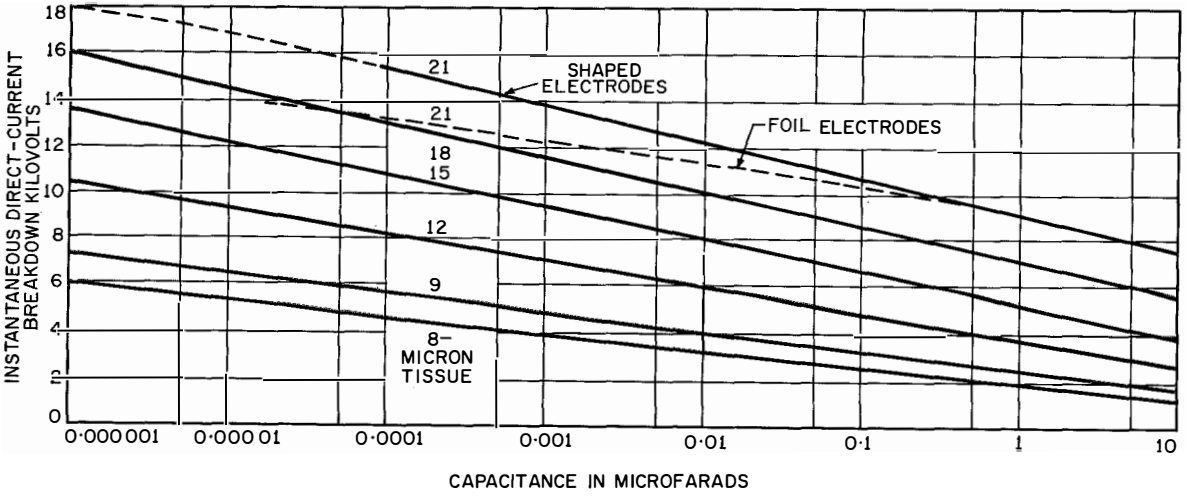

Figure 8—Breakdown voltage versus capacitance for 2 layers of rag-based tissue impregnated with mineral oil at 20 degrees centigrade.

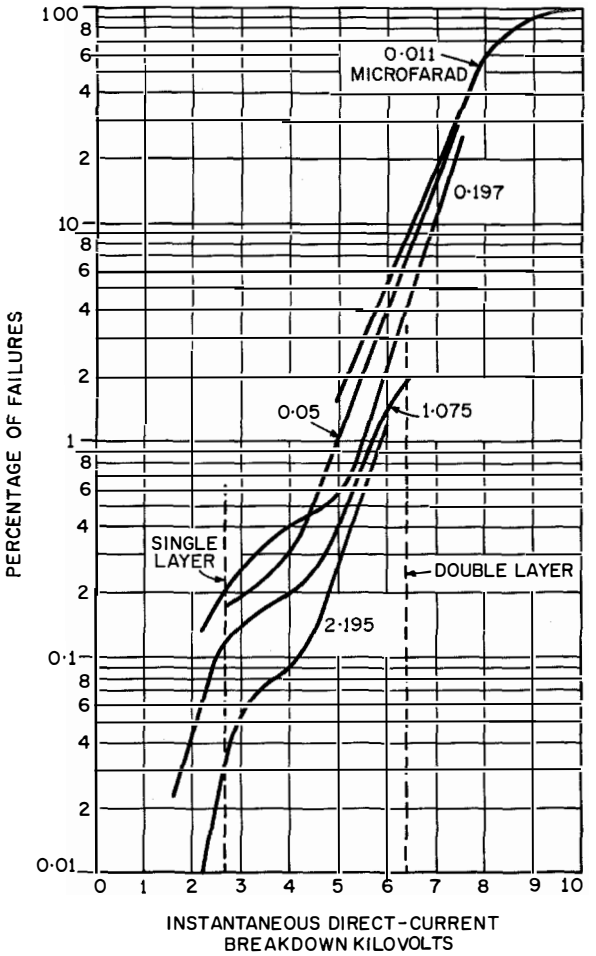

Figure 7—Breakdown voltage of capacitors consisting of 3 layers of 8-micron rag-based tissue impregnated with mineral oil, referred to 0·01 microfarad.

point plotted at 0·000 001 microfarad is for the sphere-gap test. Once again the trend is downward as the area increases. For the sphere-gap tests, no failures occurred outside the main distribution, but as the area increased there was an increasing number of such failures. The failure distribution for the 1-microfarad capacitor is one of the few clearly double-humped distributions that have been observed. It will be noted that the lower hump is centered on the strength of a single layer of tissue as determined by the sphere-gap tests.

Figure 7 shows the cumulative failure distribution for these results when referred to a 0·01-microfarad capacitance by use of (2). As for the 2-layer case, the curves should coincide if breakdown voltage is a function only of area. A second hump is apparent in all tests except that in which failures were concentrated in the upper hump. The lower hump clearly corresponds to the failure of a single layer of tissue. At 0·01 microfarad, about 0·1 per cent of the sample has one effective paper.

2.4.2 Correlation of Results

2.4.2.1 Average Values

The results of a large number of tests on different areas and different tissue thicknesses are shown in Figures 8 and 9 for the 2- and 3-layer cases, respectively. The points plotted on these graphs are the average values of at least 50 results. The test results using sphere gaps have

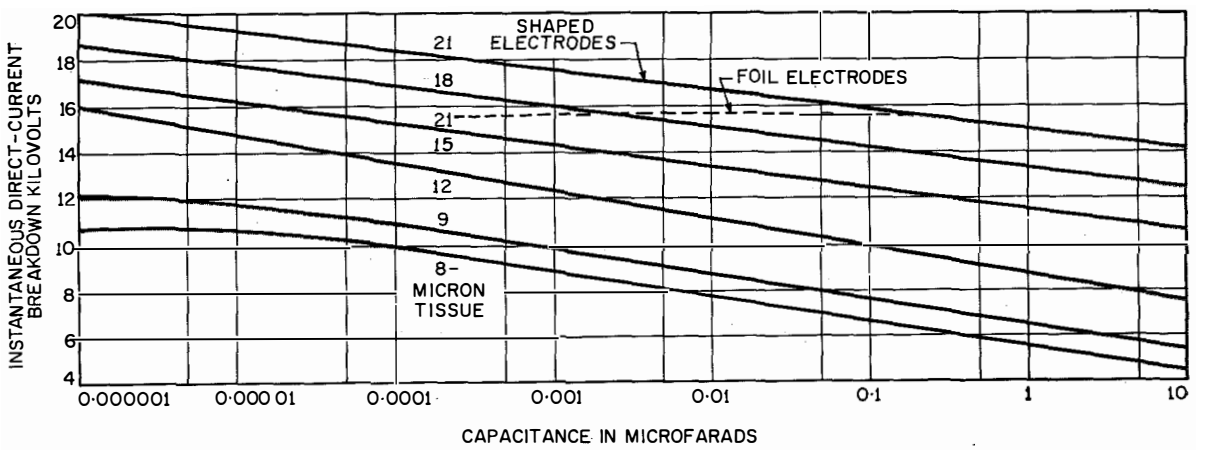

Figure 9—Breakdown voltage versus capacitance for 3 layers of rag-based tissue impregnated with mineral oil at 20 degrees centigrade.

been assumed to be the small-area limiting values and these are plotted at a 0·000 001-microfarad capacitance. A family of lines has been constructed using horizontal and vertical interpolation and, although the two sets of lines were independent of area. Tests on 21-micron tissue show that with foil electrodes, there is a marked limiting value due to stress at the edge. Tests with shaped electrodes gave only slightly higher values and did not reach the line interpolating

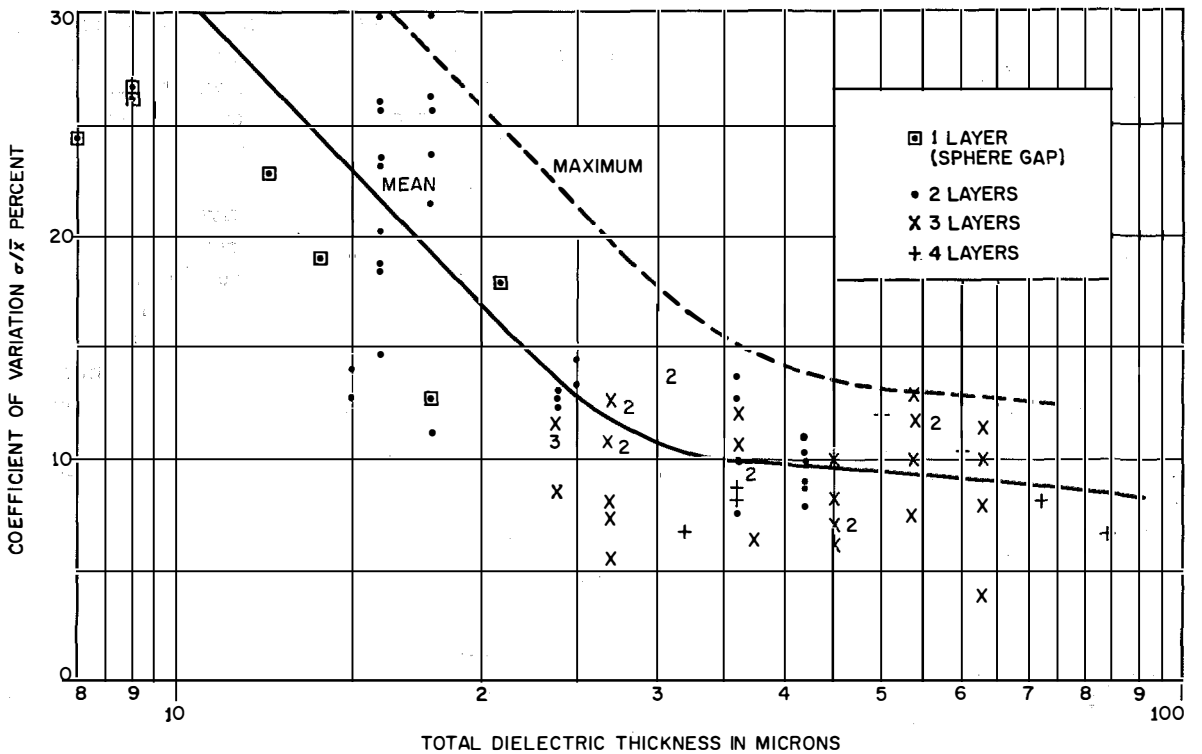

Figure 10—Coefficient of breakdown-voltage variation versus dielectric thickness of various areas of rag-based tissue impregnated with mineral oil. Points plotted are each the results of tests on 50 to 100 units.

obtained separately, it can be seen that their slopes are very similar and for the most part are parallel. For the 2-layer case with thicknesses below 12 microns, there appears a slight tendency for the lines to converge as area increases.

In the case of 2 layers of 21-micron tissue using foil electrodes, the curve tends to flatten for decreasing area and does not approach the sphere-gap limiting value. In such tests 90 per cent of the failures occurred at the edge and it was apparent that the stress at this point was the limiting factor. Tests using shaped electrodes reduced this value to about 60 per cent and resulted in a higher average value.

In the 3-layer case, it is not possible to draw a straight line covering the whole capacitance range for the thinner thicknesses and therefore the small-area breakdown strength appears to be between sphere-gap measurements and those made on large areas.

The graphs are drawn on a log-linear scale and hence the law obeyed is

$$E = A - B \log C, \qquad (4)$$

where A and B are constants. This is in the form of Milnor's equation.

2.4.2.2 Coefficient of Variation

Examination of the coefficient of variation calculated in the experiments described previously shows that, although there was some variation from one batch to the next, this was not related to increasing area. The most-reasonable assumption is that this value is independent of area. A scatter diagram of the results is shown

ı Figure 10, in which the variation coefficient is lotted against total dielectric thickness. As the hickness increases, it tends towards a value of bout 10 per cent. This value will include some xperimental error.

.4.2.3 *Skewness*

It is apparent that while the theoretical failure-requency distribution consists of a number of uperimposed distributions, each of which may ır may not be skewed, tests on small numbers of amples will reveal only a skewed distribution ather than a double hump. The result is that nore failures occur at low voltages than would ɔe expected from a knowledge of $\bar{x}$ and σ. The ɔercentages of failures that occurred at $(\bar{x} - 1{\cdot}65\,\sigma)$, $(\bar{x} - 1{\cdot}3\,\sigma)$ and $\bar{x}$ corresponding o 5, 10, and 50 per cent respectively are plotted n Figure 11, which shows that for the thinnest lielectrics the actual failures at a voltage that hould give 5-per-cent failures may, in fact, be as nuch as 12 per cent. The error is less for predic-ion of larger failure percentages and for the hicker dielectrics and becomes less as the dis-ribution skewness decreases. This information

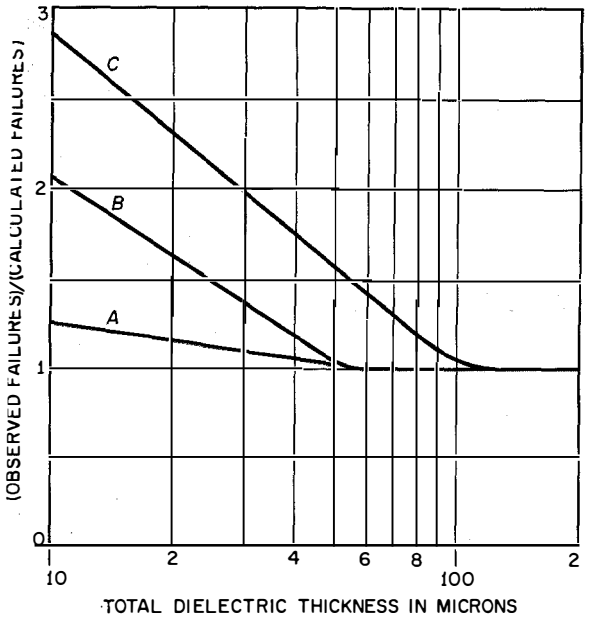

Figure 11—Calculated and measured failure rates versus dielectric thickness, plotted from averages of measurements on various areas. Curve *A* is the ratio for $\bar{x}$ (50-per-cent failure), *B* is for $\bar{x} - 1{\cdot}3\sigma$ (10-per-cent failure), and *C* is for $\bar{x} - 1{\cdot}650\sigma$ (5-per-cent failure).

can be used for rejection-rate predictions on voltage proof test.

3. *Conclusions*

A. In tests on capacitor tissues placed between 0·5-inch (12·7-millimetre) spheres, the breakdown stress increases with tissue thickness up to a certain critical value, above which it decreases. Below this value, increased strength is obtained for any one total thickness by increasing the number of tissues. Above it, the strength appears independent of the number of tissues and it is possible that this is due to the oil.

B. Mean-breakdown-voltage variation of 2-layer capacitors with area is represented adequately by Milnor's equation and sphere test results appear to be the limiting values on the assumption that they correspond to a capacitance of 0·000 001 microfarad. Deviation from this law results from edge-effect, which becomes increasingly important as thickness increases. This prevents the limiting values observed from sphere tests from being achieved with foil-type capacitors.

C. The mean breakdown voltage of 3-layer capacitors follows a similar law although the thinner tissues depart from the law, probably due to the alignment effect between conducting particles embedded in the tissues, causing breakdown distributions to become double-humped. Owing to the increased dielectric thickness, the edge effect is much-more important. As pointed out by Zingerman[12], this is a function of the edge length and not of area. The geometry of the unit must therefore be considered.

D. Breakdown-voltage comparison of 2- and 3-layer 1-microfarad capacitors of 24-micron total dielectric thickness shows that the 3-layer capacitors have a strength 50 percent greater than the 2-layer.

E. Although the coefficient of variation is itself quite variable, it appears to be independent of area and decreases with increasing thickness. The failure distribution is not normal, except possibly for the sphere tests, and the distributions are skewed towards lower values. The assumption of a normal distribution is, however, a useful one

and the errors involved have been established empirically. By this method, the fraction of a sample that will fail below a certain voltage can be predicted.

F. Prediction of the large-area breakdown-voltage distribution from tests on small areas over large ranges is liable to error unless a very-large number of samples is used; in which case it is simpler and just as economical to test the larger areas. The construction of the graphs shown permits a ready estimate of the mean breakdown voltage and coefficient of variation of any intermediate area. Owing to the coincidence effect of conducting particles, extrapolation should not be carried out over large ranges.

4. Acknowledgments

The author records his appreciation of the advice and encouragement given by Mr. R. M. Barnard, without which this paper would not have been possible, and the assistance of Messrs. W. E. R. Evans, A. Simmons, and R. S. W. Walker.

5. Bibliography

1. F. M. Farmer, "The Dielectric Strength of Thin Insulating Materials," *Transactions of the American Institute of Electrical Engineers*, volume 32, part II, pages 2097–2131; 1913: Discussion by Milnor on pages 2128–2129.
2. V. Bush and P. H. Moon, "A Precision Measurement of Puncture Voltage," *Transactions of the American Institute of Electrical Engineers*, volume 46, pages 1025–1038; 1931.
3. A. Russell, "The Electrostatic Problem of Two Conducting Spheres," *Journal of the Institute of Electrical Engineers*, volume 65, pages 517–535; 1927.
4 M. C. Holmes, "Insulation Variability—Its Influence in Determining Breakdown Voltages," *Transactions of the American Institute of Electrical Engineers*, volume 50, pages 1441–1460; December 1931.
5. S. Whitehead, "Dielectric Phenomena—III Breakdown of Solid Dielectrics," Ernest Benn Limited, London; 1932.
6. A. I. Goldstein, "A Formula for the Dependence of the Breakdown Voltage on the Electrode Area and on the Inhomogeneity of a Dielectric in a Uniform Electric Field," *Zhutnal Tekhnicheskoy Fiziki*, volume 4, number 2, pages 292–298; 1934.
7. British Standard Specification *698*, "Paper, Unvarnished, for Electrical Purposes;" 1936.
8. G. U. Yule and M. G. Kendall, "An Introduction to the Theory of Statistics," Charles Griffin and Company, Limited London; 1937.
9. H. Brooks, "The Probable Breakdown Value of Paper Dielectric Capacitors," *Transactions of the American Institute of Electrical Engineers*, volume 66, pages 1137–1145; 1947.
10. B. Epstein and H. Brooks, "The Theory of Extreme Values and its Implications in the Study of the Dielectric Strength of Paper Capacitors," *Journal of Applied Physics*, volume 19, pages 544–550; June 1948.
11. L. R. Hill and P. L. Schmidt, "Insulation Breakdown as a Function of Area," *Transactions of the American Institute of Electrical Engineers*, volume 67, part I, pages 442–446; 1948.
12. A. S. Zingerman, "A Statistical Method for Determining the Breakdown Voltage of a Dielectric," *Zhutnal Tekhnicheskoy Fiziki*, volume 18, pages 1029–1043; 1948.
13. S. Whitehead, "Dielectric Breakdown of Solids," Oxford University Press, London; 1951.
14. R. J. Hopkins, T. R. Walters, and M. E. Scoville, "Development of Corona Measurements and their Relation to the Dielectric Strength of Capacitors," *Transactions of the American Institute of Electrical Engineers*, volume 70, Part II, pages 1643–1651; 1951.

Characteristics and Applications of the Iatron Storage Tube*

By DEAN W. DAVIS

Farnsworth Electronics Company, a division of International Telephone and Telegraph Corporation; Fort Wayne, Indiana

THE OPERATION of many types of storage tubes depends on intensity modulation of an electron beam by an electrostatic charge on an insulator layer.[3–7] As early as 1927, Dr. P. T. Farnsworth suggested the method as a means of increasing brightness in cathode-ray tubes for television.

Iatron® storage tubes have been under development since 1949 and have been in experimental use since 1953. The properties of image storage and extremely high brightness at low voltage make the tube very attractive for radar indicators, oscilloscopes, and other uses.

This paper describes Iatron operation with emphasis on those unusual characteristics that have no counterpart in ordinary cathode-ray tubes and suggests modifications of an oscilloscope to use the tube. It is hoped that the applications engineer will find the answers to some of the questions that may arise when operating this storage tube for the first time.

1. Description

The Iatron is a storage cathode-ray tube in which the display can be written, stored, and viewed continuously. While it is available in a variety of bulb sizes and types of writing guns, the characteristics presented here are particularly applicable to the 5-inch (127-millimeter) *Ia10P20-25* tube, shown in Figure 1, which has an electrostatic writing gun. Continuous viewing

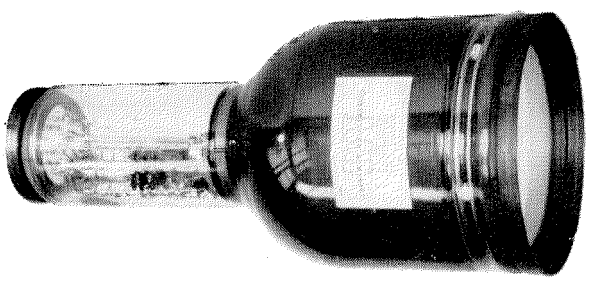

Figure 1—The 5-inch (127-millimeter) electrostatic-deflection Iatron *Ia10P20-25*.

is provided by a divergent electron beam, called the flooding beam, which expands until it covers the entire display area of the tube. Elemental areas of the large flooding beam are modulated by a conventional cathode-ray beam.

The following explanation of the method of modulating the flooding beam refers to Figure 2. The flooding gun is located on the tube axis at the juncture of the neck and bulb. The control grid of the flooding beam is an insulating layer that covers the gun-facing side of a fine-mesh metallic screen. This insulator-screen is located in the path of the beam at the distance where the beam has expanded to its maximum size. The beam passes through the metallic screen and impinges on the aluminized phosphor on the inner face of the tube. An aquadag coating on the wall of the bulb and a metallic collector screen serve to collimate the flooding beam. With proper collimation, the paths of the electrons in the expanded flooding beam are made parallel to each other and perpendicular to the plane of the insulator-screen.

The metallic screen that supports the insulator layer serves the same purpose as the screen grid of a tetrode and is operated on a fixed voltage

* Reprinted from *Communication and Electronics*, number 29, pages 47–53; March, 1957. Iatron is a registered trademark of Farnsworth Electronics Company. Dr. P. T. Farnsworth has made many notable contributions to the storage-tube art[1,2] and has personally directed the Iatron research and development work undertaken in 1949. Others who have contributed to the development of the Iatron include a majority of the Farnsworth research department. Current Iatron development has been supported primarily by the United States Navy Bureau of Ships.

[1] M. Knoll and B. Kazan, "Storage Tubes and Their Basic Principles," John Wiley & Sons, Incorporated, New York, New York, 1952.

[2] M. Knoll, H. O. Hook, and R. P. Stone, "Characteristics of a Transmission Control Viewing Storage Tube with Halftone Display," *Proceedings of the IRE*, volume 42, pages 1496–1504; October, 1954.

[3] S. T. Smith and H. E. Brown, "Direct Viewing Memory Tube," *Proceedings of the IRE*, volume 41, pages 1167–1171; September, 1953.

[4] R. C. Hergenrother and B. C. Gardner, "The Recording Storage Tube," *Proceedings of the IRE*, volume 39, pages 740–747; July, 1950.

[5] A. V. Haeff, "Memory Tube," *Electronics*, volume 20, pages 80–83; September, 1957.

[6] United States Patent 2 228 338.

[7] United States Patent 2 754 449.

of about +10 volts. Points on the insulating surface, however, can assume potentials that are quite different from each other and from the voltage on the metallic screen. These potentials fade to cutoff. Without them, the entire display area would eventually increase to maximum brightness. The increase in brightness results when positive ions, which are generated by colli-

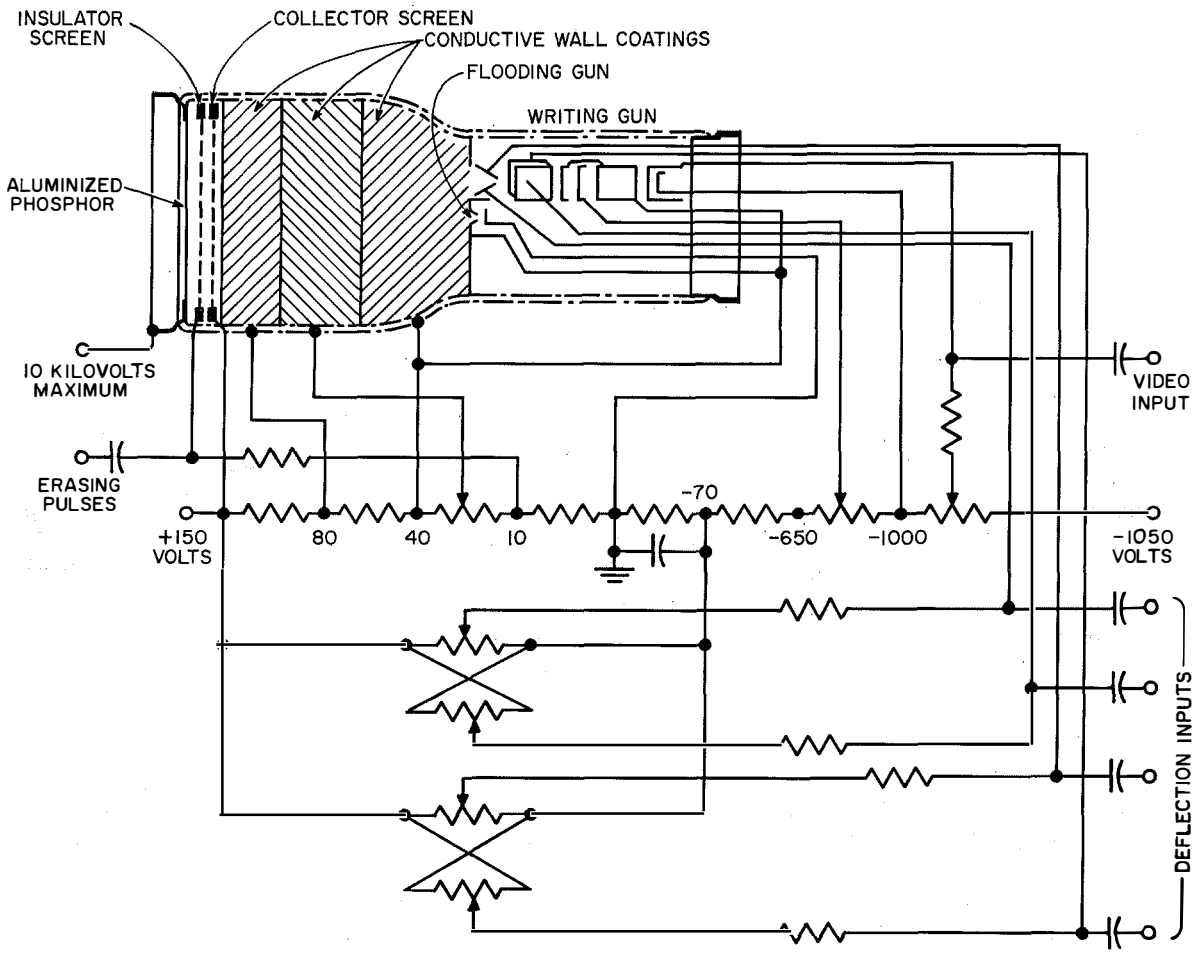

Figure 2—Diagram of Iatron model *Ia10P20-25* and associated circuits.

are established on the insulating surface by charging it with the writing beam and the flooding beam. Over the insulator control range, the number of flooding electrons that can pass through the screen at any point is roughly proportional to the potential at that point of the insulating surface.

1.1 Erasing

Erasing pulses are essential to the operation of the Iatron. These are low-voltage pulses applied to the insulator-screen that cause the display to

sion between flooding electrons and residual gas molecules, are drawn to the insulator surface, charging it positively. The ion density over the insulator surface is uniform and therefore the display area brightens everywhere at the same rate.

Further increase of insulator potential ceases when the insulator has become charged to about +2 volts with respect to the flooding-gun cathode. At this potential, some flooding electrons have enough energy to strike the insulator. Striking with low energy, these electrons adhere and, by virtue of their negative charge, prevent addi-

tional voltage increase. An equilibrium insulator potential is thereby established at which the positive ions are balanced by the electrons landing on the insulator.

When the insulator suddenly becomes more positive, as by applying a voltage pulse to the support screen, flooding current strikes the insulator, quickly charging the surface down to equilibrium again. At the end of the pulse, the support screen is returned to its original potential, but the insulator is now more negative than it was before because of the charge acquired during the pulse. Positive insulator charges written by the writing beam are erased in the same way.

1.2 Insulator Control Characteristic

Figure 3 is a curve showing average phosphor flooding current over the display area as a function of insulator surface potential. The points on the curve were obtained, using a +10-volt bias on the support screen, by first allowing ions to charge the entire insulator surface to equilibrium. At equilibrium, the insulator is charged to its most positive potential and phosphor current is a maximum. This current corresponds to zero insulator volts on the curve. The insulator surface was then charged 0.5-volt negatively by applying a +0.5-volt pulse to the insulator support screen. The phosphor current was measured at the end of the pulse and the process was repeated, increasing the amplitude of the pulse at each step until phosphor current reached cutoff. Thus it was determined that pulses of 3.2-volt amplitude are necessary to erase the tube to cutoff. The assumptions were made that the insulator surface is at zero volts at equilibrium and that the insulator is charged negatively to the amplitude of the erase pulse at each step. Although, as a matter of academic interest, the insulator surface potential at equilibrium was actually about 2 volts, the first assumption is valid in the sense that the insulator does not draw flooding current over the control range from equilibrium to cutoff.

1.3 Control of Viewing Time

It is clear that the insulator cannot be charged to a potential more negative than the absolute amplitude of the erasing pulse, because it charges to an equilibrium potential that is reached when the voltage difference between the flooding-gun cathode and insulator is just sufficient for flooding electrons to strike the insulator. But it can be prevented from charging to this equilibrium if the pulse duration is shorter than the charging

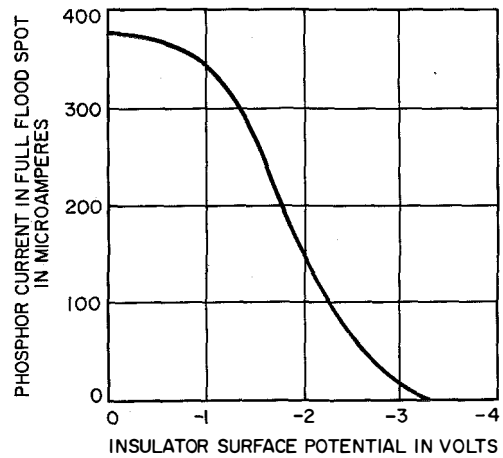

Figure 3—Static insulator control characteristic.

time required. The erasing pulses used to obtain the curve of Figure 3 were applied for a sufficient length of time to charge the insulator to equilibrium.

The average time required to charge the insulator from maximum brightness to cutoff is about 3 milliseconds and a display can be made to persist for many seconds if pulses that are narrower than 3 milliseconds are applied continuously at a suitable repetition rate. On each successive pulse, the insulator will be charged negatively a small amount and will eventually reach cutoff when the product of pulse width times the number of consecutive pulses is equal to 3 milliseconds.

Pulses having a repetition frequency of f pulses per second, which are t seconds wide and 3.2 volts in amplitude, will therefore erase signals from maximum brightness to cutoff in the approximate time $T=0.003/ft$ second, for large values of f. (The erasing-pulse amplitude required to erase to cutoff is increased slightly if the erasing-pulse frequency is reduced to very-low values, since the insulator voltage shift by ions during the interval between pulses then becomes significant.) Hence, the viewing time of the display can be varied by controlling either the frequency or the width of the erasing pulses. The proper choice

of pulse repetition frequency is influenced by flicker and contrast as well as by viewing time.

1.3.1 Flicker

During an erasing pulse, the entire display area is illuminated by flooding current which passes through the insulator screen (see Figures 5 through 7). The resulting flashes of light produce flicker at low pulse frequencies, or merge to a constant background brightness at a pulse frequency of about 45 pulses per second. However, very-narrow pulses such as would be used to obtain a viewing time of the order of 1.0 minute are hardly detectable in the display even in the flicker-frequency range.

1.3.2 Contrast

Loss of contrast is caused by background brightness. The average background contributed by erasing pulses is $B = 0.003/100T = 100\,ft$ percent of maximum display brightness.

Loss of contrast would be most severe using the erasing conditions required for minimum viewing time. However, this is an unrealistic condition for the Iatron as it defeats the very purpose of storage tubes. Nevertheless, it is interesting to estimate the maximum background brightness that might be encountered.

Since the minimum erasing time is 3 milliseconds and the repetition rate over which persistence is limited by the eyes of the observer is 45 pulses per second, these values may be taken as the pulse width and frequency that will determine minimum viewing time. Under these conditions, the display area would be viewed at maximum brightness $45 \times 0.003 = 0.135$ second per second of total viewing time. The average background brightness would, therefore, be about 13.5 percent of the maximum signal brightness.

However, by the same reasoning, B would be only 0.3 percent for a viewing time of 1.0 second. At 45 pulses per second, the pulse width for this condition would be about 67 microseconds.

1.4 Maximum Viewing Time

Viewing time can be limited by positive ions or by insulator leakage. Leakage is negligible at normal tube operating temperatures and most Iatrons will store written charges for several hours if all tube voltages are removed after writing, to avoid generation of ions.

The number of ions generated is a function of several things such as flooding-current density, length of the electron paths, pressure of residual gases in the tube, et cetera. The time required in an average tube for ions to charge the insulator from cutoff to 50 percent of maximum brightness is about 30 seconds. The measurement is significant in that there must be a minimum product of erasing frequency and pulse width, ft, which will prevent ion charge integration on the insulator and thereby maintain nearly constant insulator potential in the interval between pulses.

Figure 4 shows curves of phosphor current versus time for a typical tube using small values

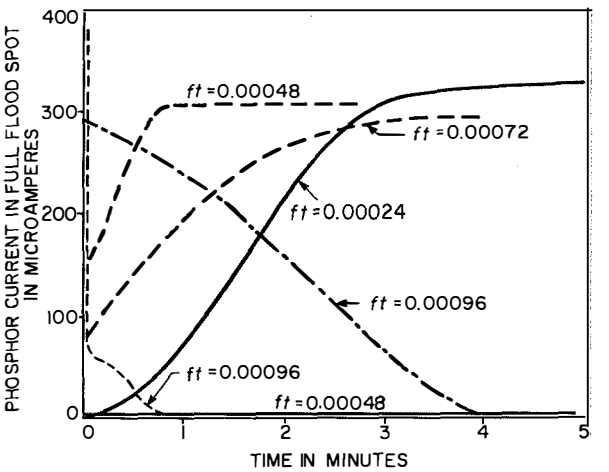

Figure 4—Change of phosphor current caused by positive ions and erasing pulses. Initial conditions: Solid line—phosphor current initially cut off. Dashed line—phosphor current initially maximum. Dash-dot line—phosphor current initially 330 microamperes. Parameters: Erase pulse width t seconds. Erase pulse frequency $f = 60$ pulses per second.

of ft. The ordinate is proportional to brightness since the flooding-spot size is constant and the power input to the phosphor is well below the level at which saturation occurs. For the condition that the insulator is initially at cutoff, an erasing product $ft = 0.000\,48$ maintains cutoff. If the insulator is initially at equilibrium (phosphor current initially maximum), however, an erasing product $ft = 0.000\,48$ will not erase the tube but will allow the insulator to charge to an intermediate potential corresponding to 310 microamperes of phosphor current. Thus it is found

that two stable potentials, one corresponding to cutoff and the other corresponding to 310 microamperes of phosphor current, are possible. They are maintained in each case because the insulator charge received from the flooding electrons during one erasing pulse is equal to the ion charge acquired during the interval between pulses.

A necessary condition for continuous operation is that signals written by the writing beam to any brightness will eventually be erased to cutoff. Lacking sufficient erasure, the display area would soon be saturated. As shown in Figure 4, if a minimum erasing product $ft = 0.000\,96$ is used, a signal that has been written to maximum brightness will assuredly be erased.

Two curves are shown for which $ft = 0.000\,96$. In the first, the pulse was not applied until the insulator had been charged to equilibrium and allowed to remain there for a considerable length of time. By suddenly applying the pulses, phosphor current drops sharply and the tube erases to cutoff. In the second curve, erasing pulses were not applied suddenly but were present continually while the tube was written to the initial phosphor current of 330 microamperes. This curve is typical of viewing-time curves obtained with continuously operating erasing pulses, the viewing time being less for larger values of ft.

The cause of the rapid decrease in brightness that is observed when an erasing pulse is suddenly applied, under the initial condition that the phosphor current is a maximum, is not fully understood. However, it is probable that the distribution of charges on the insulator on the front surface as well as on the sides of the mesh holes of the insulator screen is affected by initial conditions. Depending on the distribution of charges, the electric fields in the vicinity of the meshes will be modified, deflecting the flooding electrons and ions to selective minute areas of the insulator surface and, consequently, altering the erasing characteristic.

It is interesting to note that if the insulator is initially at cutoff and $0.000\,48 < ft < 0.000\,96$, insulator areas where a large writing charge has been deposited will charge to a definite brightness level, while weak signals will be erased to cutoff. (A small area of positive charge will not persist indefinitely however, since the escape of secondary electrons from the area is inhibited by the electric field of the less-positive surrounding insulator surface, thus causing more electrons to stick, charging the area negatively. The bright area shrinks in size and disappears.) This characteristic can be used to achieve extended viewing time but with concurrent loss of half tones. Extension of viewing time by this method is even greater if still-narrower erasing pulses of relatively high amplitude are used. The viewing time obtainable in this way is upward of 30 seconds, after which time the written areas decay rather rapidly to cutoff.

1.5 Writing Characteristic

With the tube operating and with proper erasing pulses being applied, the tube will be at cutoff and in readiness to be written on. The 1000-volt writing beam can be scanned over the insulator in any desired pattern and video signals are applied to the control grid to modulate the beam.

The collector screen, insulator, and phosphor each intercept a part of the writing beam. The current intercepted by the insulator serves to charge it in the positive direction since the beam energy is great enough to eject a greater number of secondary electrons than the number of primary electrons intercepted.

The rate at which the insulator can be charged by the writing beam is very high. This rate is determined by measuring the brightness of the stored trace after the writing beam has been deflected across the tube at a known scanning speed. In Figure 5, the brightness of a stored signal is plotted as it increases in stair-step fashion, with each passage of the writing beam during successive superimposed scans across the corresponding point on the insulator. The writing spot was scanning at a speed of 2.75×10^4 centimeters per second and the three curves are for three values of writing-beam current. After the tenth scan, an erasing pulse was applied to restore the insulator to cutoff. The bright flash which accompanies the erase pulse is shown also in Figure 5. It can be seen that the flash is never brighter than the brightness associated with equilibrium insulator potential and has a relationship to the brightness of the signal that is being erased.

The writing currents used to obtain the data in Figure 5 were necessarily very low because of the relatively low scanning speed available

for these tests. However, the writing-beam current can be as high as 150 microamperes at zero grid bias and will write to maximum brightness in a single-line scan at a speed of about 10^5 centimeters per second.

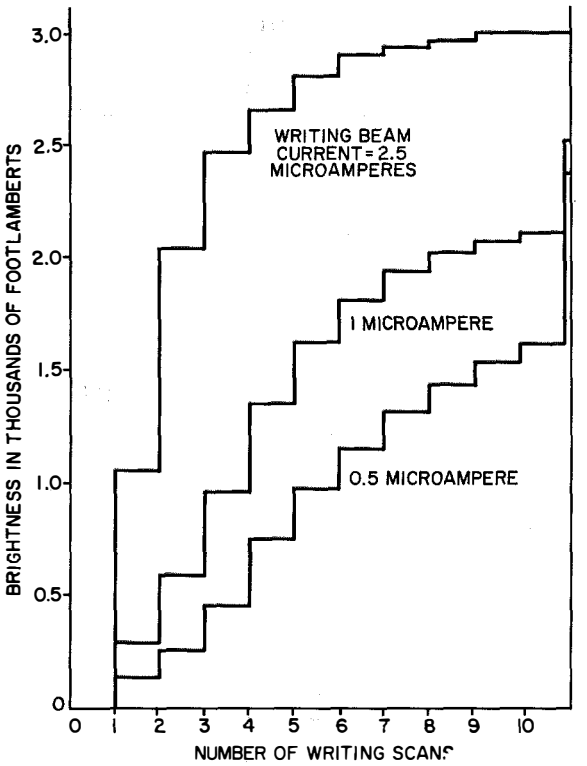

Figure 5—Brightness of a point written on for 10 successive writing scans and finally erased to cutoff; writing-spot scanning speed 2.75×10^4 centimeters per second.

At high brightness, the brightness increase per scan grows smaller. At the high-brightness limit, saturation is reached and further writing results only in a charge spreading on the insulator surface. Since an electron beam does not possess finite size, a few electrons will be found even at radii considerably larger than the dimensions of the spot defined by the usual methods. These fringe electrons continue to integrate on the insulator area surrounding the core of the spot after it has saturated.

The obvious implication is a serious one, that areas repeatedly written upon in a display will tend to bloom unless some form of insulator writing-charge limiting is used. In a plan-position-indicator radar display, for example, an equalizing signal derived from the range-deflection voltage can be added to the video signal to prevent blooming at the center. To emphasize weak targets in a display, video clipping will prevent blooming on strong signals. Proper choice of the erasing-pulse frequency is, of course, extremely important in this matter since writing charge can be erased before it has had the opportunity to integrate beyond a desired level. An erasing frequency equal to the deflection frequency is the best choice in many cases.

In almost any continuous display, the erasing-pulse frequency and pulse width are preset; after adjustments have been made to achieve the desired viewing time no further adjustments will be required during operation. Figure 6 illustrates typical continuous operation of an Iatron using an erasing frequency equal to the writing-beam scanning frequency, which in this case is 60 cycles per second. An erasing-pulse width of 0.001 35 second was used and the viewing time was consequently about 37 milliseconds. The way in which the average brightness varies with writing current is apparent from the three conditions shown. The two brightness levels in each graph

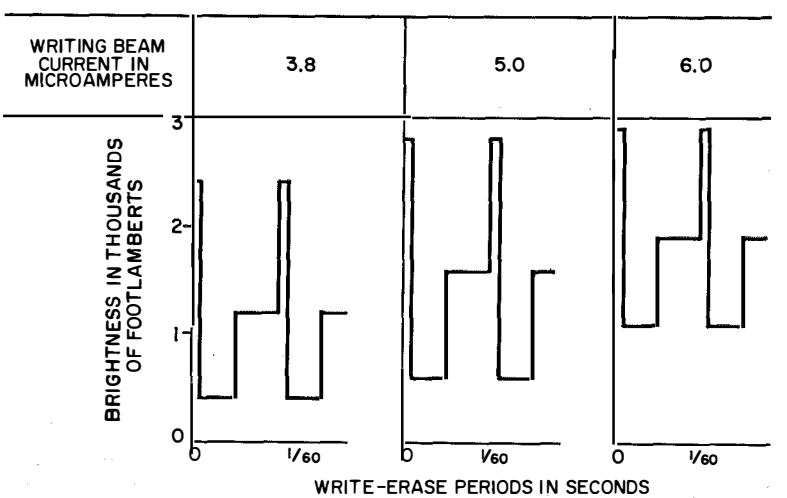

Figure 6—Stable brightness levels of a point alternately written and erased; erasing-pulse width = 1350 microseconds.

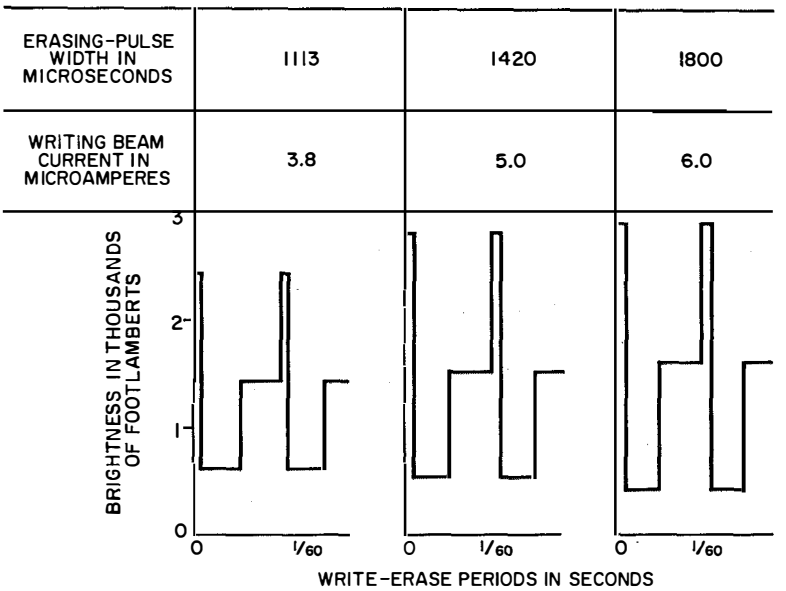

Figure 7—Stable brightness levels of a point alternately written and erased; average brightness is constant.

correspond to insulator potentials immediately after writing and immediately after erasing. These are stable potentials that will be repeated until either writing current or erasing-pulse width is changed. Each erasing pulse charges the insulator downward in potential by an amount equal to the potential increase by writing during one scan. The ability of the insulator to assume stable potentials follows from its nonlinear charging characteristic wherein the charging rate decreases toward higher brightness levels; Figure 5. If the characteristic were linear, writing charges would integrate to saturation. Since the erasing-pulse amplitude was 3.2 volts, the tube would have been erased just to cutoff if writing current were reduced to zero.

As indicated in Figure 7, a change of viewing time requires adjustment of both average writing current and the amount of erasure. In Figure 7, the average brightness was held constant by adjusting the writing current, after the viewing time was changed, by altering the erasing-pulse width.

1.6 Resolution

To measure resolution, a raster of a known number of equally spaced lines is scanned, and the raster is shrunk until the individual lines are no longer discernible. The raster width that is normal to the lines is then measured and resolution is specified in lines per inch.

Resolution measurements are meaningless unless brightness is specified concurrently. It is found that resolution is approximately the same at a given brightness regardless of how many scans or what writing-beam current were required to write to that brightness. While the resolution of a stored image at low brightness is nearly equal to the resolution of the writing beam itself, at high brightness it approaches a minimum of about 35 lines per inch (14 lines per centimeter); see Figure 8.

2. Oscilloscope Application

Operation of the Iatron storage tube probably can be understood best by noting how its characteristics apply to a particular application. Since the cathode-ray oscilloscope is commonly used

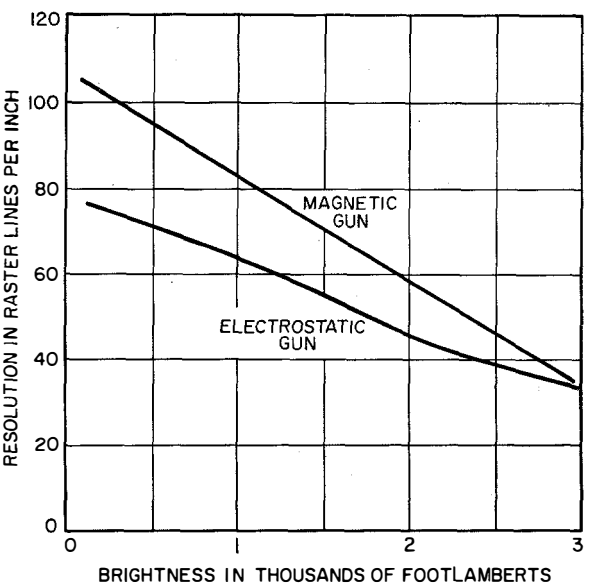

Figure 8—Resolution versus brightness. The curve for a magnetic-focus gun having a smaller writing-spot size shows limitations attributable to the writing gun.

in all engineering laboratories, this section will be concerned with the operation of the Iatron as it might be used in an oscilloscope.

The usefulness of oscilloscopes decreases rapidly for very-low sweep frequencies up to the threshold of flicker. The useful low-frequency range could be extended considerably by lengthening the persistence of the trace. Using the Iatron for this purpose, there is no flicker and the trace is bright enough to be viewed easily in a fully lighted room.

At low frequencies, storage in oscilloscope displays is ordinarily obtained by photographing the display. Another method to display low-frequency signals is to resort to mechanical means of recording. Besides the added expense and inconvenience of these methods, they also have limitations that are overcome by using the Iatron:

A. The Iatron will record transients composed of frequencies from direct current to above 1 megacycle, whereas mechanical recorders are limited to about 60 cycles.

B. Any trace can be stored for examination or it can be erased instantaneously in the Iatron.

C. The trace can be viewed immediately in the Iatron, avoiding the delay involved in development of film.

It is also practical to store superimposed sweeps taken in sequence at several test points for directly comparing waveforms.

The advantages of an Iatron oscilloscope are expected to be greatest at low sweep speeds, but it need not be restricted in operation to the low-frequency ranges, since a visible trace can be stored at writing-spot velocities up to nearly 10^6 centimeters per second.

At still-higher speeds, for which no trace will be stored, the tube can still be operated as a conventional cathode-ray tube, since the writing-beam average power input to the phosphor can be about 0.4 watt with the tube operating at 1 kilovolts; nor does the high voltage entail a loss of deflection sensitivity. A constant sensitivity of 100 volts per inch (39 volts per centimeter) is afforded by the electrostatic shielding property of the insulator screen, which isolates the 1-kilovolt deflection region of the tube completely from the 10-kilovolt phosphor potential.

By switching the insulator screen from its normal +10 volts to about −20 volts, the flooding beam can be cut off to improve contrast when it is desired to view only the writing-beam trace and not its stored image.

In normal operation, erasing pulses will keep the insulator erased to cutoff in areas where no trace is being written, and will prevent writing charges in the trace from integrating to the extent of charge spreading. For the usual repetitive-signal mode of oscilloscope operation, an erasing-pulse amplitude control and erasing-pulse width control should be accessible on the front panel to make initial adjustments of cutoff and viewing time. An intensity control is necessary to adjust writing-beam current to compensate for changes in sweep speed and waveform of the signal.

At sweep frequencies of over 45 cycles, the erasing pulse can be triggered by the sweep. This is in keeping with the discussion of writing-charge limiting in which it was pointed out that maximum charge stability of areas repeatedly written on exists when writing and erasing frequencies are equal. At lower sweep frequencies, flicker and blooming would be avoided if a constant erasing-pulse frequency of 45 cycles or higher were used. A convenient and satisfactory frequency is 60 cycles.

To display transients, maximum writing speed and storage time is desirable. A switch might be provided that, after writing, could be used to cut off the writing beam and erasing pulses simultaneously, thus avoiding over-writing of the transient trace and at the same time preventing its erasure. At extremely slow sweep speeds, it is desirable to turn off the erasing pulses before the start of the writing trace to avoid any erasure before one sweep is completed. This suggests a manual on–off erasing switch. Also, an instant-erasing button would probably be useful to restore the insulator quickly to cutoff after operating with the erasing pulse off.

The oscilloscope should be equipped with a z-axis gate to assure that the undeflected writing spot is cut off, since the undeflected spot would cause insulator charge spreading from that spot over an appreciable area of the screen and at

very-high current the insulator might even be damaged.

The controls described are the extent of the added complexity necessary to operate an oscilloscope adapted to the Iatron and the additional circuit needed to operate the flooding system is equivalent to adding one tube. An erasing-pulse generator that can perform the suggested functions could be a slave multivibrator.

Summarizing, the following controls are recommended for full utilization of the tube's capabilities:

A. Erasing-pulse gain control to adjust the amplitude of the pulses.

B. Erasing-pulse width control to adjust the duty cycle of the pulses.

C. Instant-erasing push-button switch that widens the erasing pulses momentarily to erase clutter without disturbing other erasing-control settings.

D. Erasing on–off switch to remove erasing pulses when it is desired to freeze a trace for inspection without adjusting erasing controls.

E. Writing on–off switch to bias the writing-gun control grid to cutoff to prevent over-writing a frozen trace without adjusting the intensity control.

F. Flooding-beam on–off switch to bias the insulator support screen to flooding-beam cutoff when the tube is being used as a conventional cathode-ray tube.

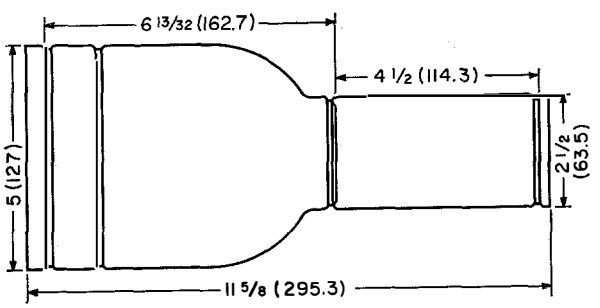

Figure 9—Outside dimensions of the 5-inch (127-millimeter) electric-field-deflection Iatron *Ia10P20-25*.

The type-*Ia10P20-25* Iatron shown in Figure 1 is the model recommended for oscilloscopes and other applications that require electric-field deflection. The useful display diameter is 4 inches (102 millimeters) and the outside dimensions are shown in Figure 9.

TABLE 1

OPERATING VOLTAGES FOR IATRON*

Electrode	Voltage	Current
Writing Gun		
Heater	6.3	0.6 ampere, alternating or direct current
Cathode	−1000	1080 microamperes, maximum
Grid	−1042 at cutoff	
First Anode	−700 at focus	−1.0 microampere, maximum
Second Anode	40	940 microamperes, maximum
Flooding system		
Heater	2.5	2.5 amperes, alternating or direct current
Cathode	0	2.6 milliamperes
Anode and First Wall Electrode	40	0.8 milliampere, minimum 1.0 milliampere, maximum
Second Wall Electrode	20	0.07 milliampere minimum 0.115 milliampere, maximum
Third Wall Electrode	80	0.035 milliampere
Collector Screen	150	1.25 milliampere
Insulator Screen	+10	
Phosphor	+10 kilovolts, maximum	0.38 milliampere, maximum

* Deflection-plate reference voltage for minimum astigmatism, 0 volts. Deflection sensitivity; 85 volts per inch for plates D_3 to D_4; 100 volts per inch for plates D_1 to D_2. Plates D_1 and D_2 connected to +90 volts draw 36-milliampere flooding current.

Some comment on the operating circuit of Figure 2 is necessary. The resistance in the final deflection-plate circuit should be lower than is ordinarily used with cathode-ray tubes, because when they are driven positive, the plates can draw about 36 microamperes of flooding current.

If the average voltage of the deflection plates is about 40 volts, the least astigmatism of the writing spot results since the second anode and first wall electrode are at that potential. An astigmatism control consisting of a dual adjustable voltage divider could be inserted in the bleeder at the points supplying the direct current to the plates to adjust the average deflection plate voltage. However, it is found in practice that good results are achieved with an average plate voltage near zero, as shown.

The maximum phosphor voltage is 10 kilovolts. However, the characteristics of the tube, other than brightness, will be relatively unchanged with operation down to less than 5 kilovolts. Therefore, to avoid any possible damage to the tube because of overvoltage accidents, particularly when extremely high brightness is not an

objective, it is recommended that reduced voltage be used.

The flooding-spot size is adjusted by small changes in voltage applied to the second wall electrode after other voltages of the flooding system have been set at their specified values. Table 1 lists operating voltages and maximum and minimum currents of flooding-system electrodes that were measured to aid in the design of power supplies and bleeders. These measurements were made on only a few tubes, since production tubes were not available at this writing to obtain average data. It is anticipated that production tubes will have fewer electrodes, but those retained will be operated very closely to their present voltages and tubes will operate interchangeably, requiring only the number of controls that have been indicated.

Recent Telecommunication Development

Space-Charge Waves

RECENTLY PUBLISHED, a book on "Space-Charge Waves" and slow electromagnetic waves has been written by A. H. W. Beck of Standard Telecommunication laboratories. It is divided into 10 chapters, 12 appendixes, and sections on problems, references, and letter symbols.

Chapter 1—General Introduction

Chapter 2—Maxwell's Equations and Wave Equations

Chapter 3—Slow-Wave Structures

Chapter 4—Space-Charge-Wave Theory

Chapter 5—Matching Specified Input Conditions with Space-Charge Waves

Chapter 6—Space-Charge Waves in Klystrons

Chapter 7—Travelling-Wave Tubes and Backward-Wave Oscillators

Chapter 8—Crossed-Field Devices

Chapter 9—Special Space-Charge-Wave Devices

Chapter 10—Noise Phenomena in Space-Charge-Wave Devices

Appendix 1—Power Flow in a Circular Guide

Appendix 2—Integrals of Products of Bessel Functions

Appendix 3—The Tape Helix

Appendix 4—Variational Methods

Appendix 5—Measurements on Slow-Wave Structures

Appendix 6—The Focusing of Long Electron Beams

Appendix 7—Annular Beams and Bessel Function Expansions

Appendix 8—Solution of Equation (134) Chapter 4

Appendix 9—Orthogonal Expansions in Bessel Functions

Appendix 10—Coupling of Modes of Propagation

Appendix 11—Excitation of the Waves in T.W.A.s and B.W.O.s

Appendix 12—Llewellyn's Electronic Equations

This is the 8th volume in the International Series of Monographs on Electronics and Instrumentation published by Pergamon Press. The dimensions are $5\frac{3}{4}$ by $8\frac{3}{4}$ inches (14.6 by 22.2 centimeters). Of the 396 pages of text, the 10 chapters occupy 321 pages and include 124 figures and 916 numbered equations. The 72 pages of appendixes are predominently mathematical. There is a 3-page index.

The book is available from Pergamon Press, 4 Fitzroy Square, London, W1, at 90 shillings and from Pergamon Press, 122 East 55th Street, New York 22, New York, at $15.00 per copy.

Storage Tube Projects Radar Plan-Position-Indicator Display*

By HARRY W. GATES

Farnsworth Electronics Company, a division of International Telephone and Telegraph Corporation; Fort Wayne, Indiana

TO PROJECT live radar or beacon information directly onto a plotting board, two basic conditions must be fulfilled; high brightness and controllable long-time storage.

The radar projector indicator described in this article fulfills these requirements by utilizing a high-brightness storage tube called an Iatron®. The equipment, consisting of a range–azimuth projection indicator and a control console, is a remote plan-position indicator providing a 50-inch (1.27-meter) display for search radars.

To make the display equipment more useful, separate inputs for radar, rafax, and mapping are included. It is possible to select five radar ranges from 20 to 200 nautical miles (37 to 370 kilometers) and range markers from 5 to 50 nautical miles (9.2 to 92 kilometers). Sweep ranges are available for use with rafax at 120, 60, and 30 pulses per second. The indicator will accept radar triggers from 200 to 1200 pulses per second.

Antenna rotation information may be from 3 to 30 revolutions per minute and a two-speed synchro system insures accurate rotational information. A cycled instant erase automatically reduces build-up of ground clutter or large slow-moving rain-cloud formations.

1. Storage Tube

The basic elements of the Iatron storage tube are a writing beam of low intensity and high definition, a high-current flooding beam of large cross-section, a fine-mesh metallic screen supporting a thin insulating layer facing the electron guns, and an aluminized phosphor screen.

The writing beam scans the insulating layer and deposits charges everywhere proportional to the instantaneous beam intensity. Writing current is modulated by application of a video signal to the control grid. The distribution of potential over the insulating layer is then an electrostatic image of the video information.

Flooding-beam electrons approaching the charged insulating layer penetrate the fine-mesh screen in quantities proportional to the local charge on the insulator and impinge on the phosphor screen. In this way, the phosphor is continuously excited by the high-current flooding beam.

While writing and display are simultaneous, means are provided for insulator-charge erasure. If the insulator surface suddenly becomes more positive, flooding electrons strike the surface and charge it in the negative direction toward flooding-gun cathode potential. This is accomplished by applying a positive voltage pulse to the metallic screen supporting the insulator.

The most-negative potential to which the insulator will charge is determined by the erasing-pulse amplitude applied to the insulator support screen. The correct amplitude is that causing the equilibrium insulator potential after erasure to be equal to the potential required barely to cut off flooding-current flow to the phosphor. Then any insulator writing charge will be erased to cutoff after an adequate number of erase pulses of fixed width have been applied. Image persistence is controlled by adjusting pulse repetition rate.

2. Servomechanism

Many of the circuits employed in the indicator are conventional. However, several features are of interest.

The servo mechanism utilizes one-speed and 10-speed or one-speed and 36-speed selsyn information to synchronize the rotating sweep with the radar antenna. The one-speed system gives approximate information of the total train angle; the 36-speed system gives accurate indication of the angle but only if it is synchronized at the proper zero.

A switching system puts the one-speed system in control until the reproduced train angle is approximately correct and then throws the control to the 36-speed synchro system. Switching is accomplished by mixing the error signals in

* Reprinted from *Electronics*, volume 29, pages 172–175; December, 1956.

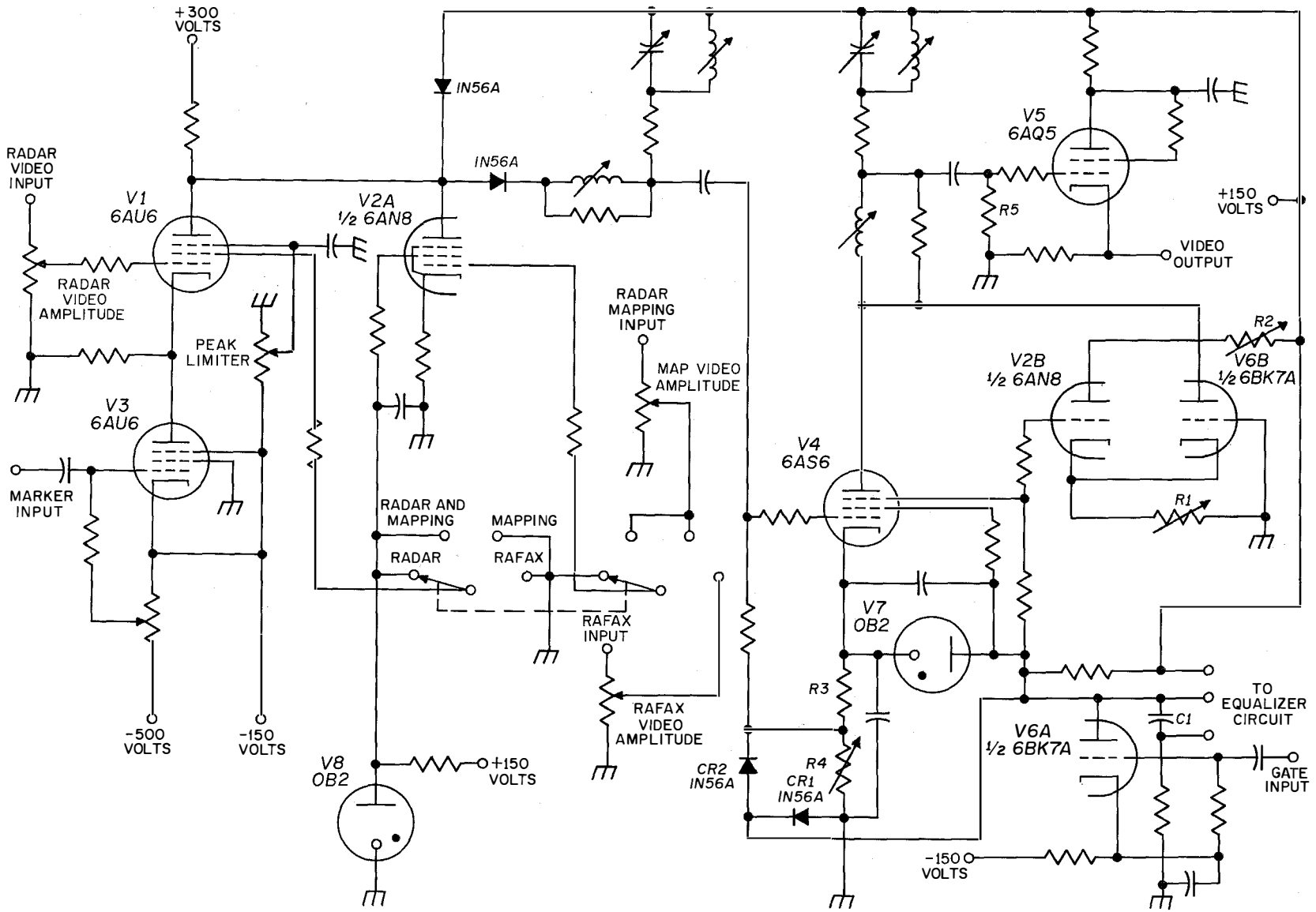

Figure 1—Radar, rafax, mapping, and marker signals are amplitude-controlled, mixed, peak-limited, and equalized in control console.

germanium diodes whose resistance decreases as the current flow increases. This insures a smooth switchover instead of a sudden switching such as is ordinarily encountered with synchronizing circuits using relays.

The video amplifier is composed of two sections. The first section, shown in Figure 1, is in the console where the radar video, mapping

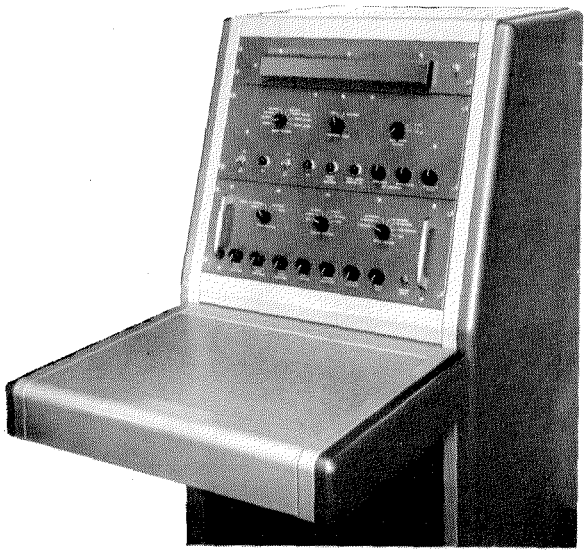

Figure 2—Control console for projector indicator.

video, and marker signals are amplitude-controlled, mixed, peak-limited, and equalized (see also Figure 2). The second section, a two-stage amplifier, is in the projection unit (Figure 3) 25 feet (7.6 meters) away, which receives the video signal from the first section over a 100-ohm coaxial cable.

3. Equalizing Circuit

Equalization of the video signal for a plan-position indicator presentation is accomplished in the second stage *V4*, of the video amplifier in Figure 1. With a rotating radial sweep, video signals of an amplitude that gives the proper brilliance near the periphery of the display tube would cause blooming near the center owing to the greater overlapping of adjacent scanning lines near the center.

To eliminate the blooming, less video gain is needed near the center of the display tube. This is accomplished by modulating the gain in accordance with a ramp function for a certain distance from the center and then continuing at constant gain for the remainder of the sweep.

The ramp-function waveform is applied to the suppressor grid of *V4*. Beside modulating the gain, the ramp-function signal of reverse polarity is also present in the plate circuit of *V4*. This is balanced out by the cathode-coupled amplifier consisting of *V2B* and *V6B*. The modulating ramp function is also applied to the grid of *V2B* which produces a signal of the same polarity in the plate circuits of *V2B* and *V4*. Adjustment of *R1* and *R2* will cancel the ramp-function signal in the plate load of *V4*.

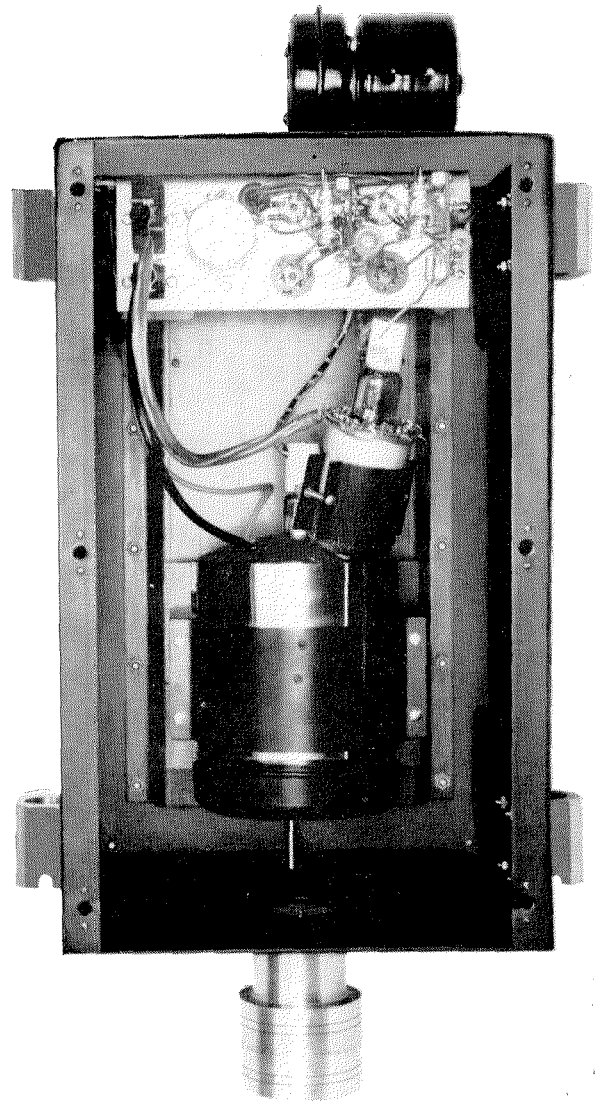

Figure 3—Inside of projector unit showing last stages of video amplifier and Iatron.

The ramp function is generated in the circuit associated with *V6A*. The cathode of *V6A* is at approximately −20 volts with respect to ground. Its plate is normally clamped to ground by *CR1*. The negative gate pulse, which initiates sweep, is applied to its grid.

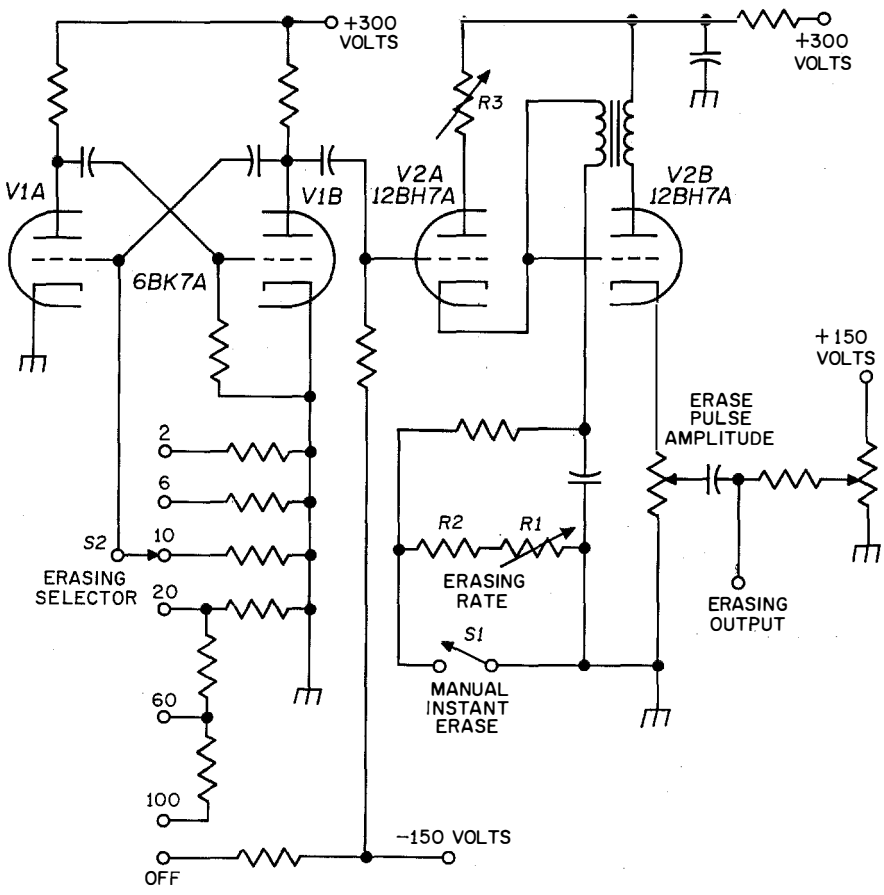

Figure 4—The pulse repetition frequency of the blocking oscillator controls the Iatron persistence.

Upon initiation of the sweep, the grid of *V6A* is driven negatively, cutting off the tube and permitting the plate voltage to rise as capacitor *C1* and a parallel capacitor, on another chassis, charge. When the plate voltage attains a value equal to that at the junction of *R3* and *R4*, *CR2* conducts, clamping the plate of *V6A* at this voltage, the maximum amplitude of the ramp function. For the remainder of the sweep it remains constant at this value.

The equalizing circuit chassis contains a capacitor and adjustable charging resistance for each range, with a separate adjustable charging resistance for each of the expanded ranges. Screwdriver controls permit adjustment of the ratio of the time the ramp function reaches its maximum to sweep time for each range and each expanded range.

Referring to Figure 1, the positive video signal from *V4* is fed to the grid of *V5*, a *6AQ5* used as a cathode-follower to change the impedance for coupling into a 93-ohm coaxial cable connecting with the projection unit. The 100-ohm cathode load resistor for *V5* is at the output end of the cable in the projection unit. Resistor *R5* prevents the cathode of *V5* from floating if the cable is disconnected while the equipment is turned on.

4. Erasing Generator

The Iatron persistence is controlled by varying the pulse repetition frequency of a blocking oscillator. The erasing-rate control on the console enables the operator to select any continuously variable persistence from 3 milliseconds to 20 seconds.

The erasing generator is a blocking oscillator, *V2B*, with the output taken from the cathode circuit as shown in Figure 4. Erasing-rate control *R1* controls the blocking-oscillator frequency. Pushbutton switch *S1*, when depressed, shorts *R1* and *R2*, causing the blocking oscillator to operate at a high frequency, which instantly erases the insulator screen.

Automatic instant erasure is provided at fixed intervals by stable multivibrator *V1*. The grid circuit of *V1A* has a long time constant that can

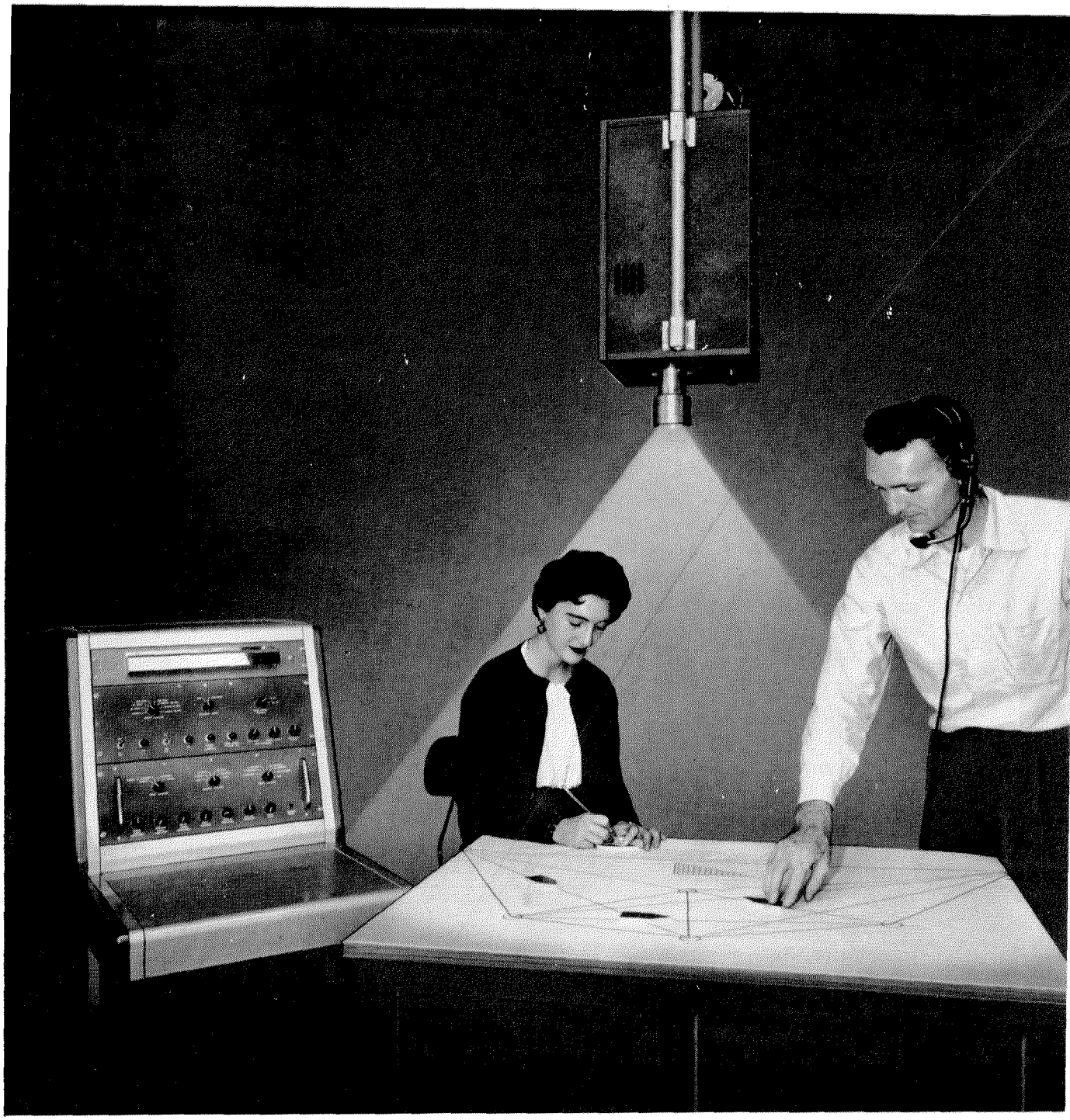

Figure 5—Radar projector indicator as used with plotting board for air-traffic control.

be varied by *S2*, causing the period to be varied in steps from 2 to 100 seconds.

The grid of *V1B* has a relatively short time constant. When the plate of *V1B* goes positive, the grid of cathode-follower *V2B* goes positive, causing the grid of the blocking oscillator to go positive. This prevents the blocking-oscillator grid from being driven negative due to the cathode-follower, which causes it to operate at a high frequency for the relatively short period that the plate of *V1B* is positive. Rheostat *R3* controls the output impedance of the cathode-follower and hence the instant-erasure frequency. When the cathode-follower has a high impedance, the grid of the blocking oscillator can be driven slightly negative, decreasing the frequency.

5. *Application*

The projection unit of the indicator is normally mounted at the ceiling of the control room and the information displayed on a horizontal plotting board (Figure 5). However, the projection unit can be mounted in any position for vertical projection on a screen or projection from below through a translucent surface.

Simple refractive optics eliminate the problems of adjustment encountered in the more-complex Schmidt-type optics. A single knob is the only adjustment.

When the indicator is used in conjunction with the rafax video-bandwidth compression system for remote radar or beacon information, a novel and interesting display is produced. Such a system, illustrated in Figure 6, was demonstrated by the Technical Development Center of the Civil Aeronautics Administration in Indianapolis.

Aircraft equipped with beacon equipment were interrogated by the beacon station in Jamestown, Ohio. The beacon video, trigger, and rotational information were transmitted by microwave link to Dayton, Ohio. At Dayton, the beacon information was reduced in bandwidth by the rafax encoder. This reduced-bandwidth information was then sent over a 100-statute-mile (161-kilometer) telephone line to Indianapolis where it was displayed by the Iatron radar projection indicator on a plotting board.

Another indicator simultaneously projected beacon information from the Indianapolis beacon on the same plotting board. The composite display was then used for traffic-control evaluation for the surrounding 400-nautical-mile (761-kilometer) radius.

The storage time of the Iatron was set for slightly greater than one antenna revolution so pertinent information was displayed at all times. Aircraft were identified and shrimp boats placed on the plotting board to be moved along as the flights progressed.

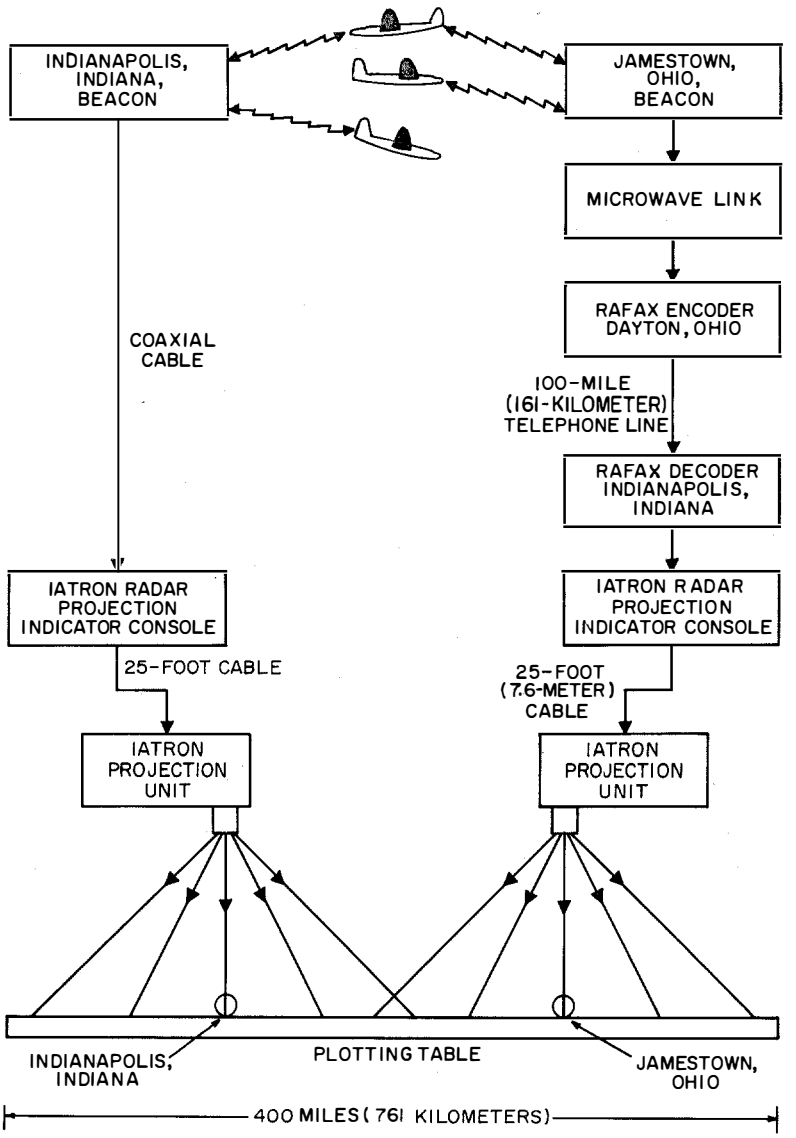

Figure 6—Civil Aeronautics Administration traffic control system using radar projector indicator.

Carrier Telecommunications Over the High-Tension Power Network in Algeria

By EDMOND A. THOMAS

Compagnie Générale de Constructions Téléphoniques; Paris, France

BEFORE the second world war, several companies had initiated the construction of networks for distributing electricity in Algeria, but their development remained limited by the comparatively low industrial activity of the country. After the war, it became apparent the increases in electric-power consumption would raise a serious problem and that a large interconnection network would have to be constructed. A working plan was then drawn up by the electricity division of the Gouvernement Général de l'Algerie to be developed by a newly formed organization, Electricité & Gaz D'Algerie (EGA).

Five years were required to erect a vast distribution network that received its main supply from 4 steam and 9 large hydroelectric plants.

With an annual production of the order of 800 million kilowatt-hours, Algeria is now in a position to meet its future needs, including those resulting from the electrification of the railways.

The large dams that are part of the hydroelectric plants were also planned to improve irrigation, which is always critical in North Africa. This important work is one of the French undertakings that honors those who were responsible for its planning and execution.

1. High-Tension Network

The more-densely populated region of Algeria, a strip of cultivatable land bordering the Mediterranean and stretching back to the edge of the desert sands, covers an area about 1100 kilometers (684 miles) long and 100 kilometers (62 miles) wide. The high-tension network necessarily took the same form. To connect the large towns, which are mainly scattered along the coastline, a main trunk line operating at 150 kilovolts was established to connect the 90- and 60-kilovolt distribution networks. This is shown in Figure 1. As rapid means of communication were not available, it was decided that an intercommunication telephone system would have to be superposed on the power network.

In 1949, a contract was signed for the application of carrier telephony to the existing and planned 90- and 60-kilovolt sections and to the 150-kilovolt principal trunk line then under construction. Automatic switching was to be provided for the whole network and would employ 3-digit dialing.

2. High-Frequency Carrier System

The first part of this program involved the installation of more than 20 carrier telephone installations with average lengths of about 100 kilometers (62 miles). The equipment had to be simple, economical, and easy to maintain. A standardized amplitude-modulated type that has been used on many power lines in metropolitan France proved to be completely suitable when manufactured for tropical service.

The transmitter includes a crystal-controlled oscillator followed by a two-stage amplifier. A carrier power of 15 watts is developed for continuous sine-wave operation. The modulation chain includes an amplifier that is adjusted so that at the zero level of 1 milliwatt on the telephone channel, the corresponding modulation of the carrier is about 35 percent.

The receiver employs two untuned radio-frequency stages preceded by a high-quality filter having a pass band of 3 kilocycles per second each side of the carrier. It provides attenuation of at least 45 decibels to interference from a carrier 6 kilocycles away.

This type of transmitter–receiver is used for duplex transmissions in the 50- to 300-kilocycle range, allowing a minimum space of 25 kilocycles between the transmitting and receiving frequencies. The selection of these two frequencies is made by associated filters at the common connection point to the power line.

On most of the connections, the high-frequency transmission is also employed for protecting the

line. For this purpose, the telephone channel is subdivided by filters that select the 300- to 2300-cycle band for speech. If a fault occurs on the line, speech is replaced by a 2580-cycle signal sent at a minimum modulation of 80 percent. This signal reduces the tripping time of the breaker at the far end of the section.

Three of these equipments are shown at the right in Figure 2.

The second part of the program was more difficult because on the long 150-kilovolt trunk line the dispatching center at Algiers had to be connected with the maximum of speed and reliability to the secondary dispatching centers at Bône and Oran and to the entire system. Long distances are involved and the line voltage was high enough to require more-complex equipment to obtain a satisfactory signal-to-noise ratio.

For these long lines, single-sideband equipments have been installed in groups of three to provide parallel channels on adjacent frequencies. Only two of these channels are used under normal conditions. The third is a spare that can be substituted for either of the other two in case of failure. If needed, it can be used for the transmission of telemetering data. The changeover of equipments can be effected quickly by switches in a connecting cabinet, which can be seen in the center of Figure 2. Connected to the lower part of it is a cabinet for connecting the three channels in parallel. A differential system employs a coaxial cable to connect the group of three bays to the single input device to the power line.

The single-sideband equipments shown at the left of Figure 2 are mounted on removable chassis in apparatus bays. Each chassis has a definite function and contains vacuum tubes and a group of air-tight boxes. They are connected to the general wiring of the bay by means of lateral rows of plugs, which allow numerous tests to be carried out.

The transmitter is designed for a theoretical bandwidth of 4 kilocycles. The frequencies transmitted are obtained by two successive modulations. The first is under control of a 24-kilocycle crystal oscillator. The upper sideband from 24 to 28 kilocycles is selected and converted to the operating frequency range between 50 and 300 kilocycles through the second modulation.

The crystal frequencies for this second modulation are spaced at 4-kilocycle intervals, placing side by side the transmission channels of the bays functioning in parallel in the same transmission direction.

The output amplifier for each bay can deliver a sine-wave power of 30 watts, but as a result of the loss introduced by the differential system,

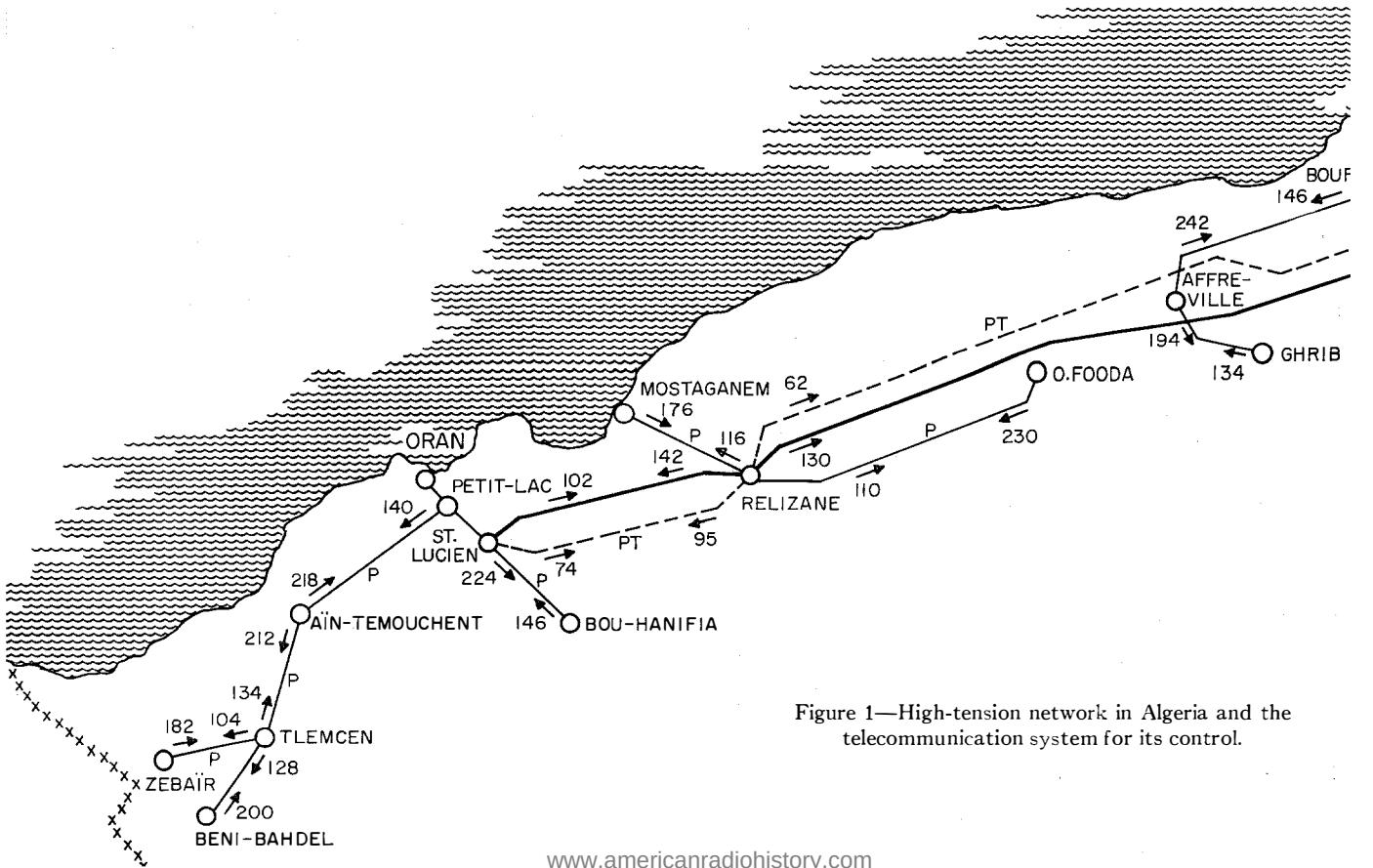

Figure 1—High-tension network in Algeria and the telecommunication system for its control.

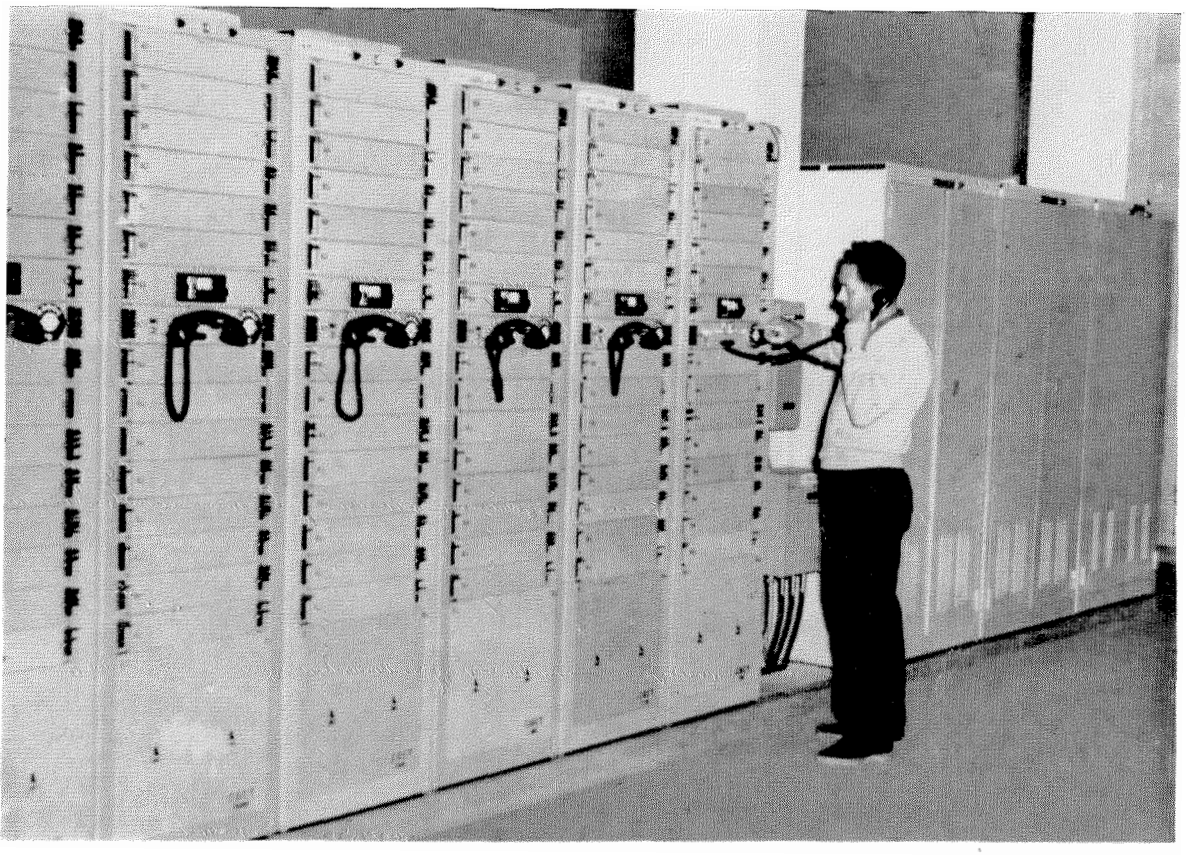

Figure 2—High-frequency equipment at Arba. The single-sideband equipment is at the left and the double-sideband apparatus is at the right. In the center are the changeover switches for the three channels.

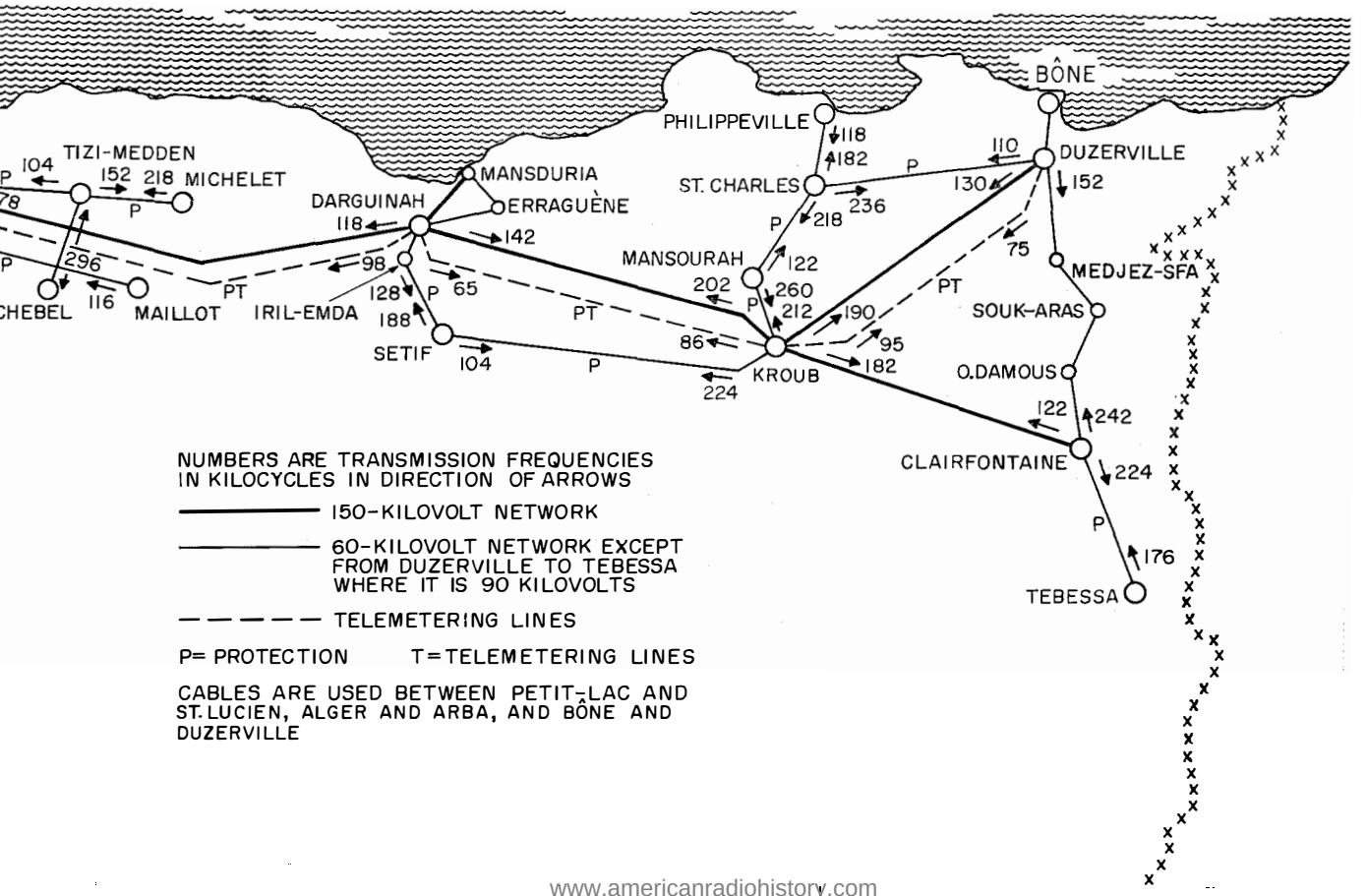

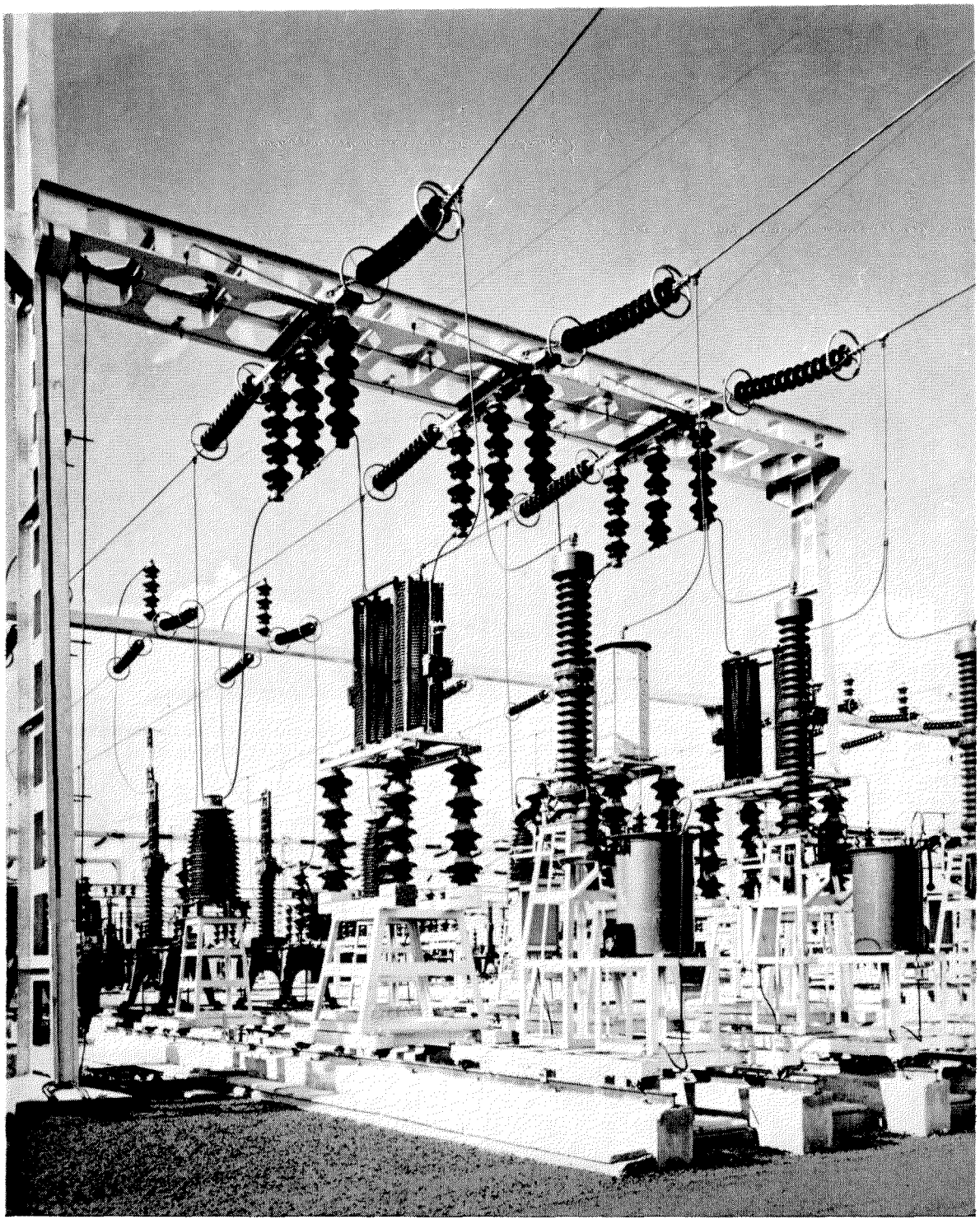

Figure 3—Line coupling installation at Duzerville. The petticoated device in the center, to which is connected the downlead from the line phase nearest the camera, is the coupling capacitor. At the base of the coupling capacitor are the drain coil and the protective devices and, partially hidden behind the framework, the line-tuning cabinet. The large vertical inductors are carrier-current line traps. The cylindrical tank contains part of the 150-kilovolt capacitive voltage divider.

the corresponding power delivered to the line is only of 10 watts in the case of three bays.

The first element in the receiver is a band-pass filter that selects the frequencies before the first demodulation. This demodulation, which is controlled by a crystal identical with that of the corresponding transmitter, brings the received frequencies back into the 24- to 28-kilocycle band. A later filter having very-sharp cutoff characteristics provides the interchannel selectivity. The voice frequencies are restored exactly to their original values by the second demodulation, which uses the 24-kilocycle voltage transmitted in an attenuated form and amplified in the receiver. This attenuated pilot is, moreover, used for the gain control since it changes with line attenuation. Regulation is obtained by controlling the heating of thermistors incorporated in an attenuator.

The theoretical 4-kilocycle channel is subdivided so as to provide a band from 300 to 2300 cycles for telephony. A channel of 2580 to 3060 cycles can thus be reserved for transmission of five frequencies in the overtone series (odd multiples of 60 cycles). Dialing is obtained through interruption of a 3300-cycle wave, the highest frequency used in the band allotted to each channel.

Of the 30 bays of this type required for the 150-kilovolt trunk line, 20 are in permanent operation for telephone traffic, which can be repeatered 4 times for communication between the most-distant dispatching centers of Oran and Bône.

Among the three dispatching centers, one of the two high-frequency channels is reserved for priority communications and the other is used for ordinary communications.

3. Line Equipment

At all substations, the high-frequency equipment is connected to the line input channeling equipment by an underground armored coaxial cable. This cable enters the coupling box, which contains a transformer with taps for adapting it to the line impedance, and is also connected to a tuning device. The tuning system generally includes the capacitor providing coupling to the power line as part of a high-pass filter. These capacitors are moreover used as voltage dividers connected to voltage transformers; at their base they are equipped with a discharge coil to bypass dangerous voltages, and with the usual protective devices, such as lightning arrestors and fuses. This subassembly appears in the center of Figure 3. At the side of the capacitors of the extreme phases may be seen the tuned circuits provided on the station side for blocking the high-frequency currents of an interphase link.

4. Telephone System

The third part of the program consisted of the organization of the telephone system. The various carrier connections to the 150-, 90-, and 60-kilovolt networks were considered to be equivalent to 4-wire telephone channels terminating in 2-wire circuits through differential devices. However, in the case of long-distance communication, the retransmissions between consecutive sections are carried out on 4 wires; the equipments are then used as base-to-carrier-frequency repeaters. It should be added that the communication channels are extended from the 150-kilovolt line to the switching stations at Algiers, Oran, and Bône through multichannel cables about 30 kilometers (19 miles) long, in accordance with the standards of the Comité Consultatif International Télégraphique et Téléphonique.

To provide automatic switching over the whole system, each subscriber's set is identified by a 3-digit number. The system is divided into 7 districts, to each of which is assigned a different figure in the hundreds position. The tens represent the various stations, and the units positions are allotted to the individual subscriber's sets in each station.

All the switching operations are effected by automatic switches, the capacity of which varies according to the size of the station and the amount of traffic. These switches are derived from four basic types that are standardized for use in similar systems in France. Racks of these switches are shown in Figure 4. They have the following capacities.

Type *C* has a capacity of 8 carrier circuits between power switching stations and 10 subscribers' lines.

Figure 4—Racks of telecommunication switches at Algiers and terminations of cables to Arba.

Type *B* has a capacity of 14 carrier circuits between power switching stations and 20 subscribers' lines.

Trada type *1* accomodates 1 trunk or main line and 6 subscribers' lines.

Trada type *2* accomodates 6 trunks or main lines and 40 subscribers' lines.

It should be added that to allow for the special connections of the carrier channels on the 150-kilovolt trunk line, two types of automatic switches are provided. Priority communications are controlled by special automatic switches that allow only priority communications between dispatching centers and between dispatching centers and certain subscribers' sets in the network. Ordinary switches normally serve all the subscribers' sets in the network and can, through their connection with the other switches, come to the aid of the priority subscribers if their network should be overloaded.

As the power network is paralleled in places with the 90- and 60-kilovolt lines, the automatic switches have been designed so that they can select a free path if the called subscriber can be reached over several routes.

Finally, as a security measure, all the large 150-kilovolt stations are equipped with a desk that allows priority telephone connections to be made manually in case of failure of the local automatic switching system. One of these desks is shown in Figure 5.

5. Conclusion

This system, which has been made entirely automatic through the installation of specially designed telephone switches, provides, by means of 3-digit dialing, for quick and reliable intercommunication over the whole territory with the standards of quality specified by the Comité Consultatif International Télégraphique et Téléphonique.

The network will be further expanded through interconnection with the Moroccan network now under construction. It allows the control centers at Algiers and Casablanca to supervise the distribution and exchange of power.

6. Acknowledgment

Compagnie Générale de Constructions Téléphoniques considers it a privilege to have collaborated with the Equipment Construction Division of Electricité & Gaz D'Algerie in providing the Algerian power distribution network with an autonomous telecommunication system.

Much information and the photographs in this article were kindly supplied by Mr. Grau of that organization.

Figure 5—Regional power-dispatching desk at Algiers. This was supplied as part of the telecommunication installation.

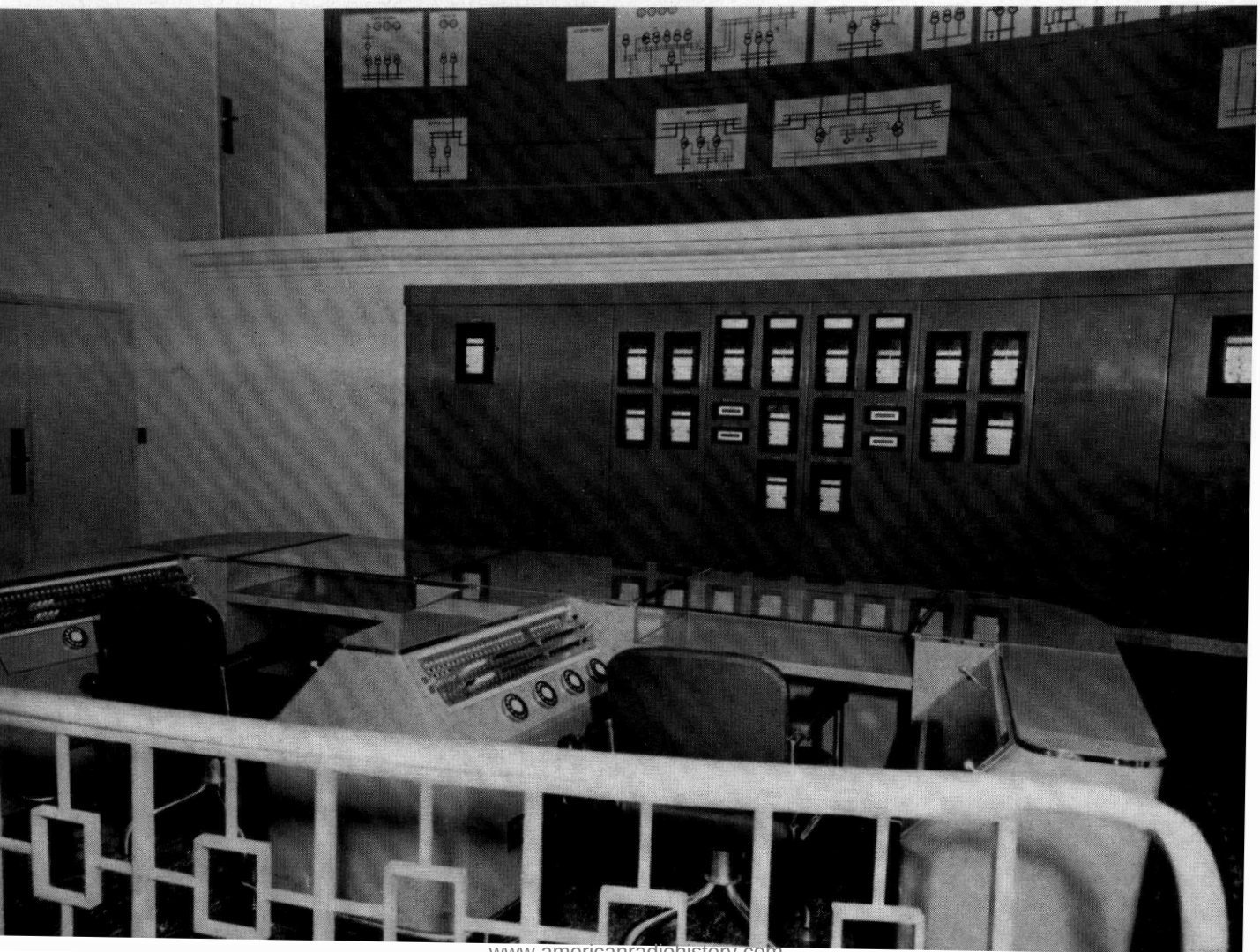

Crossbar Toll Offices in the Finnish Group Network*

By NIKOLAUS LEWEN and HEINZ KÜRTEN

Mix & Genest Werke, division of Standard Elektrik Lorenz A.G.; Stuttgart, Germany

CROSSBAR automatic telephone exchanges used as local offices with a maximum capacity of 100 lines in the subzone areas of the Finnish network are discussed. The trunking principles, testing facilities, and constructional features are described.

• • •

1. Finnish Telephone Network

The country is subdivided into 80 groups of which one is mapped in Figure 1. The toll traffic between these groups is switched through 9 toll distribution exchanges. Each group exchange is connected to at least one of the toll exchanges; direct lines between group exchanges are also provided and can alternatively be switched to the toll route. The toll exchanges are completely meshed. It is intended to introduce a subscriber toll dialing system whereby the first three digits dialed, of which the first will be a *9*, will put the subscriber through to any of the group exchanges. (Helsinki will be reached by dialing *90*.) During interim operation, toll calls will be established by dialing *09*, which will connect the calling subscriber to the toll operator's position in his group exchange.

The entire toll traffic between toll exchanges is in the hands of the public administration, while terminal exchanges are operated either by private or communal telephone companies. For the sake of uniform operation, it is intended to combine various local organizations within a group area.

A linked numbering scheme with a maximum of five digits containing the code of the terminal exchange is used within each group. Six-digit numbers are provided only for the Helsinki area.

The terminal exchanges of a group are radially connected to the group exchange via tandem exchanges. The latter are linked by direct lines, which are also provided between tandem exchanges of adjoining groups. The idea is at present being considered of establishing direct lines even between terminal exchanges of the same and of adjoining groups, if necessary.

Owing to the various proprietors of terminal exchanges, a number of different systems are in use and plants of different manufacture are encountered within one group. The administration of the national system, in its status as a supervisory authority, has issued recommendations and instructions aiming at more uniformity, at least of newly acquired switching plant.

2. Crossbar Terminal Exchange

In accordance with conditions in a thinly populated country, it is intended to equip terminal exchanges with crossbar switches serving primarily up to 50 and, with expansion, up to 100 subscribers. Each crossbar switch frame contains facilities for 50 subscribers.

Exchanges of this size have no permanent maintenance attendants. A functional check is carried out at intervals, mostly on meter readings.

Crossbar switches[1] and magnetic counters[2] are, due to their high reliability, particularly suitable for unattended operation.[3]

To check the conditions prevailing in a system from an attended central maintenance point, a so-called automatic subscriber has been provided in every terminal exchange. By dialing a certain number, this automatic subscriber will report by tone signals on the operational condition of the plant. In addition, an alarm sending device in the terminal exchange will signal disturbances that may occur in any of the more-important units of the switching plant. These signals are received in the tandem exchange.

Every line engagement causes the terminal exchange to be connected by a junction to the

* Reprinted from *SEG-Nachrichten*, volume 3, number 1, pages 35–38; 1955.

[1] J. Bernutz, "Der Koordinatenschalter KS 53," *SEG-Nachrichten*, volume 2, number 1, pages 6–10; 1954.

[2] R. Scheidig, "Der Zählmagnet ZM 53," *SEG-Nachrichten*, volume 2, number 1, pages 11–13; 1954.

[3] A. Mehlis, "Wähler oder Schalter als Verbindungsorgane in der Fernsprechvermittlungstechnik," *Fernmeldtechnische Zeitschrift*, volume 5, pages 293–296; 1952.

andem exchange, where a central register–ranslator switches into the circuit, takes all lialing digits, and remains connected to the ine until it receives the end-of-selection signal.

The dialed zone, as established by the register–translator, is passed on to a metering pulse sender permanently connected to the junction; as soon as the conversation begins, metering

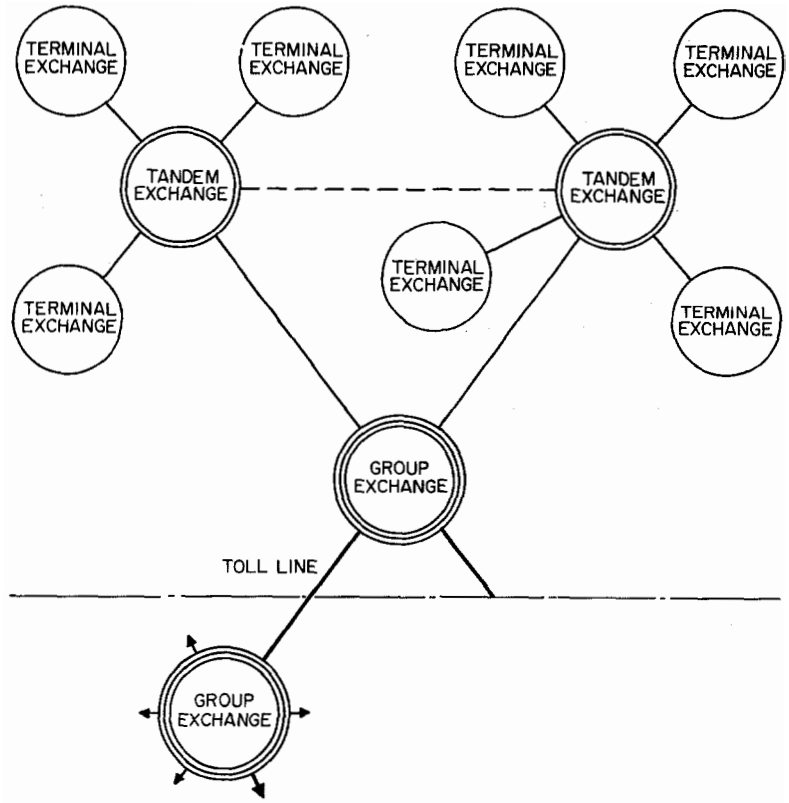

Figure 1—Layout of a group within the Finnish network.

This register–translator performs the following operations.

A. Route control; that is, selection of the shortest possible route (direct or tie lines between tandem exchange).

B. Determination of dialed zone for message metering.

C. Prevention of false engagements beyond the tandem office.

D. Upon storage of long-distance digit *9*, connection of a long-distance storage device in the group exchange to route the call.

pulses are transmitted to the calling subscriber. The interval between pulses corresponds to the zone and decreases with increasing distance.

All signals are transmitted through a junction as alternating-current signals and converted to direct-current signals at the receiving end. Since the relay repeaters are designed for simultaneous transmitting and receiving, only two signals, differentiated by their length and sequence, are necessary. This simplifies the engineering and reduces lost time. The repeater relays in any intermediate exchanges operate as pulse repeaters for a connection, requiring no counting devices. Hence, the code scheme can be modified without modification of the relay repeaters.

Using additional plant, terminal exchanges

can operate with carrier systems as well, both with in-band and out-of-band signaling, the latter being the case in which signals are regenerated in the carrier system.

The busy signal, or revertive blocking, can be a continuous signal in lines without amplifiers. In lines with amplifiers, blocking is brought about by pulsed signals to avoid overloading the group amplifiers.

the subscriber's last two digits, one magnetic counter KS to control sequence of dialing, and one magnetic counter KM checking the exchange code, which is part of the five-digit directory number. All dialing information for long-distance and short-haul (internal) traffic is received and evaluated by these magnetic counters. When a call remains within the terminal exchange, an internal linking circuit is engaged to check,

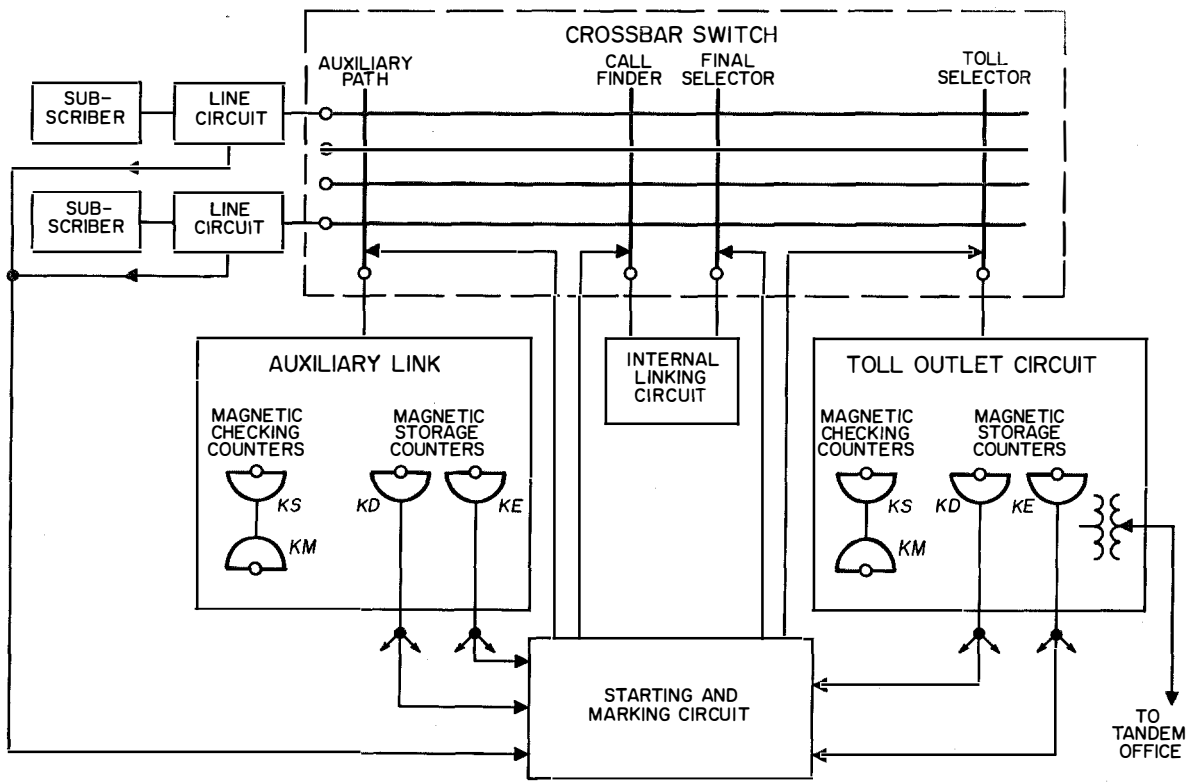

Figure 2—Starting and marking of junctions in a crossbar exchange.

3. Establishment of Connections

The establishment of a connection will be explained with reference to Figure 2. The junctions between terminal and tandem exchanges are bidirectional. In the terminal exchange, this junction leads to the long-distance outlet, connecting to one of the vertical bars of the crossbar switch. In the incoming direction, this vertical bar operates as a trunk final selector; in the outgoing direction as a call finder. Each external linking circuit has two magnetic counters, KD and KE, for the storage of the call, connect lines, and meter. Accordingly, this internal linking circuit is comparatively simple.

3.1 External Connections

For an external connection or a long-distance call, the subscriber actuates the starting and marking circuit by lifting the handset. These circuits connect a free trunk selector to the subscriber's line. At the same time, the tandem exchange end of the junction is coupled to a register–translator. The subscriber's dial pulses

are stored by the register in the tandem exchange and by the magnetic checking counter in the terminal exchange. Since the called subscriber is connected to an external terminal exchange, the dialed exchange code will not correspond to the code of the calling subscriber's exchange. In this case, the subscriber's terminal exchange does not accept further dial pulses. The evaluation of the pulse series for further routing is accomplished in the register of the tandem exchange alone.

The first revertive pulse reaching the calling subscriber's terminal exchange is the starting signal. It actuates the first counting pulse applied to the subscriber's meter and, for coin boxes, the reversal of the line conductors. Other subsequent counting pulses are emitted by the pulse sender in the tandem exchange and are counted during the conversation.

3.2 Internal Connection

When a subscriber of the same terminal exchange is being called, the long-distance outlet is seized in the same way as in the case of an external call. However, the office code dialed is now that of the same exchange; as soon as the magnetic checking counter has noted this identity, a clear-forward pulse will prevent any false engagement of the same terminal exchange on a second junction. When the last two pulse series have adjusted magnetic counter *KD* and *KE* for storage, the long-distance outlet circuit will connect to the marking circuit via a common lockout chain. The marking circuit has two functions.

A. To connect an internal linking call finder to the calling subscriber's line.

B. To connect the final selector of this internal link with that subscriber's line marked by magnetic storage counters *KD* and *KE*.

When the connection between calling and called subscribers is established—which takes about 150 to 200 milliseconds—the long-distance outlet releases the marking circuit and terminates the pulse, clearing the junction to the tandem exchange. The internal linking circuit can meter the conversation either by one pulse per conversation or by pulses timing the length of the conversation, depending on local conditions. In the first case the metering pulse is emitted at the end of conversation.

If the called subscriber is busy or if no free path in the internal linking circuit is available, all circuits engaged by the calling subscriber are immediately released and a busy tone is transmitted to the subscriber. If all long-distance outlets are busy when a subscriber tries to establish an internal connection, this connection can still be established via an auxiliary link. This auxiliary link will also release all circuits and transmit the busy tone to the calling subscriber in the case where the called subscriber belongs to another terminal exchange.

3.3 Incoming Traffic

In the case of an incoming call, the exchange code has been absorbed by the preceding selector stages; the two remaining digits actuate *KD* and *KE* in the same way as for local traffic. The called line is correspondingly marked and the crossbar-switch vertical bar is switched. The long-distance outlet circuit gives the signals for end of dialing, called-subscriber answering, and clearing. Where an incoming call is connected by an operator, there is the possibility of the operator's cutting into an existing conversation.

4. Ancillary Plant

Two-party lines, coin boxes, and grouped-number service (private-branch-exchange line hunting) are provided. The various numbers of a grouped number are not bound to a certain sequence, which would confine them to the same decade. Without any switching procedure, they can be used as night call numbers. In a fully equipped terminal exchange, eleven lines are additionally available; for instance, for grouped numbers or for coin boxes.

5. Testing Equipment

Tests of all switching facilities and metering circuits are provided. The switching plant can also be tested separately.

5.1 Testing Long-Distance Outlet Circuits, Outgoing Direction

When the test relay set (Figure 3) is connected to jack *J2* of the long-distance outlet circuit, the

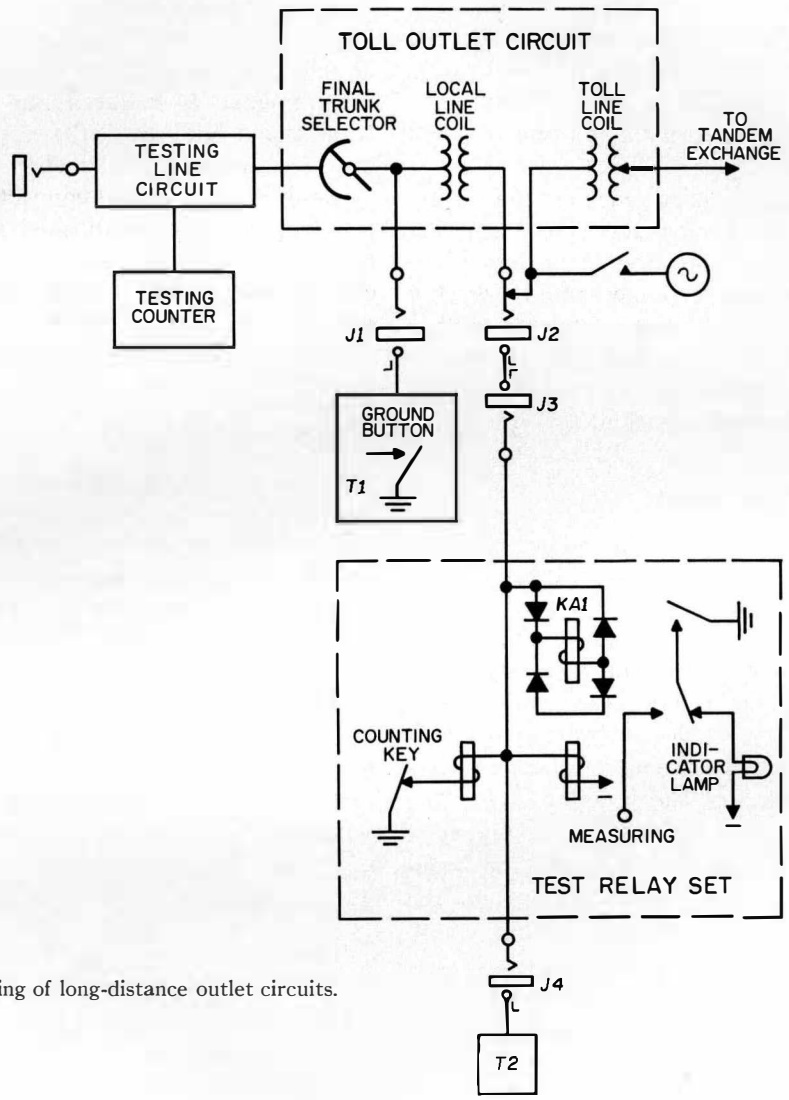

Figure 3—Testing of long-distance outlet circuits.

junction to the tandem exchange is revertively blocked. The cord of tester *T1* is connected to jack *J1*. Brief depression of the ground button in *T1* engages the long-distance outlet and generates the engaged pulse. The *KA1* relay in the test transmission circuit receives the engaged pulse, the subsequent dial pulses, and the clear-forward pulse, which are then evaluated by a test setup or made visible by an indicator lamp.

The revertive called-subscriber answering and metering pulses are initiated by a short depression of the counting key; replacing the handset is followed by a release guard signal pulse.

5.2 Testing Long-Distance Outlet Circuits, Incoming Direction

The number of the automatic subscriber serves also as a test number. The automatic subscriber is connected through jack contacts and is disconnected by the engagement of this jack with tester *T2*.

When digit *1* is dialed, *T1*—now connected to jack *J4* to establish the connection—transmits

an engaged pulse. Now the number of the automatic subscriber is dialed; the latter is connected to *T2*. In this procedure, revertive pulses are evaluated by the test relay circuit.

Instead of calling *T2*, any one of the ordinary subscribers' lines may be called.

5.3 Testing Internal Link Circuits

Tester *T1* is connected to the jack of the internal link circuit under test while *T2* is again connected to the jack of the automatic subscriber (Figure 4).

When engaged by depressing the button, the

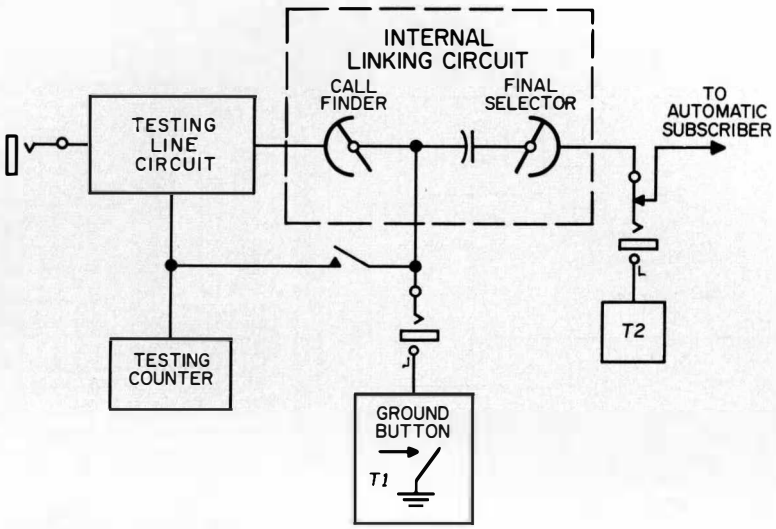

Figure 4—Testing of internal linking circuits.

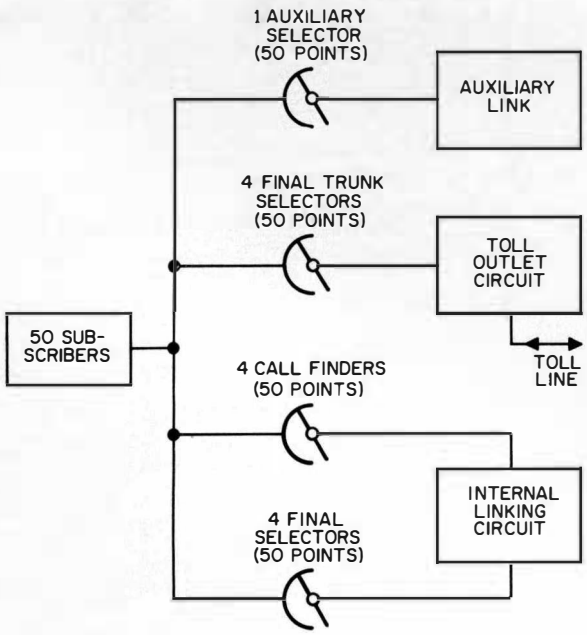

Figure 5—Trunking scheme for 50-subscriber equipment.

internal linking circuit automatically adjusts itself to the directory number of the automatic subscriber and performs all functions including metering.

5.4 Operational Test

This test requires connection of the testing line circuit to *T1*. It permits establishment of all connections outgoing from the crossbar-switch terminal exchange. The subscribers' lines are connected to the terminal exchange via a disconnecting distributor. When the plugs are disconnected, the circuits can be tested either with or without the subscribers' lines.

6. Trunking Scheme

As will be seen from Figure 5, the crossbar terminal exchange is equipped with circuits for 50 subscribers, 4 long-distance outlets, 4 internal linking circuits, and 1 auxiliary link. When

equipped to full capacity (100 subscribers), the terminal office comprises 6 long-distance, 6 internal, and 1 auxiliary circuits. The long-distance outlets, the auxiliary link, and the final selectors have a total of 100 points. The call finders of the internal linking circuits are subdivided into 4 call finders with 50 points or outlets handling the normal traffic and two 100-point call finders for the peak traffic. This is shown in Figure 6.

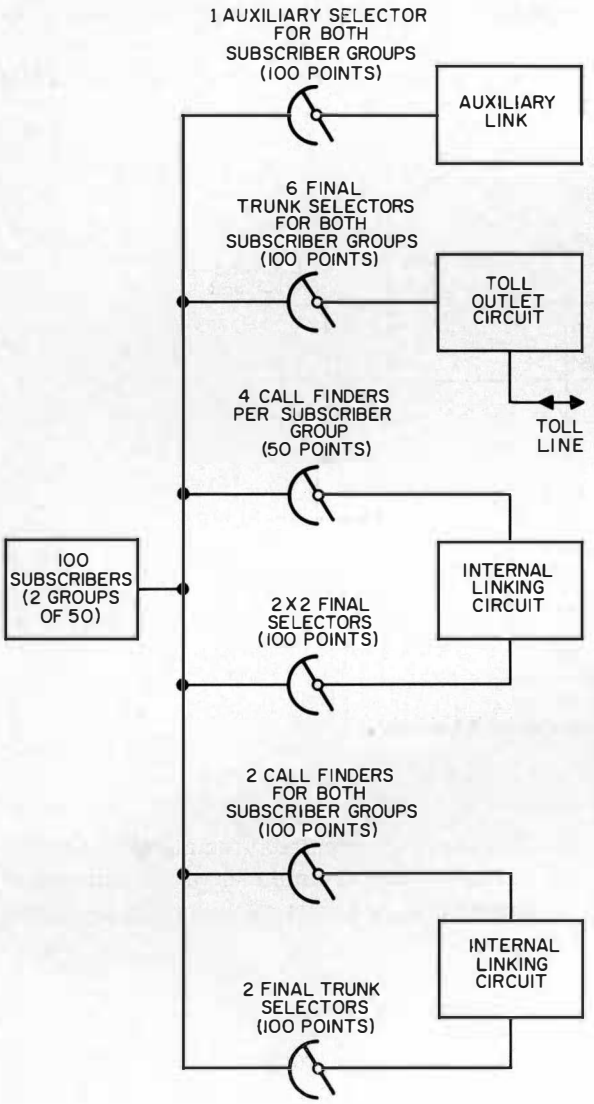

Figure 6—Trunking scheme for 100-subscriber equipment.

7. *Construction*

The crossbar exchange is mounted in a bay about 7 feet (2.1 meters) high, 40 inches (1 meter) wide, and about 20 inches (0.5 meter) deep, as shown in Figure 7. All switching circuits are arranged on two hinged frames and are easily accessible. The front frame comprises the subscribers' relays, metering circuits, the crossbar switch, and the central marking circuit. The rear frame carries the relays of the long-distance outlet circuits, internal links and auxiliary link, as well as signaling and testing equipment, jacks, and push buttons.

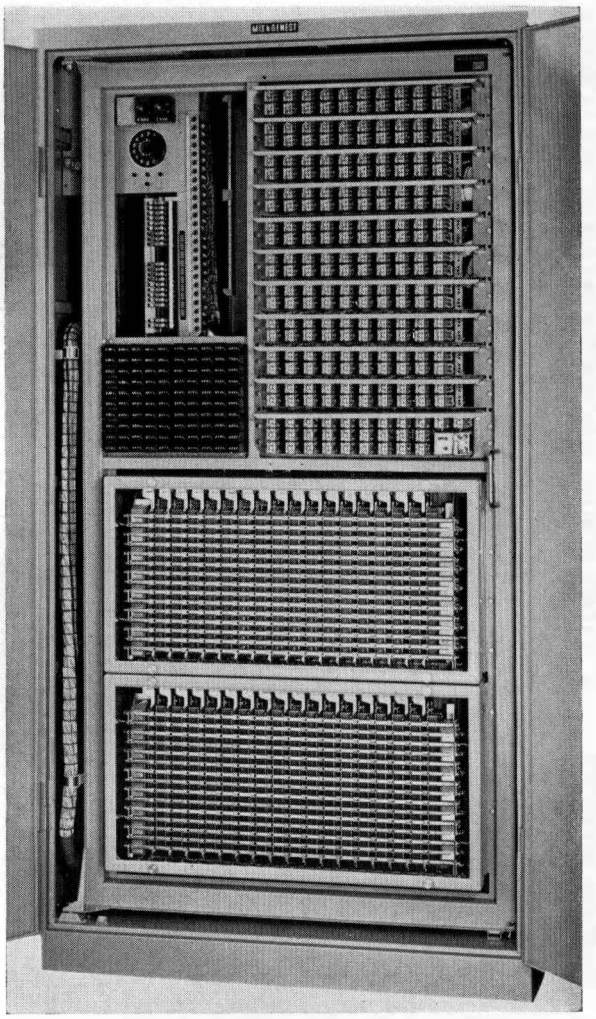

Figure 7—Crossbar terminal exchange.

Two-wire Repeater Employing Negative Impedance*

By THEODOR G. GREWE

Mix & Genest Werke, division of Standard Elektrik Lorenz A.G.; Stuttgart, Germany

COMPENSATION for losses in a nonloaded cable can be accomplished with a simple circuit having attenuation and impedance values that are similar in the voice-frequency band to those of a cable for which the circuit may be substituted. The desired properties are obtained with a bridge network consisting of a balancing inductance and two simple resistance–capacitance branches. These branches are converted into negative impedance by two single-stage transistor amplifiers. The result is an equivalent circuit having, through its negative impedances, the properties of a two-wire repeater.

1. Application

The repeater is designed for voice-frequency-operated, nonloaded two-wire lines. The circuit components determining the characteristic impedance and the gain can be inserted as individual units, which makes the repeater readily adaptable to cables having various conductor diameters. Particular care was exercised to obtain a characteristic impedance similar to that of standard cables. The remaining net loss of a repeater section is small and is only slightly dependent on the location of the repeater. The gain can be adjusted so that the net loss becomes independent of frequency. For instance, with a cable loss of 10 decibels at 800 cycles per second and 19 decibels at 3400 cycles, a reduction in attenuation to about 4 decibels can be achieved.

2. Reduction of Attenuation by Negative Resistances

Assume a structurally nonsymmetrical T network consisting of the resistances $\mathbf{R}_1$, $\mathbf{R}_2$, and $\mathbf{R}_3$ as shown in Figure 1A. The attenuation of this network can be compensated by connecting to the series resistances $\mathbf{R}_1$ and $\mathbf{R}_2$ two equivalent negative resistances $-\mathbf{R}_1$ and $-\mathbf{R}_2$ and in parallel with the shunt resistance $\mathbf{R}_3$ a negative resistance $-\mathbf{R}_3$ having the same absolute value. This is shown in Figure 1B.

The same effect can be obtained by connecting the three negative resistances as a separate T network. Alternatively, both T networks may be combined into a π network so that, at the junction points, structural symmetry of opposing signs is formed. This is shown in Figure 1C. Resistances $\mathbf{R}_3$ and $-\mathbf{R}_3$ are connected without loss by the resistances $\mathbf{R}_2$ and $-\mathbf{R}_2$. The value of the parallel resistances $\mathbf{R}_3$ and $-\mathbf{R}_3$ is infinite, and the resistances $\mathbf{R}_1$ and $-\mathbf{R}_1$ cancel each other.

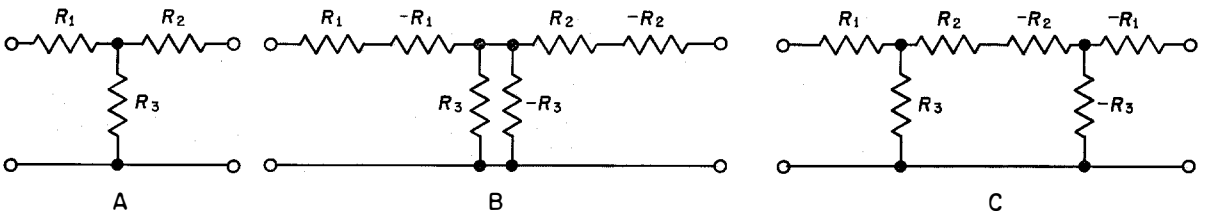

Figure 1—The attenuation of the nonsymmetrical T network at *A* may be compensated for by the insertion of corresponding negative impedances at *B*, which may also be accomplished at *C* by converting to an equivalent π network.

Within a limited frequency band, a telephone line can be approximated by a structurally symmetrical T network. Hence, the attenuation of this line could be cancelled by a symmetrical T network consisting of three negative resistances. However, the use of an equivalent circuit consisting of a bridge network with a symmetrical balancing inductor is advantageous because the number of required negative resistances is reduced to two.

* Originally published under the title "Ein Zweidrahtverstärker mit negativen Widerständen" in *Nachrichtentechnische Zeitschrift*, Volume 8, pages 610–618; November, 1955.

3. *Properties of Bridge Network*

According to Bartlett's theorem,[1] there is an equivalent bridge network for any symmetrical four-pole circuit. In the case where such a circuit represents a line of length $2l$ (see Figure 2A), the equivalent circuit is a lattice network shown in Figure 2B, where the two series impedances of the line legs $\mathbf{Z}_s$ must be equal to the short-circuit resistance and the two shunt impedances $\mathbf{Z}_o$, must be equal to the open-circuit resistance of a cable having the length l.

In the frequently used equivalent bridge network having a balancing inductor in one leg (see Figure 2C), the series impedance must be of twice the value of the short-circuit resistance and the shunt impedance must equal half the value of the open-circuit resistance. The same applies to another bridge network where the short-circuit and the open-circuit values are merely interchanged as in Figure 2D. These resistances refer to the cable length l.

The ideal negative line for compensating the attenuation of a cable of length $2l$ could, then, be constructed as shown in Figure 3. The passive impedances balancing the open-circuit and short-circuit impedances are changed by converters into negative impedances. Due to the finite bandwidth of the converter components, however, this conversion can be achieved only approximately and for a limited frequency band. The balancing of the cable impedance can also be only approximated by a limited number of components. Therefore, the properties of a bridge network having two arbitrary impedances $\mathbf{Z}_1$ and

[1] R. Feldtkeller, "Einführung in die Vierpoltheorie der Nachrichtentechnik," Hirzel, Leipzig; 1948.

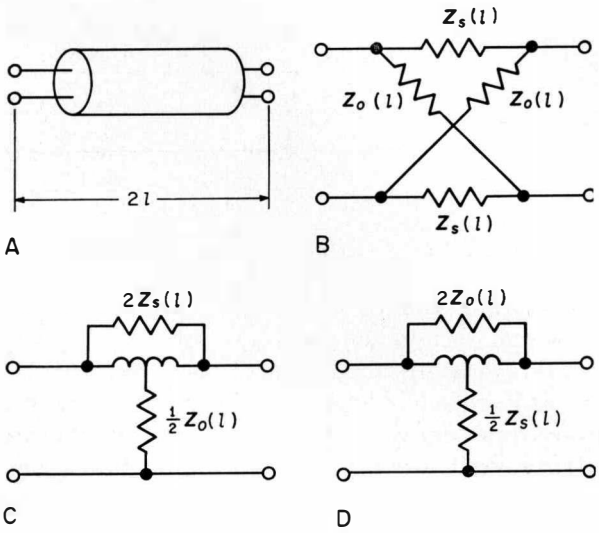

Figure 2—Equivalent lattice or bridge networks for a two-wire line.

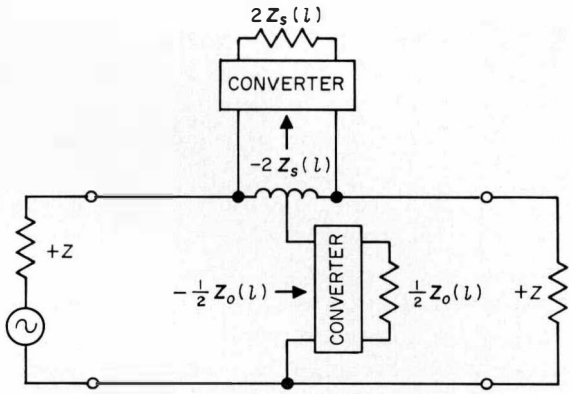

Figure 3—Construction of ideal negative line to compensate for the attenuation of a cable of length $2l$.

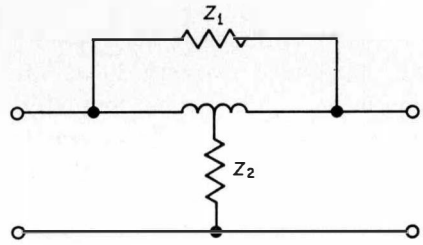

Figure 4—Bridge network having two arbitrary impedances.

$\mathbf{Z}_2$ will be discussed first. For the characteristic impedance $\mathbf{Z}$ and the image transfer constant $g = a + jb$ of the circuit shown in Figure 4, the following two equations are valid.

$$\mathbf{Z} = (\mathbf{Z}_1\mathbf{Z}_2)^{1/2} \tag{1}$$

$$g = a + jb = \ln \frac{1 + \frac{1}{2}(\mathbf{Z}_1/\mathbf{Z}_2)^{1/2}}{1 - \frac{1}{2}(\mathbf{Z}_1/\mathbf{Z}_2)^{1/2}}. \tag{2}$$

Since the characteristic impedance depends only on the product and the image transfer constant depends on the ratio of the impedances $\mathbf{Z}_1$ and $\mathbf{Z}_2$, the values for $\mathbf{Z}$ and g can be prescribed independently of each other. If the bridge-network impedance $\mathbf{Z}_1$ is related to the characteristic impedance by $\mathbf{N} = \mathbf{Z}_1/\mathbf{Z}$, where $\mathbf{N}$ is generally

the complex function of the frequency ω, then using (1),

$$\mathbf{Z}_1 = \mathbf{N}\mathbf{Z} \tag{3}$$

$$\mathbf{Z}_2 = \mathbf{Z}/\mathbf{N} \tag{4}$$

and (2) can be replaced by

$$g = \ln \frac{1 + \mathbf{N}/2}{1 - \mathbf{N}/2}. \tag{5}$$

Equation (2) is represented in Figure 5 as a diagram of the complex relation of the bridge-network branches $\mathbf{Z}_1/\mathbf{Z}_2 = |\mathbf{Z}_1/\mathbf{Z}_2| \exp j\varphi_D$ with the parameters $\mathbf{Z}_1/\mathbf{Z}_2$ and φ_D in the plane of the image transfer constant $a + jb$ for positive

Figure 5—Diagrams of the functions

$$a + jb = \ln \frac{1 + \frac{1}{2}(\mathbf{Z}_1/\mathbf{Z}_2)^{1/2}}{1 - \frac{1}{2}(\mathbf{Z}_1/\mathbf{Z}_2)^{1/2}}$$

with $\mathbf{Z}_1/\mathbf{Z}_2 = |\mathbf{Z}_1/\mathbf{Z}_2| \exp j\varphi_D$ and for $\mathbf{Z}_1/\mathbf{Z}_2$ and φ_D as parameters. Curve *1* is the propagation constant for a nonloaded cable. Curve *2* is for the circuit of Figure 4 with resistance and capacitance in parallel for $\mathbf{Z}_1$ and in series for $\mathbf{Z}_2$, for frequency limited to 3 kilocycles, and for $\mathbf{Z}_{10}/\mathbf{Z}_{20} = 1.5$. In curve *3*, $\mathbf{Z}_{10}/\mathbf{Z}_{20} = 2$. Curve *4* is for a repeater adjusted for $S_0 = 1.6$ nepers at 3 kilocycles. See Figure 25. The circles and figures on the curves designate frequency in kilocycles. The added zero subscript indicates that the impedances are adjusted for maximum power transfer.

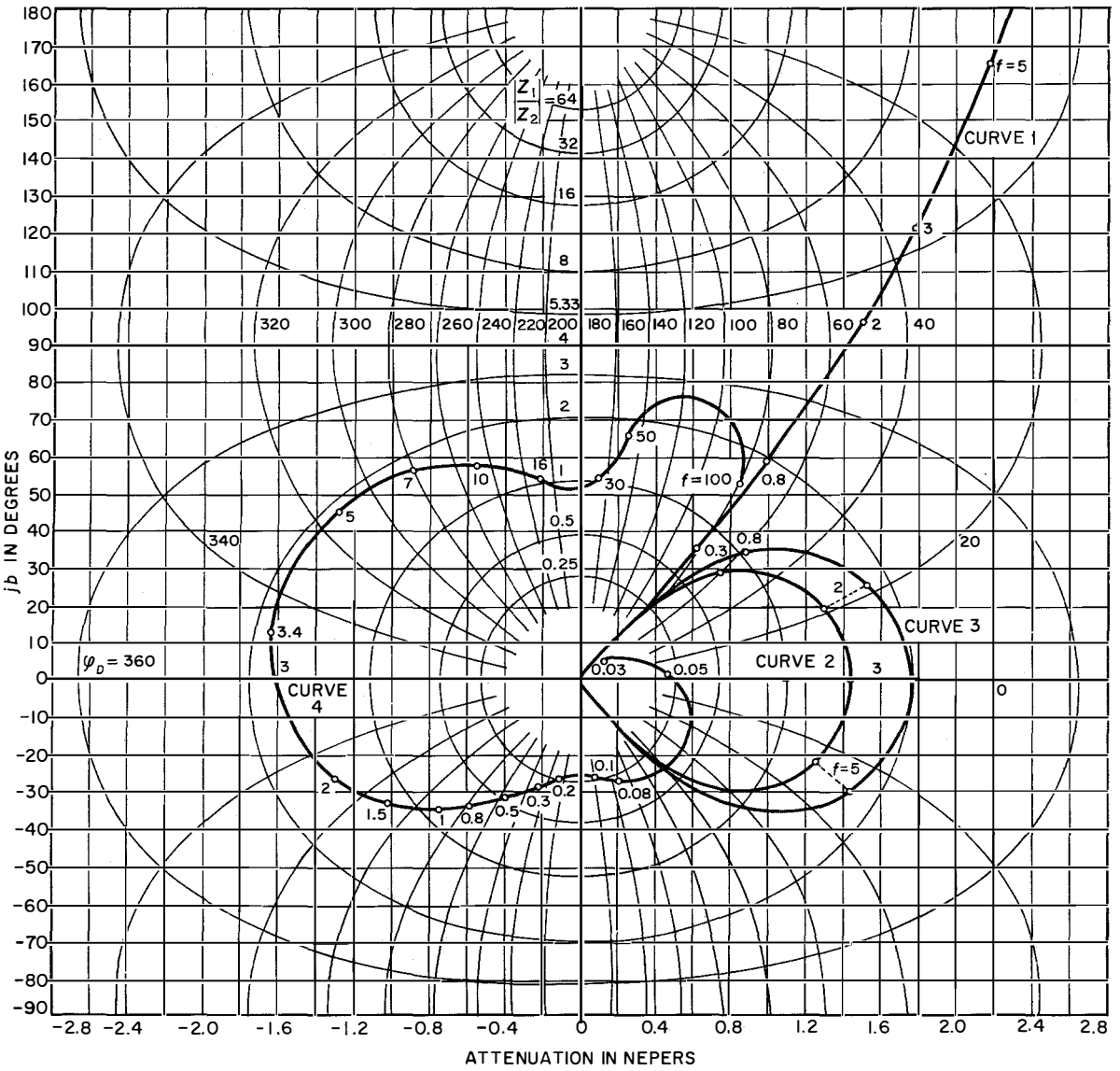

root values. It will be seen that, at a given ratio $|\mathbf{Z}_1/\mathbf{Z}_2|$, the maximum attenuation is at $\varphi_D = 0$. The wave attenuation decreases with increasing angular values and reaches zero at $\varphi_D = 180$ degrees. At this point, the image transfer constant is imaginary, as that of an all-pass network. When the difference angles increase to $\varphi_D = 180$ degrees; that is, with negative root values, the wave attenuation becomes negative. In the case under discussion, it is desirable that the network have negative wave attenuation and a positive characteristic impedance. No special dimensioning is necessary to achieve the desired polarity of

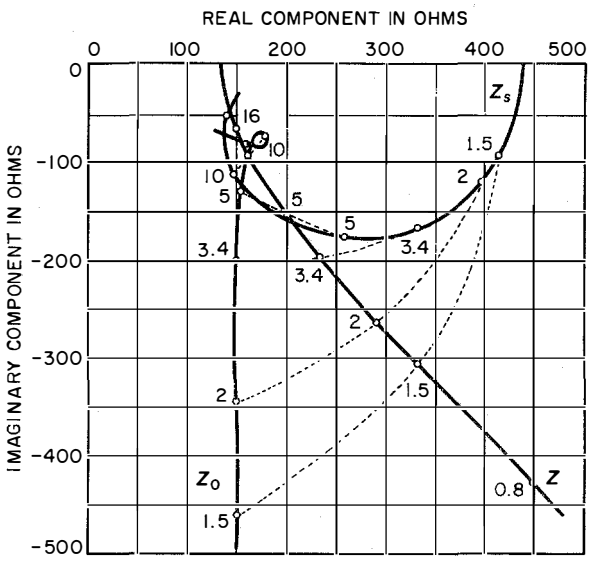

Figure 6—Impedance of 0.03-inch (0.8-millimeter) cable, 3.75 miles (6 kilometers) long, having the characteristics required by the Deutschen Post.

the characteristic impedance. If the termination impedance of an arbitrary symmetrical network equals the positive characteristic impedance of that network, then the network will also have a positive characteristic impedance. If, contrariwise, the termination impedance is equal to the negative characteristic impedance of the network, then the network will also have a negative characteristic impedance. The reason is that reflections are not admissible, whether the network be terminated by positive or by negative characteristic impedances.

The wave attenuation of any quadripole may also be either positive or negative. If the phasors of the three impedances, that is, the bridge-network impedances $\mathbf{Z}_1$ and $\mathbf{Z}_2$ and the characteristic impedance chosen for the termination are located in a semiplane, then the wave attenuation is positive; if the range of a semiplane is exceeded, the wave attenuation becomes negative. The separation line between the two semiplanes can form an arbitrary angle with the real axis. Thus, for instance, a purely resistive line will have negative attenuation if terminated by negative resistors. In the case of our repeater, the termination impedances have positive resistive components; therefore, at least one of the two bridge-network impedances must have a negative resistive component to cause the three impedances to exceed the range of a semiplane.

4. *Replacing Short- and Open-Circuit Impedances by Simple Networks*

For stability reasons, the net loss of the line repeater section must increase quickly outside the transmitted band. The ideal negative line discussed in section 3 does not comply with this requirement. Other branch networks must be examined to obtain one having the desired increase of net loss and, if possible, to require a minimum of circuit components. For instance, the repeater is to be dimensioned for a subscriber cable with a conductor diameter of 0.8 millimeter (0.03 inch) and line constants[2] of

$R' = 73.2$ ohm per kilometer
$= 117.8$ ohm per mile
$C' = 0.038$ microfarad per kilometer
$= 0.061$ microfarad per mile
$L' = 0.7$ millihenry per kilometer
$= 1.13$ millihenry per mile.

The function of this repeater is to compensate for the attenuation of the cable along a section of $2l = 12$ kilometers (7.5 miles) in the band 300 through 3400 cycles (Figure 5, Curve *1*). The open-circuit and short-circuit impedances of half of this section, $l = 6$ kilometers (3.75 miles), are shown in Figure 6. The short-circuit impedance can be approximately balanced in a limited frequency band by a parallel resistance–capacitance branch and the open-circuit impedance by a series resistance–capacitance branch. With

[2] "Telegraphenmessordnung der Deutschen Post," part 4-TMO 4; 1939.

ideal converters, the bridge network of Figure 4 could be constructed with impedance characteristics shown in Figure 7. If R_1 and C_1 are the

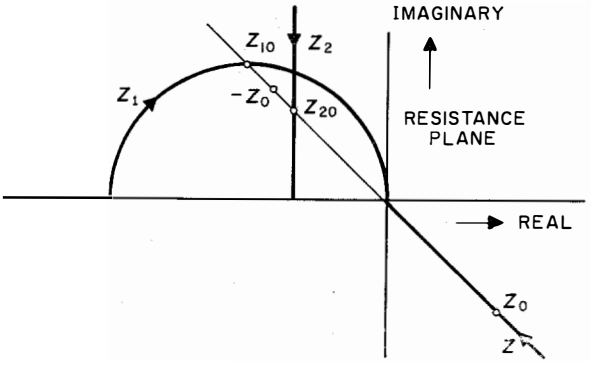

Figure 7—Impedance diagrams of resistance–capacitance branches $\mathbf{Z}_1$ and $\mathbf{Z}_2$, consisting of resistance–capacitance combinations and of the characteristic impedance $\mathbf{Z}$ of the bridge network. $\mathbf{Z}_{10}/\mathbf{Z}_{20} = 1.5$.

components of the branch $\mathbf{Z}_1$, and R_2 with C_2 are those of branch $\mathbf{Z}_2$, the following will be true.

$$\mathbf{Z}_1 = \frac{R_1}{1 + j\omega C_1 R_1} \tag{6}$$

$$\mathbf{Z}_2 = \frac{1 + j\omega C_2 R_2}{j\omega C_2} \tag{7}$$

and the characteristic impedance

$$\mathbf{Z} = \left[\frac{R_1}{j\omega C_2} \frac{1 + j\omega C_2 R_2}{1 + j\omega C_1 R_1} \right]^{1/2}. \tag{8}$$

If the same cutoff frequencies are chosen for both resistance–capacitance components, namely

$$\omega_0 = 1/(C_1 R_1) = 1/(C_2 R_2) \tag{9}$$

the simple relation

$$\mathbf{Z} = (R_1/j\omega C_2)^{1/2} \tag{10}$$

is obtained.

Now the characteristic impedance of the nonloaded cable with the line constants R', L', and C' is

$$\mathbf{Z}_k = [(R' + j\omega L')/(j\omega C')]^{1/2}. \tag{11}$$

Neglecting for the moment the effect of the inductance of the cable, the characteristic impedance of the bridge network and of the cable will coincide if

$$R_1/C_2 = R'/C'. \tag{12}$$

According to (2), the characteristic impedance depends on the ratio of the two bridge network impedances. From (6), (7), and (9), it follows that

$$\frac{\mathbf{Z}_1}{\mathbf{Z}_2} = \frac{j\omega R_1 C_2}{[1 + j(\omega/\omega_0)]^2}. \tag{13}$$

If we write

$$\frac{\mathbf{Z}_1(\omega_0)}{\mathbf{Z}_2(\omega_0)} = \frac{\mathbf{Z}_{10}}{\mathbf{Z}_{20}} = \frac{\omega_0 R_1 C_2}{2} = N_0^2 \tag{14}$$

and

$$\Omega = \omega/\omega_0, \tag{15}$$

then (13) may be rewritten

$$\mathbf{N}^2 = \frac{\mathbf{Z}_1}{\mathbf{Z}_2} = N_0^2 \frac{2j\Omega}{(1 + j\Omega)^2}. \tag{16}$$

From (16) and (5), the image transfer constant can be computed.

$$a + jb = \ln \frac{1 + \frac{1}{2}N_0\Omega^{1/2} + j(\Omega + \frac{1}{2}N_0\Omega^{1/2})}{1 - \frac{1}{2}N_0\Omega^{1/2} + j(\Omega - \frac{1}{2}N_0\Omega^{1/2})}. \tag{17}$$

The real component of (17), the wave attenuation a, is represented over the scale $\Omega^{1/2}$ of Figure 8 for the values $N_0^2 = \mathbf{Z}_{10}/\mathbf{Z}_{20} = 1.0$, 1.5, and 2.0. The wave attenuation of a nonloaded cable varies in this diagram somewhat like a straight line crossing the zero point. If the frequency $\Omega = 1$ is chosen as the upper cutoff frequency of the transmitted band, the requirements of good equalization and rapid decrease of gain outside this band can be closely approximated.

The characteristics of the image transfer constant with positive real component as per (17) are plotted in Figure 5 (Curves *2* and *3*) for the values $N_0^2 = \mathbf{Z}_{10}/\mathbf{Z}_{20} = 1.5$ and 2. The frequency $f_0 = 3$ kilocycles was chosen as the cutoff frequency of the bridge network impedances. If the bridge network shown in Figure 8 were equipped with ideal converters and the terminations consisted of positive characteristic impedances, the corresponding characteristics of the image transfer constant would have the appearance of curves *2* and *3* of Figure 5, rotated by 180 degrees around the zero point. The combination of the line and repeating network would have a smaller phase constant than the line alone. For the operation of the repeater, it would be essential to reduce the phase constant for the whole transmission band for it is well known that the phase

constant of a nearly lossless line causes at mismatch considerable ripple of the effective attenuation.

The achievable reduction is closely related to the net loss outside the transmitted band, however. The more the compensation for attenuation extends beyond the transmitted or signal band,

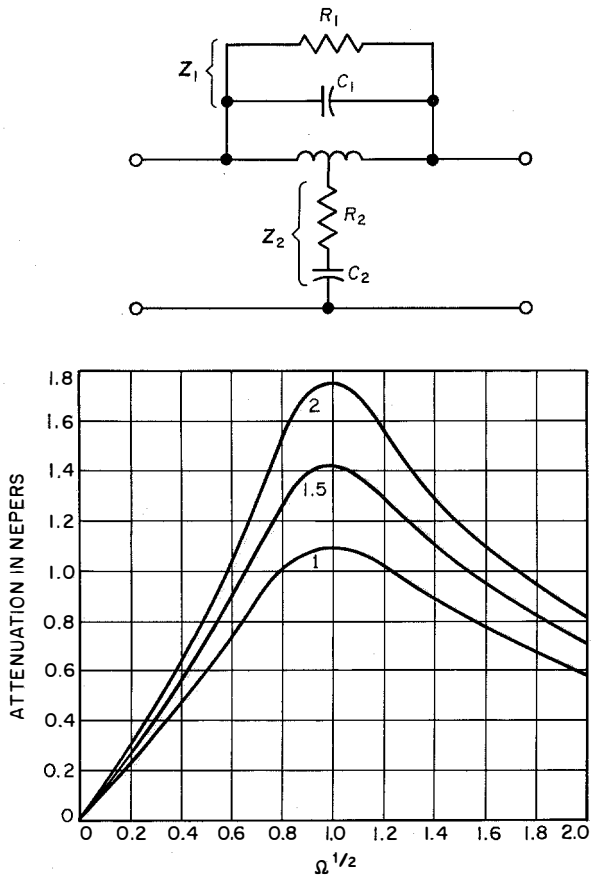

Figure 8—Example of attenuation for a bridge network of resistance and capacitance. $\mathbf{Z} = (R_1/j\omega C_2)^{1/2}$. $C_1R_1 = C_2R_2 = 1/\omega_0$. $\Omega = \omega/\omega_0$. The curves are for the indicated values of $\mathbf{Z}_{10}/\mathbf{Z}_{20}$.

the greater is the phase-rotation effect of the repeater. On the other hand, stability considerations demand that the net loss rise steeply beyond the edges of the signal band. An elimination of the phase constant in the whole frequency band, which would amount to the elimination of the delay time of a pulse, cannot be realized because any practical negative impedance would be transformed into a positive resistance, at least at high frequencies.

The following section contains an estimate of the effect of the phase constant in the particularly unfavorable case of operation where both ends of the repeater section are directly terminated by subscriber stations.

5. Line Loss of a Repeater Section

The line loss a_B of a symmetrical quadripole having propagation constant $g = a + jb$, characteristic impedance $\mathbf{Z}$, and terminations $\mathbf{R}_1$ and $\mathbf{R}_2$ can be expressed by several partial losses[3]

$$a_B = a + \ln\left|\frac{\mathbf{R}_1 + \mathbf{Z}}{2(\mathbf{R}_1\cdot\mathbf{Z})^{1/2}}\right| + \ln\left|\frac{\mathbf{R}_2 + \mathbf{Z}}{2(\mathbf{R}_2\cdot\mathbf{Z})^{1/2}}\right| + \ln|1 - \mathbf{r}_1\mathbf{r}_2\exp|-2g|, \quad (18)$$

where

$$\mathbf{r}_1 = \frac{\mathbf{R}_1 - \mathbf{Z}}{\mathbf{R}_1 + \mathbf{Z}}$$

$$\mathbf{r}_2 = \frac{\mathbf{R}_2 - \mathbf{Z}}{\mathbf{R}_2 + \mathbf{Z}}.$$

The first term a is the wave attenuation, the second is the reflection attenuation at the input, the third is the same attenuation at the output. The fourth term takes account of the effect of the reflected waves and is called the interaction term.

For the above-stated case of operation with two subscriber stations, $\mathbf{R}_1 = \mathbf{R}_2 = \mathbf{R}$ may be written. Equation (18) can thus be rewritten

$$a_B = a + \ln\left|\frac{1 - \mathbf{r}^2\exp - 2(a + jb)}{1 - \mathbf{r}^2}\right|. \quad (19)$$

Now the subscriber-station impedance has a positive phase angle of about 50 degrees while the characteristic impedance of the cable has a negative angle of about − 40 degrees. The differences of the absolute values of both impedances are not very large in midband. If the particularly adverse case of equal impedance values is considered, then the reflection coefficient will be equal to unity as a result of the angle difference of 90 degrees and will have a phase of 90 degrees ($\mathbf{r} = j$). Introducing this value $\mathbf{r} = j$ in (19), the second term will be positive at the values $b = 0, \pi, 2\pi \cdots$ and negative at the values $b = \pi/2, 3\pi/2, 5\pi/2 \cdots$. The limit values of the line loss found with these angular values are plotted in Figure 9 for wave attenuations up to 8.7 decibels (1 neper).

[3] J. Wallot, "Theorie der Schwachstromtechnik," Springer-Verlag, Berlin; 1944.

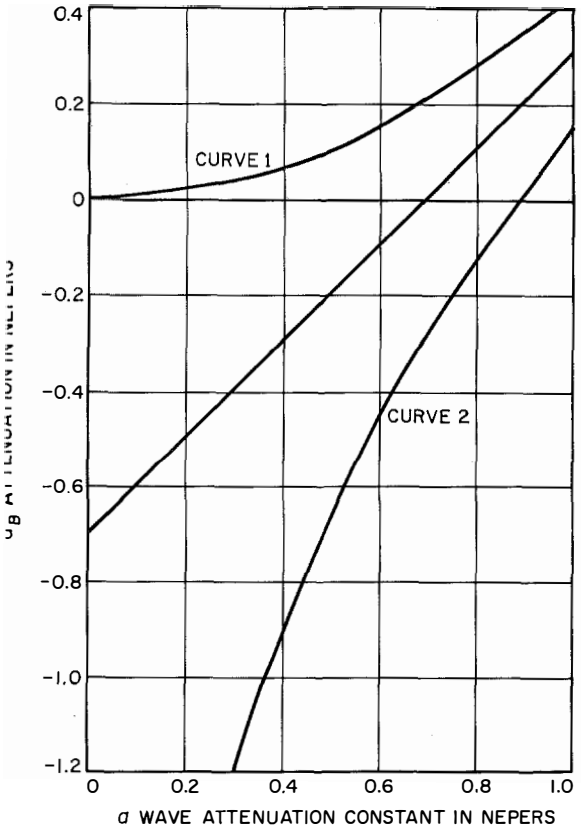

Figure 9—Limiting values of $a_B = a - \ln 2 + \ln|1 - 2\exp - 2(a + jb)|$ the attenuation of a repeater section having end-reflection coefficients corresponding to $\mathbf{r}_1 = \mathbf{r}_2 = j$. Curve *1* is for the highest values of a_B found at $b = 0, \pi, 2\pi \cdots$. Curve *2* is for the smallest values for $b = \pi/2, 3\pi/2, 5\pi/2 \cdots$. The middle curve is for $a_B = a - \ln 2$.

Figure 9 shows that the line loss can assume large negative values when the wave attenuation a of the repeater section is small. In the discussed case, this gain peak may be expected in the region of 2 kilocycles because at this frequency the phase constant of the repeater section will have the approximate value of $\pi/2$ as can be shown by curves *1* and *2* or curve *3* of Figure 5. The next critical value $3\pi/2$, is far outside the signal band.

6. *Effect of Reflections on Stability*

The varying terminations of the repeater section under operational conditions must not cause self-oscillation. This requirement is fulfilled if the loop gain in the two-wire system is always less than unity, regardless of the phase rotation.[3]

Figure 10 shows the general arrangement of a repeater section. Both ends of the repeater are connected by cables of different lengths to termination impedances. The loop gain depends on the gain $S = \exp s$ of the repeater, on the cable attenuations $A_n = \exp a_n$, and on the reflection coefficients r_n between the characteristic impedances and the termination impedances $\mathbf{Z}_n$. If, for example, the wave U_3 leaves the repeater at point *3*, the junction at this point will reflect the amount $U_3 r_3$ of the wave. The wave entering cable *2* is slightly distorted by the junction point *3*; this will be neglected in the following equation. Now the wave is propagated along the cable several times in the manner indicated in the sketch. The linear addition of the waves returning to point *3* gives

$$\begin{aligned} U'_3 &= U_3[r_3 + (r_4/A_2^2) + (r_4/A_2^2)^2 r_3 \\ &\qquad + (r_4/A_2^2)^3 r_3^2 + \cdots] \\ &= U_3\{r_3 + (r_4/A_2^2)[1 + (r_3 r_4/A_2^2) \\ &\qquad + (r_3 r_4/A_2^2)^2 + \cdots]\}. \end{aligned} \quad (20)$$

With summation formula

$$1 + x + x^2 + \cdots = 1/(1 - x), \text{ for } |x| < 1, \quad (21)$$

there is obtained

$$\begin{aligned} U_3'/U_3 &= r_3 + (r_4/A_2^2)\{1/[1 - (r_3 r_4/A_2^2)]\} \\ &= r_3 + [r_4/(A_2^2 - r_3 r_4)]. \end{aligned} \quad (22)$$

The equation for the voltage ratio U_2'/U_2 can be derived from (22) by correspondingly changing

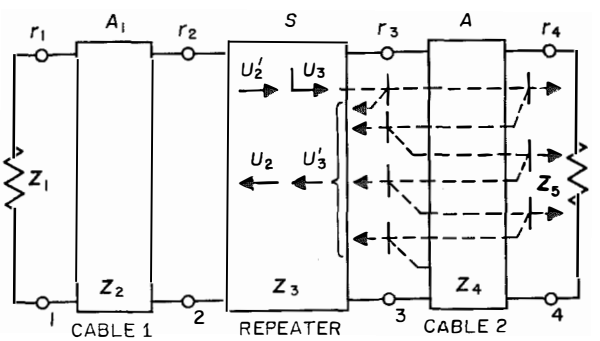

Figure 10—Calculation of loop gain of a repeater section. The cable attenuation $A_n = \exp a_n$, the reflection coefficient $r_n = \left|\dfrac{\mathbf{Z}_n + 1 - \mathbf{Z}_n}{\mathbf{Z}_n + 1 + \mathbf{Z}_n}\right|$ and repeater gain $S = \exp s$.

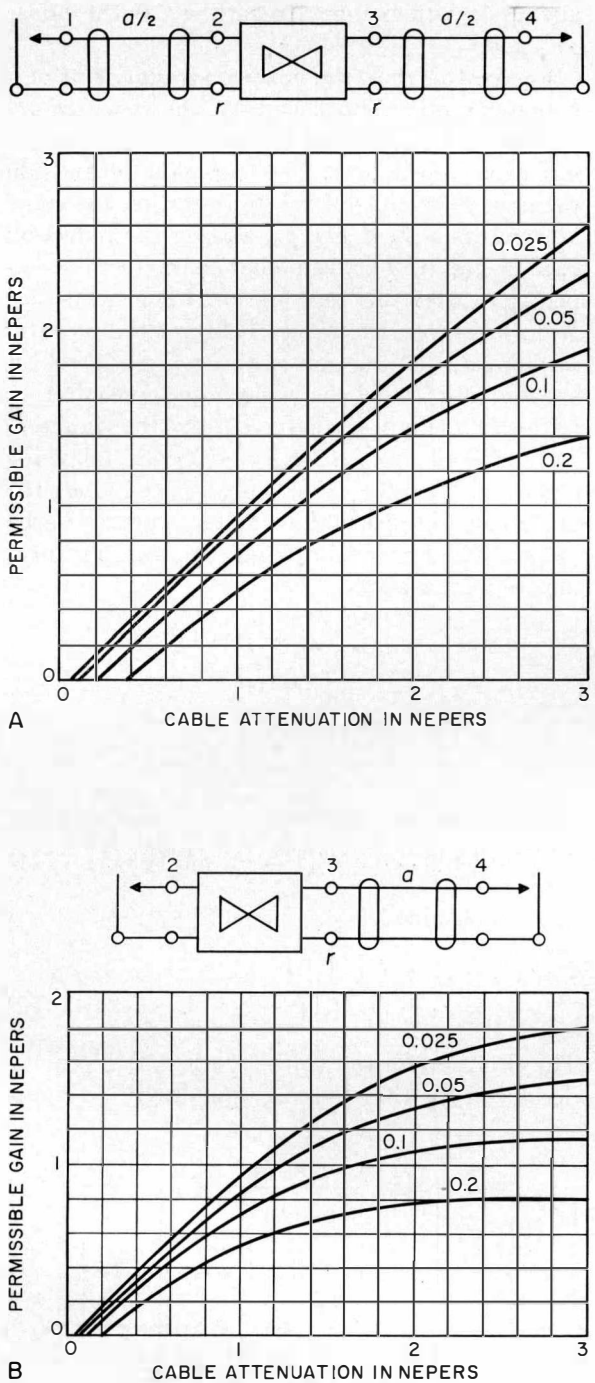

Figure 11—Permissible repeater gain plotted against cable loss for arbitrary open- and short-circuit combinations at the ends of the systems for the four indicated values of reflection coefficient r at the junctions between cable and repeater. The top figure is for the repeater in the middle and the bottom is for the repeater at one end of the cable section.

the suffixes. For the loop gain of 1, appearing at linear addition of the partial voltages, there is obtained the condition

$$S^2(U_2'/U_2)(U_3'/U_3) = 1$$

$$S^2\{r_2 + [r_1/(A_1^2 - r_1r_2)]\} \times \{r_3 + [r_4/(A_2^2 - r_3r_4)]\} = 1. \quad (23)$$

Equation (23) was used to establish the characteristics shown in Figure 11. The upper diagram is valid for the repeater installed in the middle of the repeater section, the lower diagram for an end repeater. The reflection coefficient 1 at the ends of the repeater sections was used for both repeaters.

If the reflection factor at one or both ends of the repeater section assumes values greater than 1, then the gain must be reduced at least to the value determined by (23).

The reflection coefficient existing between two arbitrary impedances $\mathbf{Z}_1$ and $\mathbf{Z}_2$ with the ratio $\mathbf{Z}_1/\mathbf{Z}_2 = x \exp j\alpha$ can be computed on the basis of the relation

$$r = (1 - x \exp j\alpha)/(1 + x \exp j\alpha)$$
$$= [(1 + x^2 - 2x \cos \alpha)/(1 + x^2 + 2x \cos \alpha)]^{1/2}. \quad (24)$$

Equation (24) indicates that the reflection coefficient becomes greater than 1 for angles of $\alpha > 90$ degrees. If, moreover, both impedances are of the same absolute value ($x = 1$), the reflection factor will assume its maximum value.

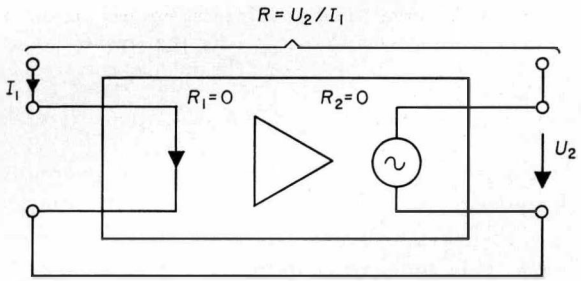

Figure 12—Open-circuit-stable negative impedance. The input current I_1 (origin) produces an output voltage U_2 (result). The input and output resistances of the amplifier are low and connected in series (current feedback).

In the unfavorable case of a repeater terminated by an inductance, the phase angle of the characteristic impedance of -40 degrees will cause a differential angle of $\alpha = 130$ degrees. When the values are the same ($x = 1$), the

reflection factor will be $r = 2.14$ according to (24).

7. *Properties of Negative Impedances*

Negative impedances can be realized by repeaters with feedback. Positive current feedback

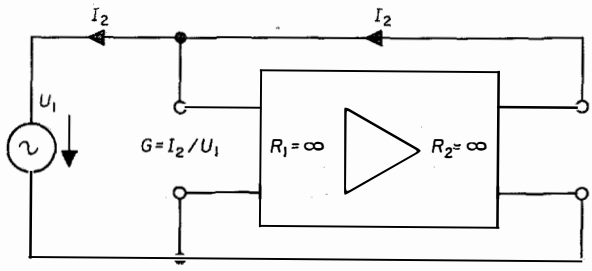

Figure 13—Short-circuit-stable negative impedance. The input voltage U_1 (origin) produces an output current I_2 (result). The amplifier input and output circuits are of high resistance and connected in parallel (voltage feedback).

results in open-circuit-stable impedance and positive voltage feedback in short-circuit-stable impedances. Figures 12 and 13 show simple equivalent circuits of these two types. In the open-circuit-stable type, input and output of the amplifiers are in series (series type), while they are parallel connected in the short-circuit-stable type (parallel type).

If series-type and parallel-type negative impedances are connected in parallel, the loop gain provides negative feedback. This can be shown by Figure 14. Assuming initially the amplification factor to be $\mu_1 = 0$, the right-hand negative impedance is short-circuited through the series-connected input and output of the left-hand

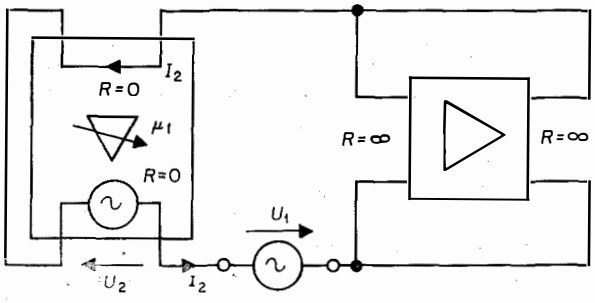

Figure 14—Stability of parallel-connected negative impedances. The test voltage U_1 (origin) produces a current of the direction I_2 (result) which develops a voltage U_2 that counteracts the origin voltage U_1.

negative impedance and thus remains stable. With increasing μ_1, a voltage U_2 is set up that counteracts the origin U_1; in other words, U_2 acts as negative feedback.

This stability of interconnected negative impedances is one of the reasons for connecting a series-type with a parallel-type impedance.

The circle diagram of negative impedances shows that the characteristics proceed partly through the right half of the impedance plane. The basic form of such characteristics will be seen from a simple example. Figure 15 shows a repeater with the input resistor R_1, the output resistor R_2, and the over-all transconductance

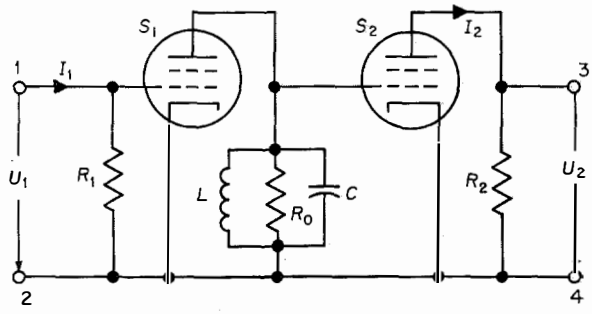

Figure 15—Amplifier producing negative impedance between input and output resistors R_1 and R_2 for cutoff frequencies ω_1 and ω_2. Lower cutoff frequency $\omega_1 = R_0/L$. Upper cutoff frequency $\omega_2 = 1/CR_0$. Transconductance $\mathbf{S} = I_2/\mathbf{Z}_1 = S_0/[1 + j(\omega/\omega_2 - \omega_1/\omega)]$ with $S_0 = S_1S_2R_0$.

$$\mathbf{S} = I_2/\mathbf{U}_1 = S_0\{1/[1+j(\omega/\omega_2 - \omega_1/\omega)]\} \quad (25)$$

with the cutoff frequencies

$$\omega_1 = R_0/L \quad (26)$$

and

$$\omega_2 = 1/CR_0. \quad (27)$$

If now the repeater input and output are connected in series, the series impedance between terminals *1* and *3* will be

$$\begin{aligned}\mathbf{Z}_1 &= R_1 + R_2 - (I_2R_2/I_1) \\ &= R_1 + R_2 - \mathbf{S}R_1R_2. \end{aligned} \quad (28)$$

When input and output are connected in parallel, the over-all admittance between terminal *2* and the short-circuited terminals *1* and *3* is

$$\frac{1}{\mathbf{Z}_1} = \frac{1}{R_1} + \frac{1}{R_2} - \frac{I_2}{\mathbf{U}_1} = \frac{1}{R_1} + \frac{1}{R_2} - \mathbf{S}. \quad (29)$$

Equations (28) and (29) lead to the equivalent circuits shown in Figures 16 and 17.

The following are valid if the impedances $\mathbf{Z}_1$ and $\mathbf{Z}_2$ are referred to their values at zero frequency.

$$\frac{\mathbf{Z}_1}{R_1 + R_2} = 1 - \mathbf{S}\frac{R_1R_2}{R_1 + R_2} \qquad (30)$$

$$\frac{1/\mathbf{Z}_2}{1/R_1 + 1/R_2} = 1 - \mathbf{S}\frac{R_1R_2}{R_1 + R_2}. \qquad (31)$$

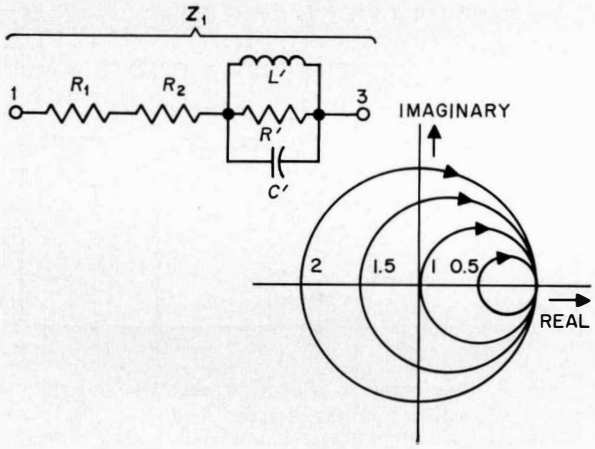

Figure 16—Equivalent circuit and impedance-characteristic diagrams for the indicated values of μ_0 of the amplifier of Figure 15 with input and output in series. $R' = -R_1R_2S_0$. $L' = -L(R_1R_2S_0)/R_0$. $C' = -C(R_0/R_1R_2S_0)$. $\mathbf{Z}_1/(R_1 + R_2) = 1 - \mu_0(\mathbf{S}/S_0)$. $\mu_0 = S_0[R_1R_2/(R_1 + R_2)]$.

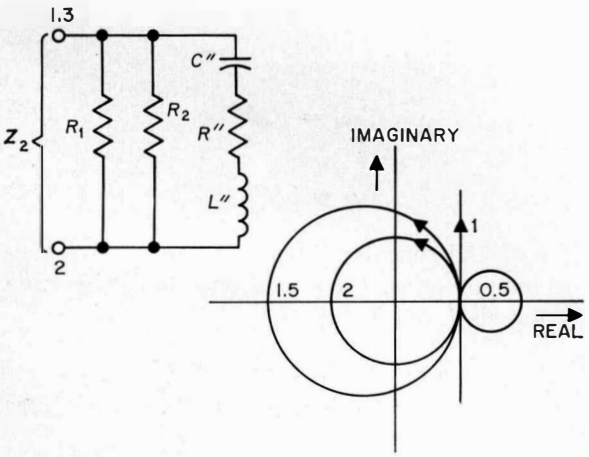

Figure 17—Equivalent circuit and impedance-characteristic diagrams for the indicated values of μ_0 of the amplifier of Figure 15 with input and output in parallel. $R'' = -(1/S_0)$. $L'' = -C(R_0/S_0)$. $C'' = -L(S_0/R_0)$. $\mathbf{Z}_2/[R_1R_2/(R_1 + R_2)] = 1/[1 - \mu_0(\mathbf{S}/S_0)]$. $\mu_0 = S_0[R_1R_2/(R_1 + R_2)]$.

The impedance characteristics of $\mathbf{Z}_1$ and $\mathbf{Z}_2$, again referred to zero frequency, are also shown with the parameter $\mu_0 = S_0(R_1R_2)/(R_1 + R_2)$ in Figures 16 and 17. It will be seen that, with increasing amplification μ_0, the impedance $\mathbf{Z}_1$ passes the zero point and becomes increasingly negative while $\mathbf{Z}_2$ becomes infinitely large before assuming negative values.

8. *Construction and Properties of Negative-Impedance Repeaters*

Basic diagrams of networks resulting in negative impedances are given in Figures 18 and 19.

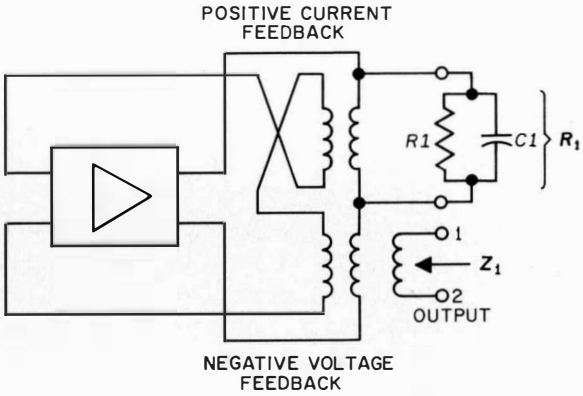

Figure 18—Basic circuit of an open-circuit-stable network in the series branch of the line.

The network destined for the series branch of the bridge network (Figure 18) has positive current feedback; it is of the series type and is, therefore, open-circuit stable; it has been called *NSI* for negative series impedance. The feedback voltage returned from the output renders the negative impedance $\mathbf{Z}_1$ insensitive to gain variations. $\mathbf{Z}_1$ is rotated in its phase by about 180 degrees against the resistance $\mathbf{R}_1$. The value of $\mathbf{Z}_1$ is about proportional to that of $\mathbf{R}_1$. The output of the negative-serves-impedance network will pass direct current.

The network for the shunt branch of the bridge (Figure 19) is of the parallel type and is called *NPI* for negative parallel impedance. This can easily be seen in the case where $\mathbf{R}_2 = 0$. The transformers must be poled so that in the case of $\mathbf{R}_2 = 0$, the input and output of the repeater are coupled by positive feedback. If the center tap of the repeating inductor is connected to the

inductor center and if the amplification is very high, then $\mathbf{Z}_2 = -R_2$. The capacitor in series with the tap renders the negative-parallel-impedance network impassable for direct current.

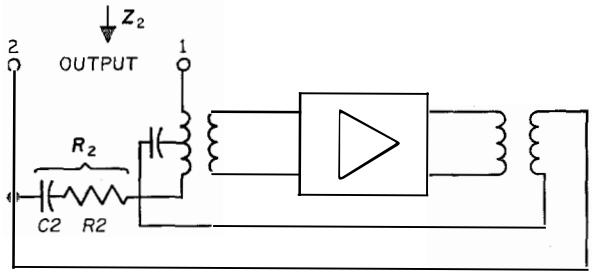

Figure 19—Basic circuit of a short-circuit-stable network in the shunt branch of the line.

transistor and the frequency characteristics of the transformer produce a translation coefficient in the transmitted band that is not constant but is of a complex frequency-dependent magnitude. Thus the negative impedance $\mathbf{Z}_1$ transformed into the line does not have the impedance characteristic of the combination *R1*, *C1* rotated by 180 degrees as in Figure 7, but rather the impedance characteristic in Figure 22. When strong speech and dial signals appear, the rectifier *CR* prevents overloading of the transistor and also reduces the loss of these signals.

The negative-parallel-impedance network producing negative impedance $\mathbf{Z}_2$ is connected by the "*NP* ON" jumper to the center tap of transformer *T1*. Capacitor *C* blocks the network

A simplified circuit diagram of a two-wire repeater with negative impedances is shown in Figure 20. Junction transistors with a power dissipation of 50 milliwatts are used as amplifiers. A 24- or 60-volt battery serves as a direct-current power supply.

The two-wire line is connected to the line windings of transformer *T1* through plug connections. These windings have direct-current resistances of not more than 10 ohms so the loss is small in the case of direct-current transmission. That *T1* winding connected to the base branch produces a negative voltage feedback and the *T4* winding connected in series with the latter produces a current feedback. The finite gain of the

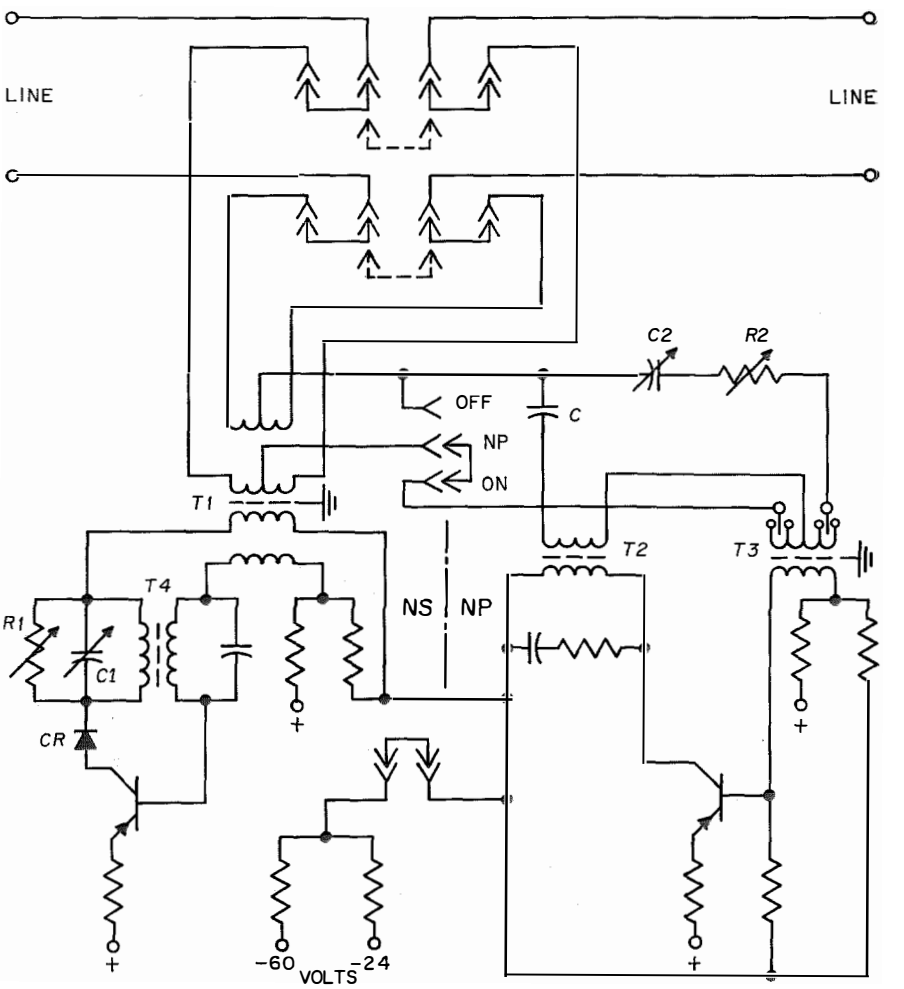

Figure 20—Simplified circuit of the repeater. *NP* and *NS* indicate negative parallel and series impedances, respectively.

against direct current. The characteristic of the negative impedance $\mathbf{Z}_2$ (Figure 22) is also quite different from the $\mathbf{Z}_2$ characteristic in Figure 7; this due to band limitations and to finite loop gain in the negative-parallel-impedance network. The deviations cause both network-loss distortion and reflections. According to Figure 11, the permissible reflection decreases with increasing gain. Therefore it is expedient to match the characteristic impedances of the cable and repeater at that frequency at which the gain is highest. Now, nonloaded cables, because of their inductivity of about $L' = 0.7$ millihenry per kilometer (1.13 millihenries per mile), have a characteristic impedance angle of only 30 to 40 degrees at the highest transmitted frequency.

The adjustment of the negative impedance by the components *R1*, *C1*, *R2*, and *C2* has to be

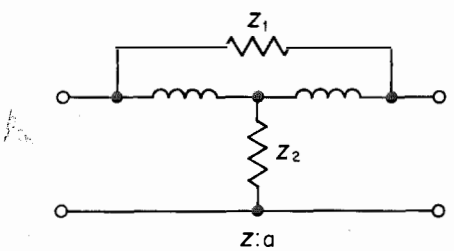

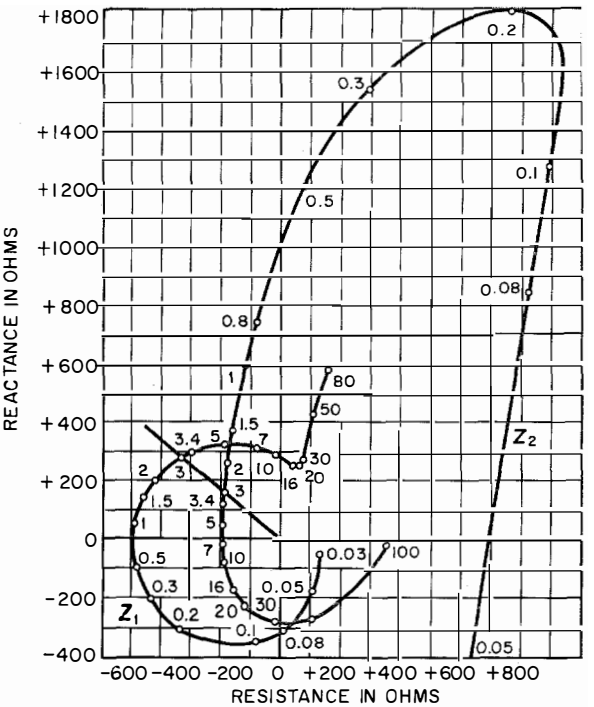

Figure 22—Characteristics of the bridge network impedances $|\mathbf{Z}_1|$ and $|\mathbf{Z}_2|$ with gain adjusted to 1.6 nepers at $f_0 = 3$ kilocycles. The frequency values in kilocycles are indicated by numbers at the various points on the curves.

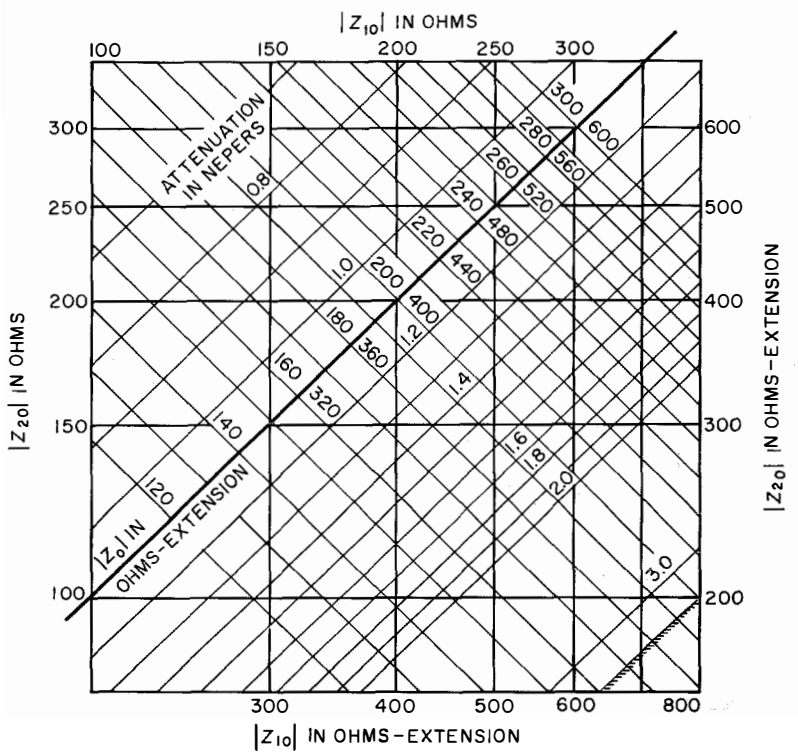

carried out in a manner differing from the requirement of (9) for the same cutoff frequency inasmuch as the repeater must assume the characteristic impedance of the cable at a frequency near the band limit. The frequency required for this alignment procedure is called the adjustment frequency f_0. The values correlated to this frequency are designated by the same subscript. Then, the requirement of a reflection-free

Figure 21—Diagram for determining the bridge network impedances $|\mathbf{Z}_{10}|$ and $|\mathbf{Z}_{20}|$ from the characteristic impedance $|\mathbf{Z}_0|$ and the attenuation α_0 in nepers at frequency f_0. Extension scales for the impedances are given in the lower right half of the chart.

matching of the repeater characteristic impedance Z_0 to the characteristic impedance of the cable, Z_{R0}, at the frequency f_0, may be expressed by the equation

$$\mathbf{Z}_{R0} = \mathbf{Z}_0 = (\mathbf{Z}_{10}\mathbf{Z}_{20})^{1/2}. \quad (32)$$

The factor $\mathbf{N}_0 = (\mathbf{Z}_{10}/\mathbf{Z}_{20})^{1/2}$ determines the gain at frequency f_0. If factor N_0 is chosen as a real one, the adjustment conditions are easily missed;

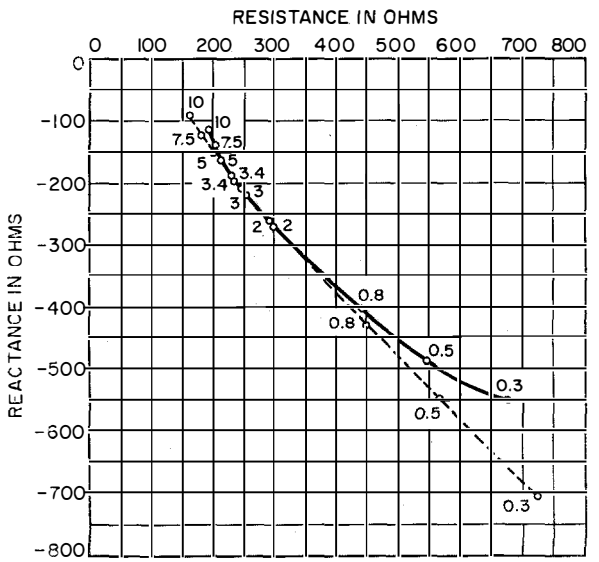

Figure 23—Characteristic impedances of repeater (solid line) and cable (broken line) adjusted to a gain of 1.6 nepers (14 decibels) at 3 kilocycles. The measurement frequencies are indicated along the curves.

however, because the characteristic-impedance angle deviates from 45 degrees, maximum gain is no longer obtained at the adjustment frequency but at a somewhat higher frequency. Therefore it is advantageous to select as the adjustment frequency a value that is smaller than the upper limit of the band, for example, $f_0 = 3.0$ kilocycles.

The factor N_0 from (5) can be found with the aid of the gain required, $S_0 = 1/A_0 = \ln a_0$.

$$N_0 = 2(A_0 - 1)/(A_0 + 1) = -2(S_0 - 1)/(S_0 + 1). \quad (33)$$

By means of the characteristic impedance $\mathbf{Z}_0$ required for frequency f_0, we obtain according to (3) and (4) the nominal impedances at frequency f_0.

$$\mathbf{Z}_{10} = N_0\mathbf{Z}_0 \quad (34)$$

and

$$\mathbf{Z}_{20} = \mathbf{Z}_0/N_0. \quad (35)$$

The angles of the negative impedances have to be chosen according to (34) and (35) equal to the angle of the positive characteristic impedance rotated by 180 degrees. Figure 21 shows the nominal values of negative impedances from the amount of characteristic impedance of the cable and from the desired reduction in attenuation.

The two impedance characteristics shown in Figure 22 were measured after the repeater was adjusted at $f_0 = 3.0$ kilocycles, to an attenuation $a_0 = 1.6$ nepers and to the characteristic impedance $Z_0 = 323$ ohms with the angle $\varphi_0 = -40$ degrees.

The characteristic impedance determined by the impedance characteristics of Figure 22 is

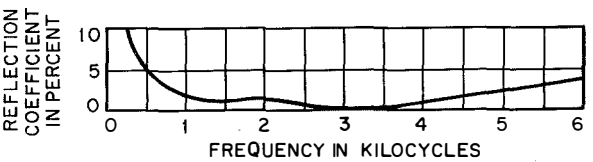

Figure 24—Reflections coefficient of the repeater as derived from Figure 23.

shown in Figure 23. The solid curve is that of the repeater and the broken curve is for the desired characteristic impedance of a cable having an 0.8-millimeter (0.03-inch) core diameter and line constants of

$R' = 73.2$ ohm per kilometer
$= 117.8$ ohm per mile
$C' = 0.038$ microfarad per kilometer
$= 0.061$ microfarad per mile
$L' = 0.7$ millihenry per kilometer
$= 1.13$ millihenry per mile

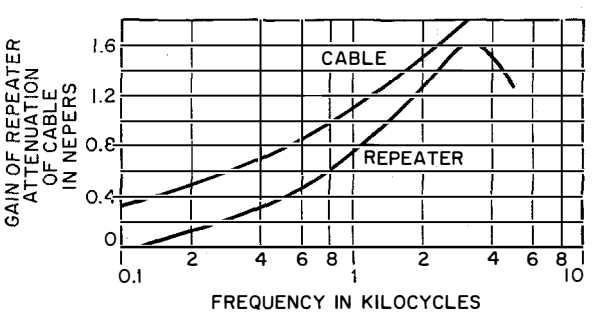

Figure 25—Gain of repeater and attenuation of cable 12 kilometers (7.5 miles) long as a function of frequency. The repeater was adjusted to a gain of 1.6 nepers (14 decibels) at 3 kilocycles.

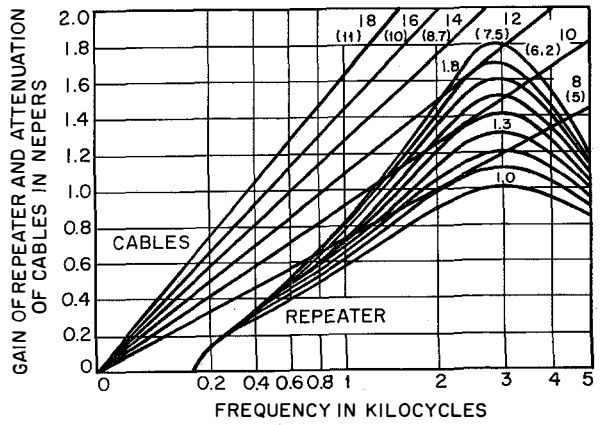

Figure 26—Gain and attenuation characteristics of repeaters and cables. The frequency scale has been dimensioned to make the cable loss linear. The length of each cable is indicated in kilometers (miles). The repeater was adjusted at 2.7 kilocycles to values between 1.0 neper (8.7 decibels) and 1.8 nepers (15.6 decibels) in steps of 0.1 neper.

which is shown for comparison purposes. The reflection coefficient found from both curves is given in Figure 24. The propagation constant was also found from Figure 22 and is shown as curve *4* of Figure 5.

The repeater gain is compared in Figure 25 with the attenuation of a cable 12 kilometers (8 miles) long.

Other gain curves were established using the adjustment frequency $f_0 = 2.7$ kilocycles (Figure 26). The equalization of the transmitted band is still good at this frequency. If the adjustment frequency chosen is as low as possible, a given cable section can be compensated for at a low value of maximum gain. This lowers the requirements for the reflection attenuation, which are highest at maximum gain.

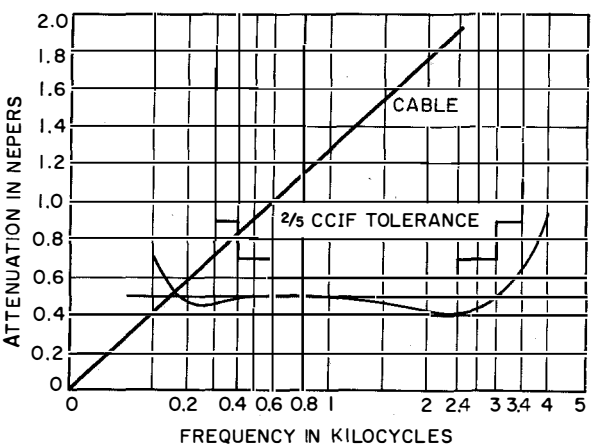

Figure 27—Net loss of repeater section for a cable 14 kilometers (8.7 miles) long. The repeater was adjusted for a gain of 1.55 nepers (13.5 decibels) at 2.7 kilocycles.

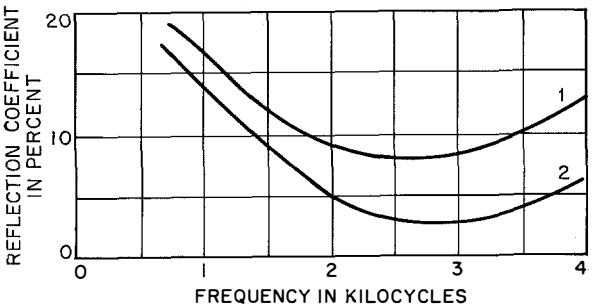

Figure 28—Permissible reflection coefficient of repeaters and cable sections of 14 kilometers (8.7 miles) having a net loss of 0.5 neper (4.3 decibels). Curve *1* is for the repeater in the middle of the line and *2* is for the repeater at the end of the line.

Figure 27 is an example for the net loss of a cable that is 14 kilometers (8.7 miles) long, having an attenuation $a_{800} = 1.15$ nepers (10 decibels) at 800 cycles. A net loss of 0.5 neper (4.3 decibels) is obtained with the repeater for 800 cycles, the gain being adjusted to 1.55 nepers (13 decibels) at the adjustment frequency

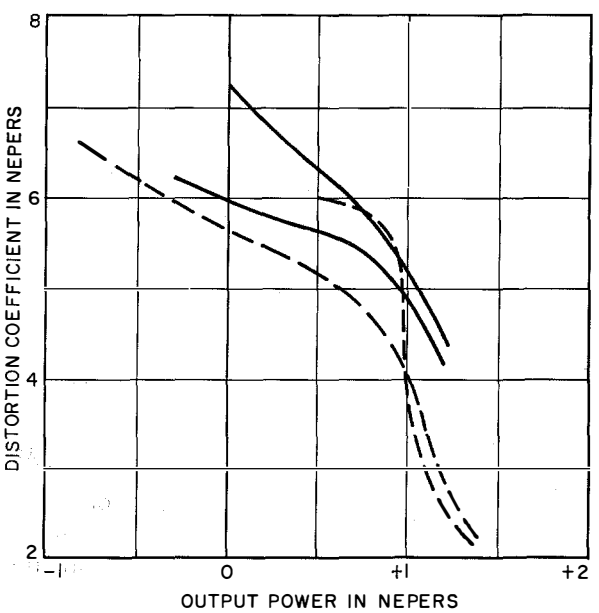

Figure 29—Distortion coefficient of the repeater terminated by cable balancing networks.

f_0 = 2.7 kilocycles. The linear distortion, referred to 800 cycles, is within the $\frac{2}{5}$ tolerances recommended by the Comité Consultatif International Téléphonique.

The permissible reflections between the characteristic impedances of the cable and the repeater terminals for this net loss were found in Figure 11 and plotted in Figure 28. These values lead to self-excitation of the repeater section only in those cases where the reflected waves can be added linearly.

Apart from the precise adjustment of its characteristic impedance, the repeater has another feature of importance: its constancy, on which the singing stability of the repeater section depends. When the supply voltage varies by ± 20 percent, the additional reflection amounts to not more than ± 0.5 percent, the gain being changed by a maximum of ± 0.01 neper (0.08 decibel).

The distortion coefficient for a termination by positive characteristic impedances of the cable is shown in Figure 29. The solid curves are valid for a cutoff frequency of 3400 cycles and the broken-line curves for 800 cycles. In the band 300 through 3400 cycles, the point of overload is reached at a voltage level of about + 1.0 neper (8.7 decibels).

Telephone Statistics of the World*

DURING 1956, about 8.8 million telephones were added throughout the world, making a total of 109.8 million on January 1, 1957. More than half of the world's telephones were in the United States, where several thousand privately owned and operated systems provided a telephone for one out of every three individuals. In Europe, which had 29.7 percent of the world's telephones, mostly under public operation, there was a telephone for approximately every 17 individuals.

For the purpose of this compilation, only those telephones that can be connected to a commercial public system are counted. Fourteen countries reported more than 1 million telephones in service January 1, 1957: United States, United Kingdom, Canada, Western Germany, Japan, France, Italy, Sweden, Australia, Switzerland The Netherlands, Argentina, Spain, and Eastern Germany. Of the world's principal countries, had more than 15 telephones per 100 of population: United States (35.4), Sweden (31.5) Canada (27.6), New Zealand (25.6), Switzerland (25.5), Denmark (20.5), Australia (18.5), Norway (17.8), and Iceland (17.4).

TELEPHONES IN CONTINENTAL AREAS

Partly estimated; statistics reported as of other dates have been adjusted to January 1, 1957

Continental Area	Total Telephones			Privately Owned		Automatic (Dial)	
	Number	Percent of Total World	Per 100 Population	Number	Percent of Total	Number	Percent of Total
North America	64 723 700	58.9	34.7	64 046 000	99.0	55 719 800	86.1
Middle America	772 800	0.7	1.3	695 700	90.0	596 500	77.2
South America	2 695 300	2.5	2.1	1 268 600	47.1	2 229 000	82.7
Europe	32 606 600	29.7	5.8	5 218 100	16.0	25 957 000	79.6
Africa	1 546 100	1.4	0.7	22 400	1.4	1 091 500	70.6
Asia	4 929 900	4.5	0.3	3 521 900	71.4	2 889 800	58.6
Oceania	2 525 600	2.3	16.7	178 400	7.1	1 794 700	71.1
World	109 800 000	100.0	4.0	74 951 100	68.3	90 278 300	82.2

New York, with more telephones than any other city, had almost twice as many as Greater London, which ranked second. On a per-capita basis, Washington, District of Columbia, led among the world's large cities with 65.3 telephones per 100 population and Stockholm, Sweden, was first outside the United States with 55.9.

A subdivision in certain of the tables shows the number of telephones operated under private and government ownership. The latter category has reference to municipal and state, as well as national, ownership.

The statistics in this compilation are based on questionnaires sent to the telephone administrations of the various countries throughout the world.

* Abridgement from a booklet issued by the American Telephone and Telegraph Company; New York, New York. After the issuance of the statistics published here, and thus not reflected in them, the government of the Union of Soviet Socialist Republics informed the American Telephone and Telegraph Company that on January 1, 1957, there were 3 366 000 telephones in that country, 1 504 000 of them automatic, and there were 431 000 telephones in Moscow. The corresponding figures for January 1, 1958 were 3 558 000 total, 1 640 000 automatic, and 454 000 in Moscow.

TELEPHONES IN COUNTRIES OF THE WORLD AS OF JANUARY 1, 1957

Country	Total Telephones	Per 100 Population	Percent Automatic (Dial)	Ownership	
				Private	Government
NORTH AMERICA					
Alaska	30 655	17.52	80.2	7 478	23 177
Canada	4 502 326	27.56	77.3	3 848 137	654 189
Greenland	0	—	—	—	—
St. Pierre and Miquelon	300	6.00	0	0	300
United States	60 190 377	35.45	86.8	60 190 377	0
MIDDLE AMERICA					
Bahamas	7 220	6.20	98.8	0	7 220
Barbados	6 968	3.04	100	6 968	0
Bermuda	8 810	20.02	100	8 810	0
British Honduras	924	1.13	0	45	879
Canal Zone (1) (2)	7 564	28.01	100	0	7 564
Costa Rica	11 245	1.12	2.2	10 856	389
Cuba	143 730	2.37	89.3	143 730	0
Dominican Republic	11 750	0.44	92.9	11 630	120
El Salvador	10 316	0.45	75	0	10 316
Guadeloupe and Dependencies	1 855	0.81	0	0	1 855
Guatemala	11 000	0.32	80	0	11 000
Haiti (3)	4 400	0.13	90	0	4 400
Honduras	5 486	0.33	90	0	5 486
Jamaica and Dependencies	25 000	1.58	97.6	25 000	0
Leeward Islands:					
Antigua	500	0.96	0	0	500
Montserrat	98	0.75	0	0	98
St. Christopher-Nevis	325	0.61	0	0	325
Virgin Islands (United Kingdom)	1	0.01	0	0	1
Total	924	0.72	0	0	924
Martinique	4 143	1.73	70	0	4 143
Mexico	383 257	1.24	73.2	382 609	648
Netherlands Antilles	6 061	3.25	97.1	0	6 061
Nicaragua	5 735	0.45	68.7	0	5 735
Panama	21 635	2.28	82.1	21 080	555
Puerto Rico	65 190	2.84	65.8	60 440	4 750
Trinidad and Tobago	25 431	3.42	87.5	25 431	0
Virgin Islands (United States)	2 780	10.30	0	0	2 780
Windward Islands:					
Dominica	351	0.55	0	0	351
Grenada	1 200	1.50	0	0	1 200
St. Lucia	452	0.51	68.6	0	452
St. Vincent	426	0.53	0	0	426
Total	2 429	0.78	12.8	0	2 429
SOUTH AMERICA					
Argentina	1 155 198	5.87	82.8	82 189	1 073 009
Bolivia	11 700	0.36	91	11 700	0
Brazil	842 800	1.41	82.8	842 800	0
British Guiana	4 819	0.95	14.7	0	4 819
Chile	152 690	2.17	69.8	151 840	850
Colombia	197 752	1.52	94.4	0	197 752
Ecuador	17 000	0.44	60	2 000	15 000
Falkland Islands and Dependencies	391	17.77	0	0	391
French Guiana	779	2.78	0	0	779
Paraguay (3)	6 400	0.40	86	0	6 400
Peru	67 832	0.69	80.3	67 832	0
Surinam	3 883	1.55	94.7	0	3 883
Uruguay (3)	122 600	4.63	75	0	122 600
Venezuela (3)	111 500	1.85	94	110 250	1 250
EUROPE					
Albania (4)	1 555	0.14	10.6	0	1 555
Andorra	100	1.67	0	0	100
Austria	540 524	7.74	87.7	0	540 524
Belgium	931 439	10.41	81.8	0	931 439
Bulgaria (5)	54 347	0.77	39.4	0	54 347
Channel Islands:					
Guernsey and Dependencies	10 660	23.17	27.3	0	10 660
Jersey	14 647	25.70	0	0	14 647
Total	25 307	24.57	11.5	0	25 307
Czechoslovakia (5)	350 708	2.88	59.4	0	350 708
Denmark	922 881	20.52	47.3	813 841	109 040
Finland	486 193	11.27	70.1	372 066	114 127
France	3 313 426	7.57	70.2	0	3 313 426

(1) Excluding telephone systems of the military forces.
(2) June 30, 1956.
(3) Data partly estimated.
(4) January 1, 1943 (latest official statistics).
(5) January 1, 1948 (latest official statistics).
(6) March 31, 1957.
(7) January 1, 1947 (latest official statistics).
(8) Under government operation since 1949.
(9) January 1, 1936 (latest official statistics available during this compilation; but see footnote on page 138).
(10) Includes data for the Isle of Man.

TELEPHONES IN COUNTRIES OF THE WORLD AS OF JANUARY 1, 1957—*Continued*

Country	Total Telephones	Per 100 Population	Percent Automatic (Dial)	Ownership	
				Private	Government
EUROPE (Continued)					
Germany, Democratic Republic	1 066 582	5.98	92.2	0	1 066 582
Germany, Federal Republic	4 323 225	8.26	96	0	4 323 225
Gibraltar	1 928	7.71	100	0	1 928
Greece	136 835	1.70	93.6	0	136 835
Hungary	347 672	3.55	77.8	0	347 672
Iceland	28 260	17.44	63.6	0	28 260
Ireland	123 619	4.27	69.1	0	123 619
Italy	2 609 127	5.40	95.6	2 609 127	0
Liechtenstein	2 929	19.53	100	0	2 929
Luxemburg	35 540	11.39	84.4	0	35 540
Malta and Gozo (6)	9 170	2.88	0	0	9 170
Monaco	6 953	33.11	100	0	6 953
Netherlands	1 229 174	11.22	96.1	0	1 229 174
Norway (2)	614 523	17.75	66.3	51 862	562 661
Poland	378 000	1.37	68.8	0	378 000
Portugal	279 537	3.15	65 2	188 895	90 642
Rumania (7)	127 153	0.77	75.8	126 131 (8)	1 022
Saar	59 955	6.00	100	0	59 955
San Marino	450	3.21	100	0	450
Spain	1 199 078	4.09	79.2	1 181 437	17 641
Sweden	2 312 223	31.50	78.7	0	2 312 223
Switzerland	1 293 743	25.50	99.6	0	1 293 743
Turkey	173 730	0.70	86.8	0	173 730
Union Soviet Socialist Republics (9)	861 181	0.52	19.9	0	861 181
United Kingdom (6) (10)	7 218 791	14.04	78.2	0	7 218 791
Yugoslavia	175 341	0.98	70.1	0	175 341
AFRICA					
Algeria	144 402	1.41	79.6	0	144 402
Angola	3 802	0.09	95.9	0	3 802
Ascension Island	44	22.00	68.2	44	0
Basutoland	770	0.12	5	0	770
Bechuanaland	254	0.08	0	0	254
Belgian Congo	18 046	0.14	78	0	18 046
Cameroons (French Administration)	3 616	0.11	58.1	0	3 616
Cape Verde Islands	127	0.07	0	0	127
Comoro Islands	0	—	—	—	—
Egypt	179 988	0.75	78.8	0	179 988
Ethiopia and Eritrea	7 264	0.04	80.5	0	7 264
French Equatorial Africa	5 735	0.12	36.5	0	5 735
French West Africa	25 351	0.13	57.1	0	25 351
Gambia	489	0.17	99.2	0	489
Ghana (6)	15 821	0.34	40.3	0	15 821
Ifni	121	0.27	0	121	0
Kenya	29 447	0.48	76.5	0	29 447
Liberia (3)	1 500	0.12	100	425	1 075
Libya (3)	7 500	0.67	77	0	7 500
Madagascar and Dependencies	10 284	0.21	46.1	1 279	9 005
Mauritius and Dependencies	7 282	1.26	8	0	7 282
Morocco	124 893	1.26	83.2	19 533	105 360
Mozambique	8 271	0.14	75.1	0	8 271
Nigeria, Federation of, and British Cameroons	24 536	0.07	48.4	0	24 536
Portuguese Guinea	346	0.06	0	0	346
Reunion	4 649	1.67	0	0	4 649
Rhodesia and Nyasaland:					
Northern Rhodesia	14 113	0.64	93.8	1 477	12 636
Nyasaland	3 604	0.14	89.6	0	3 604
Southern Rhodesia	54 579	2.16	81.7	0	54 579
Total	72 296	0.98	84.4	1 477	70 819
Ruanda-Urundi	1 071	0.03	92.3	0	1 071
St. Helena	112	2.24	0	0	112
São Tomé and Principe	312	0.52	0	0	312
Seychelles and Dependencies	160	0.41	100	160	0
Sierra Leone	2 257	0.09	81.1	0	2 257
Somaliland, British Protectorate	330	0.05	0	0	330
Somaliland, French	762	1.17	100	0	762
Somaliland (Italian Administration)	1 228	0.10	0	0	1 228
South West Africa	10 614	2.23	42.2	0	10 614
Spanish Guinea	827	0.40	71.2	827	0
Spanish North Africa	6 199	4.30	100	6 199	0
Spanish Sahara	40	0.08	0	40	0
Sudan	18 569	0.18	80.2	0	18 569
Swaziland	997	0.45	35.5	0	997
Tanganyika	11 462	0.14	53.8	0	11 462

TELEPHONES IN COUNTRIES OF THE WORLD AS OF JANUARY 1, 1957—*Continued*

Country		Total Telephones	Per 100 Population	Percent Automatic (Dial)	Ownership	
					Private	Government
AFRICA (continued)						
Togoland		1 095	0.09	68.1	0	1 095
Tunisia		33 710	0.88	57.3	0	33 710
Uganda		10 697	0.19	75.8	0	10 697
Union of South Africa	(6)	765 540	5.40	67.4	0	765 540
Zanzibar and Pemba		1 045	0.38	4.3	0	1 045
ASIA						
Aden Colony		3 165	2.26	100	0	3 165
Aden Protectorate		0	—	—	—	—
Afghanistan	(3)	6 200	0.05	30	0	6 200
Bahrain		1 756	1.40	100	1 756	0
Bhutan		0	—	—	—	—
Brunei		160	0.29	0	0	160
Burma	(3)	7 400	0.04	0	0	7 400
Cambodia		2 637	0.06	0	0	2 637
Ceylon		28 757	0.32	93.8	0	28 757
China	(5)	244 028	0.05	72.9	94 945 (7)	149 083
Cyprus		12 913	2.43	83.8	0	12 913
Hong Kong		63 760	2.56	100	63 760	0
India	(6)	314 885	0.08	52.6	3 528	311 357
Indonesia		79 227	0.09	12.1	0	79 227
Iran		63 927	0.29	55	0	63 927
Iraq	(6)	41 725	0.83	77.2	0	41 725
Israel		72 445	3.87	92.1	0	72 445
Japan	(6)	3 486 821	3.84	55.7	3 486 821	0
Jordan		11 034	0.74	72.4	0	11 034
Korea, Republic of		50 256	0.23	40.3	0	50 256
Kuwait		1 800	0.87	80	0	1 800
Laos		536	0.03	51.1	0	536
Lebanon		38 497	2.65	90.5	0	38 497
Macao		1 865	0.93	100	0	1 865
Malaya		57 358	0.90	66	0	57 358
Maldive Islands		0	—	—	—	—
Muscat and Oman		152	0.03	100	152	0
Nepál		0	—	—	—	—
Netherlands New Guinea	(3)	1 100	0.16	0	0	1 100
North Borneo		1 705	0.44	81.8	0	1 705
Pakistan		49 892	0.06	68.8	0	49 892
Philippine Republic		63 400	0.28	68.7	56 400	7 000
Portuguese India		266	0.04	0	0	266
Portuguese Timor		443	0.09	0	0	443
Qatar		443	1.11	100	443	0
Ryukyu Islands	(1)	3 924	0.48	37	0	3 924
Sarawak		1 931	0.31	63.4	0	1 931
Saudi Arabia		13 835	0.20	4.3	0	13 835
Singapore		41 672	3.23	100	0	41 672
Syria		36 650	0.91	83.4	0	36 650
Taiwan		47 112	0.50	49.4	0	47 112
Thailand		11 832	0.05	100	0	11 832
Trucial Oman		0	—	—	—	—
Viet-Nam, Republic of		12 054	0.09	85.1	0	12 054
Yemen		0	—	—	—	—
OCEANIA						
Australia		1 762 173	18.48	71	0	1 762 173
British Solomon Islands		208	0.20	0	0	208
Caroline Islands		191	0.44	0	0	191
Cocos (Keeling) Islands		59	9.08	100	0	59
Cook Islands		174	1.09	0	82	92
Fiji Islands		4 327	1.25	58.9	0	4 327
French Oceania		888	1.22	0	0	888
Gilbert and Ellice Islands		108	0.26	74.1	77	31
Guam		10 233	14.83	93.6	0	10 233
Hawaii		178 165	30.10	99.8	178 165	0
Mariana Islands (less Guam)		350	5.00	71.4	0	350
Marshall Islands		485	3.46	99	0	485
Nauru		0	—	—	—	—
New Caledonia and Dependencies		2 504	3.85	64.7	0	2 504
New Hebrides Condominium		250	0.46	0	0	250
New Zealand	(6)	568 339	25.59	62.3	0	568 339
Niue Island		63	1.26	0	0	63
Norfolk Island		50	5.00	0	0	50
Papua and New Guinea		3 883	0.22	51.4	120	3 763
Pitcairn Island		0	—	—	—	—
Samoa, American		331	1.66	100	0	331
Samoa, Western		690	0.71	0	0	690
Tokelau Islands		0	—	—	—	—
Tonga (Friendly) Islands		535	0.94	0	0	535

Telephone Conversations for the Year 1955

Conversation data were not available for all countries

Country	Number of Conversations in Thousands			Conversations Per Capita
	Local	Toll	Total	
Alaska	106 300	800	107 100	630.0
Algeria	72 300	26 200*	98 500	9.9
Argentina	3 532 000	41 200	3 573 200	183.5
Australia	1 285 400	103 100	1 388 500	147.3
Belgium	522 400	91 100	613 500	68.7
Brazil	3 926 600	52 200	3 978 800	66.5
Canada	7 559 500	171 300	7 730 800	480.7
Ceylon	60 800	4 900	65 700	7.5
Channel Islands	17 600	200	17 800	172.8
Chile	378 500	23 100	401 600	57.9
Colombia	690 400	9 700	700 100	54.1
Cuba	502 000	6 400	508 400	83.7
Denmark	1 056 400	183 300	1 239 700	277.6
Egypt	450 000	12 700	462 700	19.8
El Salvador	21 200	2 400	23 600	10.4
Finland	593 800	83 000	676 800	157.8
France	2 053 200	571 500	2 624 700	60.2
French West Africa	15 600	1 600	17 200	0.9
Germany, Democratic Republic	772 900	119 300	892 200	50.3
Germany, Federal Republic	2 733 900	636 800	3 370 700	66.6
Greece	329 400	6 800	336 200	41.9
Hawaii	294 900	2 400	297 300	530.9
Hungary	438 300	25 900	464 200	47.4
Iceland	63 200	1800	65 000	403.7
Ireland	91 800	14 600	106 400	36.8
Israel	122 500	5 200	127 700	70.4
Italy	4 135 000	268 200*	4 403 200	91.3
Jamaica	55 600	900	56 500	36.1
Japan (1)	8 520 000	712 900	9 232 900	102.6
Lebanon	51 800	4 600	56 400	38.9
Madagascar	10 700	1 100	11 800	2.4
Malaya	140 800	17 000	157 800	25.2
Mexico	820 500	12 000	832 500	27.3
Morocco	95 700	16 500*	112 200	11.4
Netherlands	872 800	302 600	1 175 400	108.0
Norway (2)	484 500	58 000	542 500	157.5
Peru	245 800	3 900	249 700	25.9
Philippines	425 500	1 100	426 600	19.2
Portugal	257 000	48 600	305 600	34.6
Puerto Rico	130 400	2 800	133 200	58.5
Saar	80 900	1 400	82 300	82.3
Singapore	148 800	800	149 600	118.4
South West Africa	10 900	1 600	12 500	26.7
Spain	2 770 000	93 700	2 863 700	98.1
Sweden (3)	3 222 100	120 600	3 342 700	455.3
Switzerland	516 700	444 500*	961 200	191.4
Syria	94 700	6 100	100 800	25.4
Trinidad and Tobago	78 400	4 600	83 000	113.4
Tunisia	26 300	6 900	33 200	8.8
Turkey	228 000	9 200	237 200	9.6
Union of South Africa (1)	873 500	59 800	933 300	67.1
United Kingdom (1)	3 781 000	323 000	4 104 000	80.1
United States	68 545 000	3 080 000	71 625 000	425.7
Viet-Nam, Republic of	12 200	200	12 400	0.9
Yugoslavia	285 000	22 600	307 600	17.3

(1) Year ended March 31, 1957.
(2) Year ended June 30, 1956.
(3) Year ended June 30, 1957
* Three-minute units

United States Patents Issued to International Telephone and Telegraph System; November 1957–January 1958

BETWEEN November 1, 1957 and January 31, 1958, the United States Patent Office issued 50 patents to the International System. The names of the inventors, company affiliations, subject, and patent numbers are listed below.

H. H. Adelaar, Bell Telephone Manufacturing Company (Antwerp), Binary Electrical Counting Circuit, 2 812 134.

E. Albert, Bell Telephone Manufacturing Company (Antwerp), Measuring Instrument, 2 817 817.

R. A. Andre and L. J. G. Nys, Bell Telephone Manufacturing Company (Antwerp), Matrix for Detachably Mounting Electrical Components, 2 821 691.

M. Arditi, G. A. Deschamps, and J. Elefant, Federal Telecommunication Laboratories, Microwave Filters, 2 819 452.

M. Arditi, G. A. Deschamps, and J. Elefant, Federal Telecommunication Laboratories, Microwave Filters, 2 820 206.

H. Bartels, Süddeutsche Apparatefabrik (Nürnberg), Method of Making Dry-Contact Rectifiers, Particularly Selenium Rectifiers, 2 819 436.

H. Bartels and H. Fritsch, Süddeutsche Apparatefabrik (Nürnberg), Process for Connecting a Tantalum Electrode Pin to an Electrode Body, 2 819 961.

A. H. W. Beck and A. B. Cutting, Standard Telephones and Cables Limited (London), Ionization Manometers, 2 817 030.

G. R. Clark, Federal Telecommunication Laboratories, Selective Gate System for Radar Beacons, 2 815 504.

E. C. L. deFaymoreau, Federal Telecommunication Laboratories, Electromechanical Delay Device, 2 815 490.

E. C. L. deFaymoreau, Federal Telecommunication Laboratories, Signaling System, 2 815 507.

M. Dishal and M. Rogoff, Federal Telecommunication Laboratories, Continuous-Wave Beacon System, 2 817 082.

C. L. Estes, Federal Telecommunication Laboratories, Electrical Signal-Translating System, 2 815 486.

L. Goldstein, M. A. Lampert, and J. F. Heney, Federal Telecommunication Laboratories, Electromagnetic Wave Generator, 2 817 045.

H. Grottrup, C. Lorenz A. G. (Stuttgart), Sensing Arrangement for Stored Information Concerning Positioning of a Mechanical Element, 2 820 216.

S. J. Harris and J. A. Henderson, Capehart–Farnsworth Company, Television Film Scanners Having Sprocket Hole Sensing Means Responsive to Film Refraction Between Holes, 2 818 467.

W. Hauer, Mix & Genest (Stuttgart), Dispatch-Tube System, 2 815 183.

H. L. Horwitz and G. L. Hasser, Federal Telephone and Radio Company, Two-Party-Line Individual Metering, 2 820 848.

J. F. Houdek, Jr., Kellogg Switchboard and Supply Company, Selectively Amplifying Loud-Speaking Telephone, 2 821 572.

T. M. Jackson and E. A. F. Sell, Standard Telephones and Cables Limited (London), Stepping Circuit Arrangement Using Trigger Devices, 2 814 762.

R. V. Judy, Kellogg Switchboard and Supply Company, Dual-Switch Finder Combination, 2 821 573.

K. A. Karow, Kellogg Switchboard and Supply Company, Digit-Absorbing Selector, 2 818 469.

M. Kenmoku, Nippon Electric Company, Limited (Tokyo), Microwave Discharge Tube, 2 814 756.

W. Klein and W. Fritz, C. Lorenz A. G. (Stuttgart), Traveling-Wave-Tube Arrangement, 2 812 469.

K. Klinkhammer, K. Steinbuch, G. Merk, and H. Bretschneider, Mix & Genest (Stuttgart), Digital Register for Communication System, 2 820 849.

G. Kratt, C. Lorenz A. G. (Stuttgart), Translating Device for Type Printing Machines, 2 821 570.

G. Kratt and O. Holstein, C. Lorenz A. G. (Stuttgart), Telegraph Signal Translation Mechanism, 2 820 094.

C. C. Larson, Farnsworth Electronics Company, Jump Compensation for Continuous Motion Film Projection, 2 818 466.

P. E. Lighty, Federal Telecommunication Laboratories, Selenium Rectifier, 2 815 475.

F. Malsch, C. Lorenz A. G. (Stuttgart), Tuning-Indicator Valve of Small Dimensions and High Sensitivity, 2 820 916.

E. M. S. McWhirter and F. W. Warden, Intelex Systems Incorporated, Memory System, 2 814 440.

M. Mattheyses, Federal Telephone and Radio Company, Rectifier Stack, 2 819 434.

R. C. Miles, Federal Telephone and Radio Company, Moving-Target Indicator, 2 818 561.

F. H. Mittag and H. Ringhandt, Standard Elektrik A. G. (Stuttgart), Dispatch Tube System, 2 815 182.

H. Nopp and K. Wernick, Mix & Genest (Stuttgart), Circuit Arrangement for Loudspeaker Telephone Systems, 2 820 096.

R. L. Plouffe, Jr., Federal Telecommunication Laboratories, Delay-Line Pulse Shaper, 2 820 909.

M. C. Poylo, Federal Telecommunication Laboratories, Information Transmission System, 2 815 400.

E. A. Richards and L. J. Ellison, Standard Telephones and Cables Limited (London), Dry Contact Rectifiers, 2 817 047.

E. Richert, Mix & Genest (Stuttgart), Arrangement for the Stopping and Dispatching of Carrier Capsules in Pneumatic Tube Systems, 2 816 719.

T. P. Robinson and B. W. Glover, Standard Telephones and Cables Limited (London), Electrical Control Circuits, 2 821 679.

R. D. Salmon and F. J. L. Turner, Creed & Company, Limited (Croydon), Telegraph-Code Perforating Apparatus, 2 818 116.

K. Sass and K. Klinkhammer, Mix & Genest, Circuit Arrangement for Final Selectors with Three Line Groups Arranged in One Plane, 2 821 574.

W. Sichak, Federal Telecommunication Laboratories, Dual Polarization Antenna, 2 820 965.

E. Stein, Federal Telecommunication Laboratories, Waveform Monitor, 2 817 043.

D. L. Thomas, Standard Telephones and Cables Limited (London), Two-Way Repeaters, 2 812 388.

H. E. Thomas, Federal Telecommunication Laboratories, Sweep Wave Generators, 2 819 392.

L. R. Ullery and R. K. Orthuber, Capehart–Farnsworth Company, Radiation Detector, 2 818 511.

C. Weill, C. Hannigsberg, and H. Adelaar, Bell Telephone Manufacturing Company (Antwerp), Control Circuit for Pulse Generator, 2 820 141.

H. Wolfson, Standard Telephones and Cables Limited (London), Germanium Diodes, 2 818 537.

W. W. Wright, P. Welch, and D. A. Day, Standard Telephones and Cables Limited (London), Electron Discharge Device, 2 815 464.

Memory System

2 814 440

E. M. S. McWhirter and F. W. Warden

A data-card storage and reading system is described. The storage cabinet has a record transfer mechanism for feeding the cards from a particular drawer or tray past heads reading the data on the cards, which are then replaced in their drawer.

Contributors in This Issue

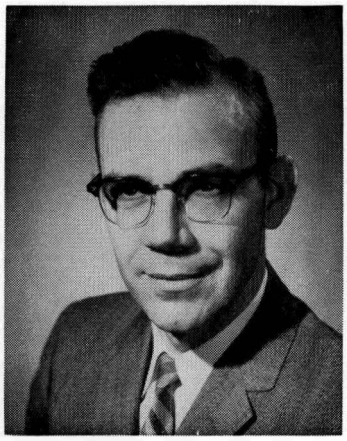

DEAN W. DAVIS

DEAN W. DAVIS was born in 1921 in Fort Wayne, Indiana. He received a degree of Bachelor of Science in electrical engineering from Purdue University in 1943. He then served for three years in the United States Army Signal Corps.

He joined the research department of the Farnsworth Electronics Company in 1946, working on special-purpose tubes. He has been in charge of storage-tube development since its inception at Farnsworth in 1949 and now heads the special-tube development laboratory. He reports in this issue on the latron storage tube.

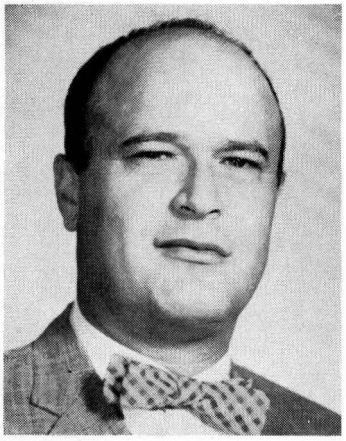

HARRY W. GATES

Mr. Davis is a member of the Institute of Radio Engineers.

• • •

HARRY W. GATES was born on May 18, 1921 in Tulsa, Oklahoma. He received BS and MS degrees in electrical engineering from the University of New Mexico in 1949.

From 1942 to 1946, he served as a radar and communications officer in the United States Marine Corps. From 1949 to 1952, he taught ultra-high-frequency theory and did research at the University of New Mexico and the University of Florida.

In 1952, Mr. Gates joined Farnsworth Electronics Company, where he is a senior engineer concerned with air-traffic-control systems design. His paper in this issue describes the Farnsworth Iatron storage tube as used in an indicator for air-traffic control.

• • •

D. S. GIRLING was educated at Leicester City Boys' Grammar School. As a member of the Territorial Army he was called up at the outbreak of war and served with the British Expeditionary Force in their campaign in Belgium in May 1940. He was later commissioned in Royal Signals and was responsible for the training of line mechanics on line carrier equipment.

In May 1946, he joined the capacitor department of Standard Telephones and Cables at North Woolwich. He took charge of the development laboratory in 1948, since when his main interests have been the statistics of capacitor failure, on which he reports in this issue, and techniques for the manufacture of miniature capacitors. He has recently taken charge of the capacitor engineering department. He is an Associate Member of the Institution of Electrical Engineers.

• • •

THEODOR GRANZ GREWE was born in Lippstadt, Germany, on July 20, 1916. He completed his studies at the Technical State College, Dortmund, in 1937 and the Technical University, Stuttgart, in 1948.

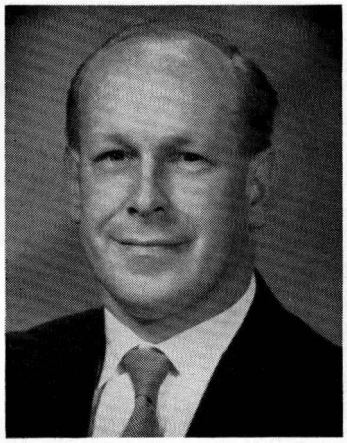

D. S. GIRLING

In 1938 and 1939, Mr. Grewe worked in the Research Institute of AEG, Berlin, on the development of acoustic altitude meters. During the second world war, he was employed in the torpedo testing installations at Eckenförde and Gotenhafen. On completion of his studies in 1948, he joined Standard Elektrik Lorenz A.G., Stuttgart, where he is a staff member in the transmission-technique laboratory.

Mr. Grewe reports in this issue on the theory of the negative-impedance two-wire repeater.

• • •

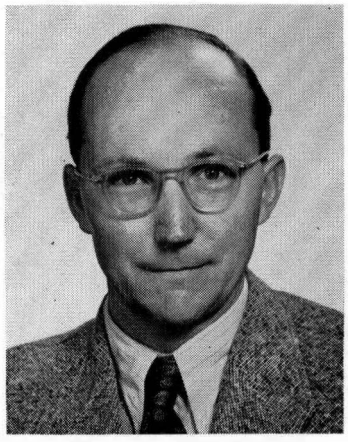

THEODOR G. GREWE

HEINZ KÜRTEN

HEINZ KÜRTEN was born in Kempen, Germany, on November 26, 1925. He served as an aviator in the German Air Force from 1943 to 1945.

While working in industry, he also attended the Technical University at Aachen from 1949 to 1953. As a student, he visited Finland in 1951 and 1952.

On graduation as Diploma-Ingenieur, he joined Standard Elektrik Lorenz. He is now a project engineer in the export division. He is coauthor of a paper in this issue on Finnish crossbar toll offices.

NIKOLAUS LEWEN was born in Wintrich, Germany, on February 17, 1910. After three years at Rheinische Elektrizitaets AG in Mannhein, he attended the Technical College at Bingen from 1933 to 1936.

He served as a telecommunication engineer for Siemens and Halske from 1936 to 1942. He then worked on the improvement of aircraft engines for Daimler-Benz in Stuttgart.

In 1946, Mr. Lewen jointed Standard Elektrik Lorenz as a circuit designer. He is coauthor of a paper on the Finnish crossbar toll offices in this issue.

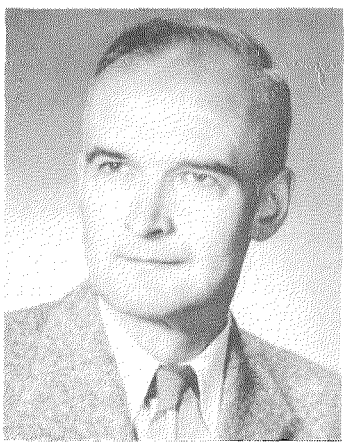

NIKOLAUS LEWEN

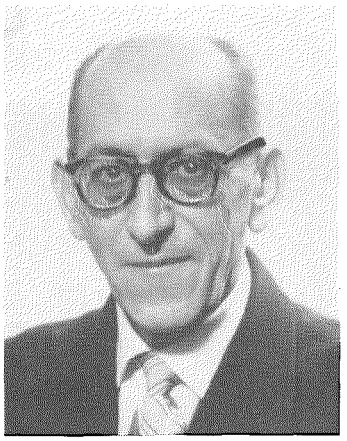

EDMOND A. THOMAS

EDMOND A. THOMAS was born in Chambery, France, on July 21st 1899. He graduated as an engineer from Institut Electrotechnique de Grénoble in 1922.

He joined the Compagnie Générale de Constructions Téléphoniques in 1936 and was assigned to the power-line carrier telephony division of the technical department. Mr. Thomas is the author of the paper in this issue on the carrier system for the Algerian power network.

INTERNATIONAL TELEPHONE AND TELEGRAPH CORPORATION

Principal U. S. Divisions and Subsidiaries

DIVISIONS

Components Division, Clifton, N. J.
Kuthe Laboratories, Inc., Newark, N. J.
Farnsworth Electronics Company, Fort Wayne, Ind.
Federal Telephone and Radio Company, Clifton, N. J.
Industrial Products Division, San Fernando, Calif.
ITT Laboratories, Nutley, N. J.
Kellogg Switchboard and Supply Company, Chicago, Ill.

SUBSIDIARIES

American Cable & Radio Corporation, New York, N. Y.
All America Cables and Radio, Inc., New York, N. Y.
Commercial Cable Company, The, New York, N. Y.
Mackay Radio and Telegraph Company, New York, N. Y.
Federal Electric Corporation, Paramus, N. J.
Intelex Systems Incorporated, New York, N. Y.
Airmatic Systems Corporation, Rochelle Park, N. J.
Kellogg Credit Corporation, New York, N. Y.
Royal Electric Corporation, Pawtucket, R. I.

and... International Standard Electric Corporation, New York, N. Y. whose principal research, manufacturing, and sales affiliates are:

ARGENTINA
Capehart Argentina S.A.I.C. (50% owned), Buenos Aires
Compañía Standard Electric Argentina, S.A.I.C. Buenos Aires

AUSTRALIA
Standard Telephones and Cables Pty. Limited, Sydney
Austral Standard Cables Pty. Limited (50% owned), Melbourne
Silovac Electrical Products Pty. Limited, Sydney
Standard Telephones and Cables (Qld.) Pty. Limited, Brisbane

AUSTRIA
Standard Telephon und Telegraphen Aktiengesellschaft, Czeija, Nissl & Co., Vienna

BELGIUM
Bell Telephone Manufacturing Company, Antwerp

BRAZIL
Standard Eléctrica, S.A., Rio de Janeiro

CANADA
Standard Telephones & Cables Mfg. Co. (Canada), Ltd., Montreal

CHILE
Compañía Standard Electric, S.A.C., Santiago

CUBA
Equipos Telefónicos Standard de Cuba, Havana
International Standard Products Corporation, Havana

DENMARK
Standard Electric Aktieselskab, Copenhagen

FINLAND
Oy Suomen Standard Electric AB, Helsinki

FRANCE
Compagnie Générale de Constructions Téléphoniques, Paris
Les Téléimprimeurs, Paris
Laboratoire Central de Télécommunications, Paris
Le Matériel Téléphonique, Paris

GERMANY
Standard Elektrik Lorenz A.G., Stuttgart
Bauelemente Werk S.A.F. (division), Nuremberg
Informatikwerk (division), Stuttgart
Kabelwerk (division), Stuttgart
Lorenz Werke (division), Stuttgart
Mix & Genest Werke (division), Stuttgart
Schaub Werk (division), Pforzheim

IRAN
Standard Electric Iran A.G., Teheran

ITALY
Fabbrica Apparecchiature per Comunicazioni Elettriche Standard S.p.A., Milan

MEXICO
Industria de Telecomunicación, S.A. de C.V. (50% owned), Mexico City
Standard Eléctrica de México, S.A., Mexico City

NETHERLANDS
Nederlandsche Standard Electric Maatschappij N.V., The Hague

NEW ZEALAND
New Zealand Electric Totalisators Limited. Wellington

NORWAY
Standard Telefon og Kabelfabrik A/S, Oslo

PORTUGAL
Standard Eléctrica, S.A.R.L., Lisbon

PUERTO RICO
Standard Electric Corporation of Puerto Rico, San Juan

SPAIN
Standard Eléctrica, S.A., Madrid

SWEDEN
Standard Radio & Telefon AB, Stockholm

SWITZERLAND
Standard Téléphone et Radio S.A., Zurich

TURKEY
Standard Elektrik Ve Telekomunikasyon Limited Sirketi, Ankara

UNITED KINGDOM
Creed & Company, Limited, Croydon
Standard Telephones and Cables Limited, London
Kolster-Brandes Limited, Sidcup
Standard Telecommunication Laboratories Limited, London

VENEZUELA
Standard Telecommunications C.A., Caracas

OVERSEAS TELECOMMUNICATION COMPANIES

ARGENTINA
Compañía Internacional de Radio, S.A., Buenos Aires
Sociedad Anónima Radio Argentina (subsidiary of American Cable & Radio Corporation), Buenos Aires

BOLIVIA
Compañia Internacional de Radio Boliviana, La Paz

BRAZIL
Companhia Rádio Internacional do Brasil, Rio de Janeiro
Companhia Telefônica Nacional, Curitiba and Pôrto Alegre

CHILE
Compañía de Teléfonos de Chile, Santiago
Compañia Internacional de Radio, S.A., Santiago

CUBA
Cuban American Telephone and Telegraph Company (50% owned), Havana
Cuban Telephone Company, Havana
Radio Corporation of Cuba, Havana

PERU
Compañía Peruana de Teléfonos Limitada, Lima

PUERTO RICO
Puerto Rico Telephone Company, San Juan
Radio Corporation of Puerto Rico, San Juan

SPAIN
Compañía Radio Aérea Marítima Española, S.A., Madrid

UNITED KINGDOM
International Marine Radio Company Limited, Croydon

ASSOCIATE LICENSEES FOR MANUFACTURE AND SALES

FRANCE
Lignes Télégraphiques et Téléphoniques, Paris

ITALY
Società Italiana Reti Telefoniche Interurbane, Milan

JAPAN
Nippon Electric Company, Limited, Tokyo
Sumitomo Electric Industries, Limited, Osaka

SPAIN
Marconi Española, S.A., Madrid